Advanced Functional Materials

ADVANCED FUNCTIONAL MATERIALS
www.afm-journal.de

REVIEW

Machine Learning-Based Inverse Design for Functional Materials: Methods, Challenges, and Engineering Applications

Weihao Lin[1,2] | Liuchao Jin[3] | Zhifei Jiang[4] | Mingjing Cai[5] | Zhihui Lai[1,2] | Daniil Yurchenko[6] | Bo Yan[7] | Shengxi Zhou[8] | Kostya S. Novoselov[4] | Wei-Hsin Liao[3,9] | Shitong Fang[1,2]

[1]Guangdong Key Laboratory of Electromagnetic Control and Intelligent Robots, College of Mechatronics and Control Engineering, Shenzhen University, Shenzhen, China | [2]National Key Laboratory of Green and Long-Life Road Engineering in Extreme Environment (Shenzhen), Shenzhen University, Shenzhen, China | [3]Department of Mechanical and Automation Engineering, The Chinese University of Hong Kong, Hong Kong, China | [4]Department of Materials Science and Engineering, National University of Singapore, Singapore, Singapore | [5]Guangzhou Institute of Technology and School of Mechano-Electronic Engineering, Xidian University, Guangzhou, China | [6]Institute of Sound and Vibration Research, University of Southampton, Southampton, UK | [7]School of Mechanical Engineering, Zhejiang Sci-Tech University, Hangzhou, Zhejiang, China | [8]School of Aeronautics, Northwestern Polytechnical University, Xi'an, China | [9]Institute of Intelligent Design and Manufacturing, The Chinese University of Hong Kong, Hong Kong, China

Correspondence: Shitong Fang (stfang@szu.edu.cn)

Received: 12 December 2025 | **Revised:** 4 March 2026 | **Accepted:** 10 March 2026

Keywords: data-driven design | design optimization | functional material | inverse design | machine learning | surrogate modeling | topology optimization

ABSTRACT

Inverse design of functional materials—using target performance to guide optimal parameters—provides a powerful alternative to traditional forward methods, especially for complex, high-dimensional problems. Advances in machine learning (ML) enhance its feasibility through fast surrogate modeling, efficient design-space exploration, and direct mapping from desired properties to material solutions. This review presents a unified overview of ML-driven inverse design methodologies, covering topology optimization, direct inverse mapping, and hybrid frameworks. We analyze key ML models, optimization algorithms, and adaptive schemes that tackle challenges including data scarcity and coupled physical constraints. Focusing on diverse functional materials, we highlight and illustrate how ML-based inverse design is accelerating innovation across diverse classes of materials by rapid generation of microstructures and geometries tailored to specific functionalities, including mechanical and architected materials, acoustic and thermal metamaterials, optical materials, energy functional materials, biomedical and chemical materials. Finally, we outline key challenges and future directions toward autonomous, physics-integrated, and generative pipelines for advanced functional materials. This review aims to provide a unified foundation for ML-based inverse design and to guide the development of intelligent discovery pipelines for advanced materials.

1 | Introduction

Traditional design of engineering functional materials typically follows a forward process (Figure 1: blue part): an initial configuration, often based on empirical knowledge or designer intuition, is evaluated and iteratively refined using physics-based simulations until the desired performance criteria are satisfied [1–5]. However, compared to inverse design, forward design suffers from several limitations, including heavy reliance on designer knowledge and intuition, high computational costs, a

Weihao Lin and Liuchao Jin contributed equally to this work.

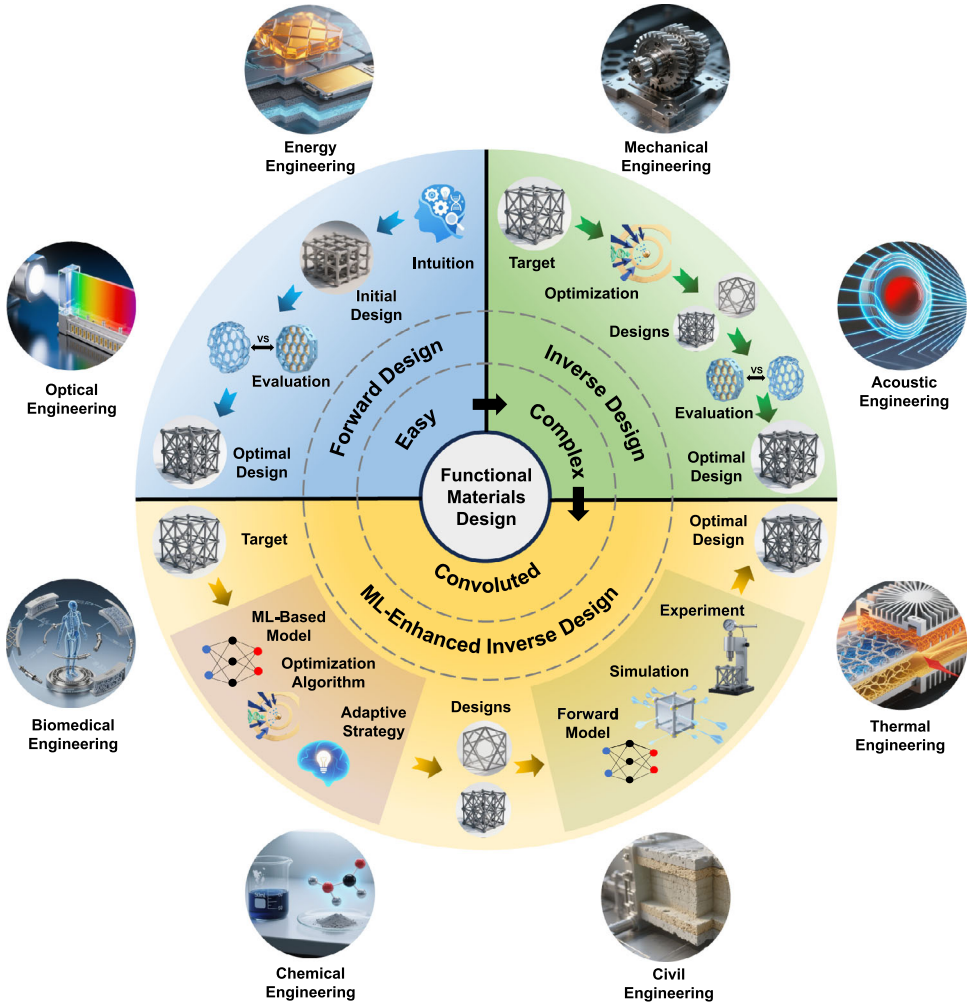

FIGURE 1 | Overview of functional materials design methodologies and application domains in engineering.

tendency to converge to local rather than global optima, and difficulties in handling high-dimensional and complex design problems [6, 7]. In contrast, inverse design offers an alternative methodology [8, 9]. Rather than starting from a predefined structure, it begins with a specification of the target performance or functional objectives and seeks to determine the optimal physical configuration that satisfies these requirements (Figure 1: green part). This performance-driven strategy enables the systematic exploration of non-intuitive, mechanical metamaterials with energy absorption properties [10], alloy with high-strength characteristics [11], energy structure with high conversion efficiency and high energy density [12], high-performance solutions—such as ultra-broadband acoustic metamaterials [13] and photonic crystals with tailored light-manipulation properties [14, 15]—that are often inaccessible through conventional design methods.

However, the practical realization of inverse design has some significant, inherent challenges. The computational cost of navigating vast, high-dimensional design spaces using iterative high-fidelity simulations is often prohibitive [16–18]. Another problem is that multiple distinct designs can satisfy the same performance target, and it is sensitive, where small changes in the desired performance necessitate radically different solutions [19–21]. Furthermore, generating sufficient high-quality and high-dimensional data (design-performance pairs) to explore these complex spaces is costly and time-consuming, while incorporating real-world constraints like manufacturability and multi-physics interactions adds further layers of complexity and uncertainty [22, 23]. These challenges historically hinder the development of complex inverse design.

The use of machine learning in inverse design has significantly advanced the inverse design (Figure 1: yellow part), offering practical tools to address longstanding challenges such as high computational cost, complex design spaces, and limited data availability [24–31]. By learning the relationship between design inputs and performance outputs from data, ML models can provide fast approximations to traditional simulations, reducing the time needed for design evaluation and enabling more efficient optimization [32]. In addition to improving computational efficiency, ML methods help manage problems related to high-dimensional input and output spaces. Generative models—such as Variational Autoencoders (VAEs) and Generative Adversarial Networks (GANs)—can reduce the size of the design space or identify feasible design regions, allowing optimization algorithms to work more effectively. Recent models like diffusion-based and transformer-based networks also show promise in capturing complex patterns in design data [33]. To address data scarcity,

several approaches have been developed. Physics-informed neural networks (PINNs) incorporate known physical laws into the learning process, improving accuracy even when training data is limited. Multi-fidelity modeling combines low-cost, low-accuracy simulations with more accurate but expensive data sources, while transfer learning and meta-learning use information from related problems to improve learning efficiency. Active learning methods can further reduce data requirements by selecting the most informative samples to evaluate [34]. In some cases, ML models can learn to directly map target performance specifications to suitable design parameters, providing a more direct route for inverse design that does not rely on iterative optimization. These approaches are especially effective when integrated with traditional physics-based methods, combining the speed and flexibility of ML with the accuracy and reliability of established modeling techniques [35].

Although machine learning-driven inverse design has been applied across a wide range of engineering disciplines, its underlying strategies and guiding principles share a common foundation. At its core, the inverse design process—whether applied to mechanical structures, optical devices, or biomedical and chemical materials—relies on learning or approximating the mapping from desired performance targets back to feasible design configurations. Across various applications, similar components are commonly adopted, including surrogate modeling, optimization under constraints, dimensionality reduction, and adaptation to data availability. Despite differences in specific implementations and domain requirements, the methodological framework remains largely unified.

However, most current research remains focused within disciplinary boundaries, with limited cross-referencing between subfields [36]. This has led to the repeated development of similar techniques, such as types and frameworks of machine learning, and the design of optimization algorithms, without a shared language or comparative analysis. A comprehensive synthesis is therefore essential to understand how these methods are being adapted to different problem settings, and to identify the core techniques that can be transferred or generalized across domains.

This review aims to fill this gap by presenting a unified perspective on ML-based inverse design. Rather than treating individual applications in isolation, we emphasize the common methodological framework that underpins inverse design across diverse classes of functional materials. We structure the discussion around core strategies—including topology-optimization-based approaches, direct inverse mapping, and hybrid forward-inverse schemes—and analyze how different machine learning models and optimization algorithms operate under varying data regimes and design-space dimensionalities. Furthermore, we highlight not only the methodological consistency of ML-driven inverse design but also its ability to accelerate the discovery, optimization, and multifunctional integration of mechanical, acoustic, thermal, optical, energy, civil, electrical, biomedical, chemical, and other emerging functional materials. Finally, we identify the key challenges that persist in this rapidly evolving field and outline promising directions for future research, aiming to guide the development of next-generation inverse design frameworks for advanced functional materials.

2 | From Classical to Machine Learning-Enabled Inverse Design

In this section, we review and summarize the technological advancements in inverse design, along with commonly used machine learning models, methods, and optimization algorithms, aiming to provide readers with a comprehensive, clear, and concrete framework for inverse design. In Section 2.1, we primarily discuss the development of inverse design methodologies. In Section 2.2, we summarize the frequently employed machine learning models and methods in inverse design. In Section 2.3, we summarize the optimization techniques commonly applied in inverse design. In Section 2.4, based on the commonly used machine learning models, methods and optimization methods in inverse design, we summarize three inverse design processes based on machine learning.

2.1 | Evolution of Inverse Design

The inverse engineering of materials has undergone a progressive evolution from traditional manual methods to modern ML-driven intelligent processes. In traditional inverse engineering methodologies, physical experimentation, empirical analysis, and trial-and-error processes were predominantly employed for design optimization, but these approaches suffered from inherent limitations, including low procedural efficiency, high experimental costs, and inadequate capability for handling complex systems [37]. With the rapid advancement of numerical computational methods, they are widely used for simulating or validating experimental results. When a target outcome is inversely designed, its performance can be evaluated through high-fidelity numerical simulations. Numerical computational methods include the finite element method (FEM) [38], the finite difference time domain (FDTD) [39, 40], the finite integration technique (FIT) [41], the finite volume method (FVM) [42, 43], and the discrete element method (DEM) [44, 45] as shown in Table 1. Numerical calculation methods primarily rely on solving partial differential equations (PDEs) to simulate physical field distributions (e.g., mechanical equations to stress-strain models [38], Maxwell's equations to electromagnetic fields [39, 40]). Numerical calculation methods primarily rely on solving partial differential equations to simulate the distribution of physical fields. In electromagnetic simulations, Kanyee et al. [40] applied the FDTD method to forward-model the propagation and scattering of electromagnetic waves. This approach discretizes the continuous Maxwell's equations into difference equations in time and space, and iteratively solves for updated field components at grid points. For stress–strain modeling, Marcal & King [38] employed the FEM to perform incremental elastoplastic analysis of two-dimensional stress systems. By incorporating the Prandtl–Reuss equations and the Von Mises yield criterion to establish stress–strain relationships, equilibrium equations were solved iteratively, simulating the progressive expansion of plastic zones. These advancements in numerical techniques have enabled the simulation of physical properties during the material design process.

With the increasing maturity of optimization algorithms such as gradient descent and Newton's method, their application in

TABLE 1 | Numerical methods in inverse design applications.

Methods	Applications	Advantages	Limitations
FEM [38, 46–48]	Structural mechanics, fluid dynamics, electromagnetic analysis, thermodynamics, biomedical engineering	- Complex geometry handling - Parameter inversion capability - Intuitive field variable visualization (e.g., stress, temperature)	- Mesh sensitivity (accuracy heavily depends on mesh quality)
FDTD [39, 40, 49–51]	Optics (metasurfaces), biomedical engineering, electromagnetic analysis (design of electromagnetic compatibility, metamaterials)	- Time-domain electromagnetic transient simulation - Broadband analysis capability - Parallel computing compatibility	- The requirement for the refinement of the grid structure
FIT [41]	Electromagnetic analysis (electromagnetic compatibility, particle accelerators)	- Electromagnetic conservation property - High-frequency domain precision	- Structured grid dependency - Complex geometry limitation
FVM [42, 43, 52, 53]	Fluid dynamics (aerodynamic design), thermal management (layout optimization, heat pipe design)	- Conservation law adaptability (e.g., hyperbolic, mass, momentum, energy)	- Discretization scheme complexity - Numerical diffusion susceptibility
DEM [44, 45, 54]	Multibody dynamics (granular systems), biomedical engineering (structural interaction analysis, drug delivery)	- Discontinuous media modeling (e.g., particle interactions, multiscale adaptation) - Mesh-free formulation	- High computational cost (large particle systems) - Parameter sensitivity (e.g., friction coefficients, restitution)

structural design has deepened, demonstrating notable optimization outcomes. Through systematic iterative updates of design variables, these methods can effectively determine sensitivity relationships between various structural responses—such as displacement, stress, and temperature fields—and target performance, thereby guiding adjustments in structural morphology and parameters. For instance, in gradient-based optimization, the adjoint variable method is commonly employed to efficiently compute sensitivity coefficients, avoiding repeated forward computations and significantly enhancing the efficiency of the optimization process [55]. When addressing design problems with complex boundary conditions, gradient-based algorithms can achieve inverse design of intricate structures, such as porous cooling channels, by minimizing objective functions like temperature error or stress overrun, ensuring that results satisfy practical engineering constraints [56]. It is evident that the advent of gradient-based optimization algorithms has introduced directional guidance into structural optimization, laying the groundwork for subsequent optimization strategies in functional material design.

Subsequently, in 1997, Professor Olson introduced the concept of "materials by design [57]," advocating an inverse design approach following the closed-loop of "performance–properties–structure–process." This means first defining the desired end performance of a product, then employing optimization algorithms (e.g., topology optimization, evolutionary algorithms) and computational models (physical or machine learning models) to inversely design material structures across multiple scales, from micro to macro. This concept has led to a series of new inverse design methods based on optimization algorithms and computational models. For instance, in multi-material topology optimization in inverse design, Bendsøe et al. [58] applied the SIMP model to inverse topology optimization design, proposing a topology optimization method based on material interpolation schemes, including the SIMP model and inverse homogenization. The SIMP model suppressed intermediate densities via density variables and penalty factors, driving the design toward a binary (0-1) distribution to generate clear topological structures. Through inverse design of periodic microstructures, the effective properties were matched to the target interpolation model, enabling precise control of material volume fractions in multi-material designs. Later, the development of global search algorithms, such as evolutionary algorithms and particle swarm optimization, has addressed challenges in material structure optimization, including discrete design spaces, discontinuities, and the difficulty of balancing kinematic stability. Early research often integrated global optimization algorithms with multidisciplinary theories for the inverse design of material structures. For example, in the inverse design of photonic crystal devices, multiple scattering theory was combined with the genetic algorithm (GA), where GA was used to adjust binary parameters to optimize device performance [59]. Subsequently, the particle swarm optimization (PSO) algorithm was also applied to assist in the design and optimization of functional material structures. For instance, in multidimensional crystal structure design, PSO can serve as a global search algorithm to efficiently identify silicon phases with targeted electronic bandgap properties [60].

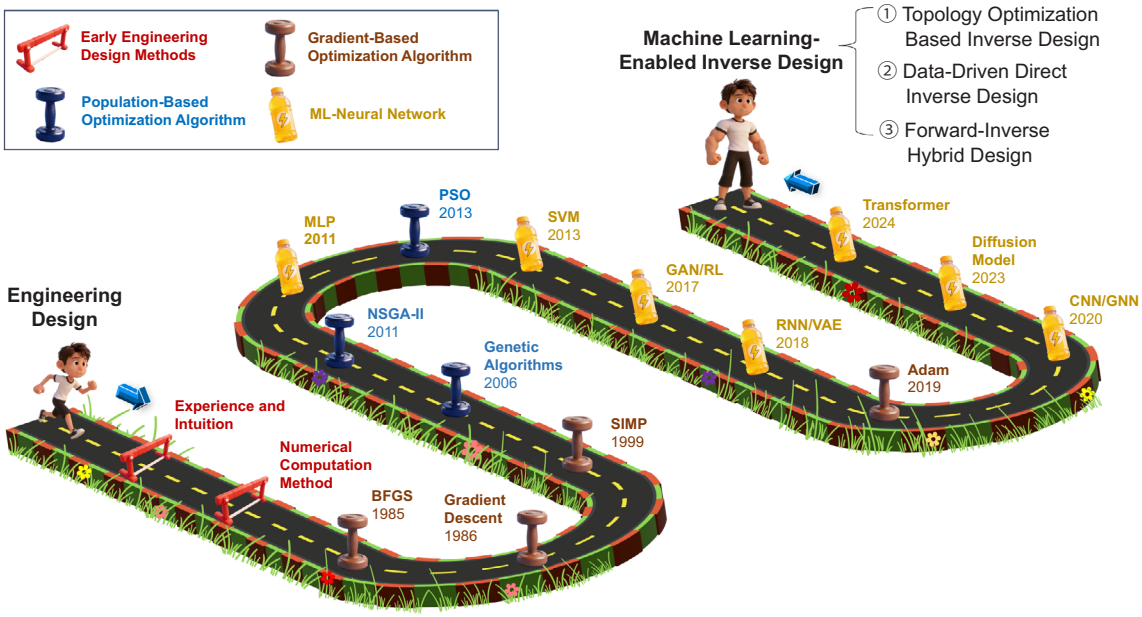

FIGURE 2 | The development history of inverse design in the field of engineering. From the initial trial-and-error approach to the current three machine learning-based inverse design methods.

Currently, numerical computation methods, optimization algorithms, and topology optimization techniques have been extensively applied to inverse structural design across multiple engineering disciplines. In numerous works, these approaches are synergistically integrated to achieve comprehensive solutions [39, 61–65]. Nelson et al. [63] adopted a topology optimization framework combined with adjoint sensitivity analysis for plasmonic nanostructure inverse design, utilizing gradient descent algorithms to iteratively update design variables until convergence. Their methodology produces a trapping potential that is 1.95 times greater than previous representative studies on algorithm designed. Thillaithevan et al. [64] implemented the SIMP method for material distribution interpolation during inverse design of periodic microstructures. This approach incorporated objective functions with intermediate density penalty constraints, employed FEM for automatic computation of objective function and constraint sensitivities, and integrated gradient-based optimization algorithms to progressively adjust penalty factors and projection parameters. The SIMP method significantly improved design binarization. Zeng et al. [66] developed a GA-based topology optimization framework for inverse design of energy-absorbing metamaterials with target stress-strain curves, successfully achieving structure-property mapping with minimal error. Additionally, Cui et al. [65] proposed an intelligent design system for material topology inverse design, enabling users to input target elastic parameters (e.g., effective elastic modulus, Poisson's ratio) and directly generate compliant structures through integration of PSO with moving morphable component topology optimization. While these methodologies remain highly effective and crucial in contemporary research, significant potential for methodological advancement persists.

As the complexity of material design continues to increase, traditional numerical computational methods have shown limitations in efficiency when dealing with intricate material systems. In conventional topology optimization, gradient-based sensitivity analysis also suffers from high computational cost and difficulty in providing accurate optimization directions [66, 67]. Moreover, as the design dimensionality rises, such methods struggle to generate comprehensive structural datasets, leading to deviations in predicted structural performance. Consequently, researchers start to base material design on big data, exemplified by the Integrated Computational Materials Engineering approach supported by the Materials Genome, as proposed by Xiong and Olson [68]. Its core lies in the multi-scale, interdisciplinary integrated design following the processing-structure-property-performance paradigm, enabling rational material design and development. Later, to achieve lower-cost and more efficient inverse material design, researchers have turned to vast material structure databases to train machine learning models. These models serve as surrogates for expensive physics-based simulations, accelerating forward prediction of structure-property relationships (e.g., Multilayer Perceptron (MLP) [69], Support Vector Machine (SVM) [70], Reinforcement Learning [71], Recurrent Neural Network (RNN) [72], Convolutional Neural Network (CNN) [73], and Graph Neural Network (GNN) [74]). On the other hand, by training generative models to directly invert the "structure-property" mapping, truly efficient inverse design is realized (e.g., GAN [71], VAE [75]). Emerging machine learning models such as Diffusion models [76] and Transformer models [77] are now demonstrating strong potential in inverse material design. ML-based inverse design methods have been widely applied across various fields, including mechanical engineering [78–81], energy systems [82, 83], civil and architectural engineering [84], optics and electromagnetics [85–88], materials science [89–92], and biomedical engineering [93–96]. These ML-based approaches can be broadly categorized into three strategic paradigms: topology optimization-based inverse design, pure inverse design, and forward-inverse hybrid design. In summary, the evolution of design methodologies from simple to complex, high-dimensional engineering problems is summarized in Figure 2.

2.2 | Machine Learning Models and Methods in Inverse Design

Machine learning models and methods serve distinct roles in inverse design, which can broadly be categorized into two primary functions. First, machine learning models serve as inverse solvers to directly output inverse design results, thereby accelerating the efficiency of inverse design [73, 97–99]. Notably, generative models, owing to their high generative efficiency, can effectively expand the dataset [100]. Second, machine learning models can act as performance predictors to replace traditional mathematical solvers such as numerical simulations and sensitivity calculations, enabling rapid performance prediction and result validation [101, 102]. When combined with active learning methods, these models significantly enhance their own quality [103]. From this analysis, it is evident that machine learning models are pivotal for inverse design. Therefore, in this section, we conduct a systematic classification of machine learning models based on learning patterns, categorizing them into supervised learning, unsupervised learning, semi-supervised learning, and reinforcement learning.

Supervised learning typically relies on labeled datasets for model training [104, 105]. For classification, SVMs and Nearest Neighbor classifiers are quintessential supervised models. In inverse design, machine learning models are commonly used for prediction, generation, and optimization, leveraging their high predictive accuracy and computational efficiency [106]. Unsupervised learning focuses on identifying underlying patterns in unlabeled data. Without explicit guidance, training such models is significantly more challenging than supervised learning [107]. It is precisely this autonomous learning capability, however, that enables unsupervised models to discover novel patterns from data more effectively than supervised models [76]. Semi-supervised models represent a combination of supervised and unsupervised learning, typically utilizing a small amount of labeled data alongside abundant unlabeled data. This approach mitigates data scarcity [108] and enhances either generative model diversity or proxy model robustness via self-supervised pretraining. Reinforcement learning is a strategy for learning dynamic decisions through environmental interaction [109]. It embeds reward mechanisms to optimize design parameters, eliminating the need for labeled data. RL excels at resolving multi-objective trade-offs and enables dynamic adaptive optimization. Table 2 summarizes commonly used machine learning models in inverse design, classified according to four learning patterns, and further analyzes their advantages and disadvantages based on existing research.

2.3 | Optimization Algorithms in Inverse Design

Optimization algorithms play a pivotal role in inverse design, not only broadening the scope of addressable problems but also enhancing design efficiency. Overall, these can be classified into five uses. First, optimization algorithms are employed to iteratively optimize network model parameters, i.e., adjusting design parameters to match target performance. Second, they facilitate structural generation and topology optimization. Third, these algorithms address multi-objective collaborative optimization [133]. Fourth, optimization algorithms impose constraints or penalties in inverse design processes, ensuring that design parameters satisfy physical limitations while achieving optimal performance. Lastly, they enable adaptive adjustment of design schemes in dynamically changing environments or through real-time feedback mechanisms. The choice of optimization method directly influences design efficiency and result reliability. Based on the differences in algorithmic principles and implementation mechanisms, mainstream optimization methods can be systematically classified into the following five categories: gradient-based optimization algorithms, population-based optimization algorithms, probability-model-based optimization algorithms, physics-based optimization algorithms, and reinforcement learning algorithms.

Basic gradient methods adjust design parameters using gradient information to approach a minimum in inverse design [134], proving efficient and intuitive for convex optimization. Incorporating enhancements like adaptive learning rates or regularization, such as Adam, enables adaptation to sparse data [135] and high-dimensional non-convex optimization [125]. Within topology optimization, the SIMP method iteratively derives optimal structures by leveraging gradients of the objective function with respect to design variables.

Population-based optimization algorithms locate global optima through iterative information exchange among individuals. Based on distinct core mechanisms, they fall into two categories: evolutionary algorithms, simulating biological evolution via cycles of mutation, selection, and recombination [136], and swarm intelligence algorithms, mimicking collective animal behavior by emphasizing collaborative interactions among individuals [137].

Probability-model-based optimization leverages prior knowledge and historical data to construct surrogate models predicting performance distributions in unexplored regions. By integrating acquisition functions, it efficiently locates global optima. In inverse design, this approach significantly reduces reliance on costly experiments or simulations, particularly for multivariate, high-dimensional nonlinear problems [138].

Physics-guided optimization algorithms achieve optimal structural performance through physically driven design variable adjustment. For instance, Bidirectional Evolutionary Structural Optimization adjusts member thickness based on von Mises stress distribution within lattice struts, progressively enhancing structural stiffness and lightweighting [139].

RL optimization enables agents to autonomously learn optimal policies by interacting with an environment to maximize cumulative rewards. Algorithms like DQN and Proximal Policy Optimization (PPO) utilize neural networks to approximate value or policy functions, employing experience replay and target networks to stabilize training. This approach exhibits particular strength in handling high-dimensional non-convex spaces and dynamic constraints [132, 140].

In Table 3, we summarize the five types of optimization algorithms described above, encompassing common optimization algorithms currently used in inverse design.

TABLE 2 | Common machine learning models and methods for inverse design of functional materials.

Category	Model and method	Advantage	Disadvantage	Refs.
Supervised-Learning	SVM	- Suitable for small sample datasets - Avoids dependence on activation functions - Kernel functions can handle non-linear relationships	- Unsuitable for large-scale data - Sensitive to kernel function selection	[73]
	Random Forest	- Ensemble mechanism improves model robustness - Handles mixed-type datasets	- Unsuitable for very small sample data - Limited extrapolation capability	[110–112]
	MLP	- Suitable for continuous numerical data - Suitable for high-dimensional input-output mapping	- Lack of feature extraction capability - Requirement for large amounts of data	[113, 114]
	CNN	- Efficient local feature extraction - Suitable for processing 1D sequence data, 2D image data, 3D voxel data	- Weak sequential data processing capability - Unsuitable for unstructured data	[106, 115]
	GNN	- Suitable for data with graph structures - GNN can progressively analyze structural information through multiple layers	- Unsuitable for datasets without structural relationships - High model complexity, difficult hyperparameter tuning	[45, 116]
	RNN	- Strong sequence feature extraction capability - Suitable for variable-length sequence data - Strong capability in capturing sequence dependencies	- Highly sensitive to sequence order	[72]
	Long Short-Term Memory (LSTM)	- Suitable for sequence data with sequential dependencies - Stronger capability in processing long sequences - Improves temporal modeling performance	- Difficult to handle extremely long sequences - Computation cannot be parallelized	[117]
	Conditional VAE (cVAE)	- Diverse design samples generation - Suitable for data with explicit conditional information	- Generated results can be blurry - Relationship between latent space and physical properties is unclear	[118, 119]
	Conditional GAN (cGAN)	- Adversarial training enhances generation quality - Suitable for data with explicit conditional information	- Unstable training - Long training time - Risk of mode collapse	[120, 121]

(Continues)

TABLE 2 | (Continued)

Category	Model and method	Advantage	Disadvantage	Refs.
	Supervised Transformer Model	- High parallel computing efficiency - Suitable for processing multimodal data - Self-attention mechanism captures long-range dependencies	- Requirement for large amounts of high-quality data - Reliance on positional encoding to add sequential information	[77, 117]
Unsupervised Learning	VAE	- Continuous latent space facilitates integration with optimization algorithms - Suitable for high-dimensional data with underlying low-dimensional structures	- Generated samples may lack sharpness - KL divergence trade-off can be difficult	[113, 122]
	GAN	- Highly realistic data generation - Suitable to handle "one-to-many" mapping problems	- Risk of mode collapse - Not suitable for high-precision tasks	[123, 124]
	Diffusion Model	- Suitable for high-dimensional data - Multi-step iterative denoising avoids mode collapse - Probabilistic generation solves "one-to-many" inverse problems	- Slow sampling, unsuitable for rapid iterative design needs - Not suitable for low-dimensional data	[76, 98, 106, 125–129]
Semi-Supervised Learning	Semi-Supervised VAE	- Utilizing unlabeled data can improve model generalization - Latent space optimized jointly by unsupervised and supervised parts	- Unsuitable for datasets where distribution of unlabeled data differs significantly from labeled data - Noise from unlabeled data can affect latent space construction	[130, 131]
	Semi-Supervised GAN	- Utilizing unlabeled data can help model capture material features - Adversarial training avoids overfitting to unlabeled data	- Difficult to handle mixed features with discrete and constrained types - Model may learn irrelevant features	[108]
Reinforcement Learning	Deep Q-Network (DQN)	- DQN autonomously explores design space through interaction with the environment - Experience replay breaks temporal correlations in data, improving training stability - Cumulative rewards allow optimization of long-term goals	- Long interaction time with the environment - DQN can only output one action, making it less flexible than generative models	[132]

2.4 | Workflows of Machine Learning-Enabled Inverse Design

Based on a systematic review of the development of inverse design, along with machine learning models and optimization algorithms, we further focus on the current architecture of ML-based inverse design workflows. With the deepening application of data-driven methods in materials and structural design, three representative processes of inverse design have emerged: topology optimization-based inverse design,

TABLE 3 | Commonly used optimization algorithms for inverse design.

Category	Subclass	Algorithm	Fundamental principle	Function	Refs.
Gradient-Based	Basic Gradient Method	GD	Iterative parameter update along the gradient of the loss function	Minimization of the loss function	[103, 141–144]
	Improved Gradient Method	Stochastic Gradient Descent (SGD)	Parameter update using gradients computed from randomly sampled data	Acceleration of large-scale data training	[145]
		Adjoint Method	Transformation of gradient computation into solving adjoint equations	Significant reduction in computational cost for complex optimization problems	[146, 147]
		Adaptive Moment Estimation (Adam)	Dynamic parameter adjustment combining momentum and adaptive learning rates	High-dimensional parameter optimization; automatic adjustment of update magnitude	[67, 72, 106, 115, 117, 118, 124, 125, 135, 138, 143, 148–159]
		Adam with Weight Decay (AdamW)	Decoupling of weight decay from parameter updates	Prevention of overfitting; enhanced generalization capability	[77, 98, 126, 143, 160, 161]
		Limited Memory BFGS (L-BFGS)	Iterative parameter update using quasi-Newton methods within a bounded region	Avoidance of divergence or local optima	[45, 143, 154, 156]
		Moving Asymptotes Method (MMA)	Sequential adjustment of movable asymptotes to approximate the original problem	Balance of convergence and robustness; avoidance of oscillation or premature local optima	[102, 162]
		Adaptive Gradient Algorithm (Adagrad)	Adaptive learning rate adjustment; larger updates for sparse features	Sparse data optimization	[143]
		Nesterov-accelerated Adam (Nadam)	Combination of Nesterov momentum and Adam's adaptive learning rates	Accelerated convergence; reduced oscillation	[143]
		Root Mean Square Propagation (RMSprop)	Learning rate adjustment via exponentially weighted averages	Optimization of non-stationary objective functions	[124, 143]

(Continues)

TABLE 3 | (Continued)

Category	Subclass	Algorithm	Fundamental principle	Function	Refs.
	Material Density Distribution based Method	SIMP	Association of material density with physical properties via penalty functions; suppression of intermediate densities	Efficient handling of complex material layout; elimination of gray-scale intermediates; ensuring manufacturability	[64, 127, 162]
Population-Based	Evolutionary	GA	Emulates natural selection via crossover, mutation, and selection	Global search for multi-objective/nonlinear problems	[133, 144, 146, 163–165]
		Differential Evolution (DE)	Generation of new individuals via vector differential mutation	Continuous space global optimization	[122, 166, 167]
		NSGA-II	Multi-objective optimization via non-dominated sorting, crowding distance, and elitism	Solution of multi-objective optimization problems	[133, 168]
	Swarm Intelligence	PSO	Simulates collective behavior of bird flocks for information sharing	Fast convergence in continuous optimization	[65, 113, 166, 169, 170]
		ABC	Simulation of honeybee foraging division of labor and cooperation	Strong global search with delayed convergence	[73]
		Simulated Annealing (SA)	Probabilistic acceptance of suboptimal solutions with temperature scheduling	Escapes local optima in multimodal landscapes	[171]
		Quantum Annealing	Leverages quantum tunneling to bypass energy barriers	Tunneling effect enables rapid sampling from complex quantum probability distributions for efficient training of high-quality models	[171]

(Continues)

TABLE 3 | (Continued)

Category	Subclass	Algorithm	Fundamental principle	Function	Refs.
Probability Model-Based	Model-Based Sequential Optimization	Bayesian Optimization	Modeling of the objective function (e.g., using Gaussian Processes); sequential optimization guided by the surrogate model	Suitable for high-cost black-box functions and hyperparameter tuning	[138, 163]
	Sampling-Based Probability Distribution Update	Cross-Entropy Method (CEM)	Optimization of importance sampling density; re-estimation using elite samples	Significant reduction in computation required for estimating small probabilities	[172]
Physics-Based	Material Addition/Subtraction	Bidirectional Evolutionary Structural Optimization	Dynamic material distribution adjustment driven by objective and constraint functions	Performance enhancement; lightweight design; complex geometry adaptation; multi-scale compatibility	[139, 173]
	Physical Field Modeling	Level Set Method	Implicit definition of material distribution via a continuous level-set function	Direct boundary control; multi-parameter co-optimization	[174, 175]
Reinforcement Learning	Policy Gradient Methods	PPO	Clipped objective function and adaptive KL divergence penalty to limit policy changes	Enhanced training stability for high-dimensional, non-convex design spaces	[132]
	Q-Factor Optimization	Q-Learning	Stepwise Q-value error correction converging to the optimal policy	Global optimum exploration via stochastic policy using only reward signals; adaptation to dynamic complex scenarios	[140]

data-driven direct inverse design, and forward-inverse hybrid design. Beyond establishing mapping mechanisms from performance targets to structural parameters, these frameworks fundamentally differ in their typical failure modes, suitability under different data–physics regimes, and trade-offs among data efficiency, physical consistency, and computational scalability (Table 4). This section therefore not only elaborates on their core logic and implementation pathways but also critically compares their limitations and regime-dependent applicability, aiming to provide a decision-guiding framework for selecting appropriate strategies in practical engineering contexts.

2.4.1 | Topology Optimization based Inverse Design

Inverse design via topology optimization is a design methodology that inversely derives the optimal topological structure from target performance by adjusting material distribution and structural topological morphology [98, 162, 176, 177]. Its core lies in iteratively evolving to find optimal parameter designs through topology-evolved structures combined with physical models and optimization algorithms, as illustrated in Figure 3a. Topology optimization for inverse design is grounded in explicit physical formulations, establishing clear relationships between design and

TABLE 4 | Three commonly-used inverse design processes.

Inverse design strategy	Topology optimization based inverse design	Data-driven direct inverse design	Forward-inverse hybrid design
Core operational principle	Topology evolution-based structural optimization	Direct performance-to-parameter mapping	Alternating forward-inverse iterative optimization
Physical embedding mechanism (constraint formalism)	Explicit material distribution constraints (e.g., SIMP method)	Implicit data-driven constraints	Explicit physics-based constraints (e.g., FEM)
Functional role of machine learning	Auxiliary sensitivity analysis and structural generation	Core inverse solver	Optimization acceleration, performance prediction, parameter correction
Functional role of optimization algorithms	Structural distribution generation	Inverse solver optimization and optimal structure screening	Forward prediction model optimization and inverse generation model refinement
Characteristic outputs	Continuum topology configurations	Non-intuitive innovative configurations	Parametric geometric models

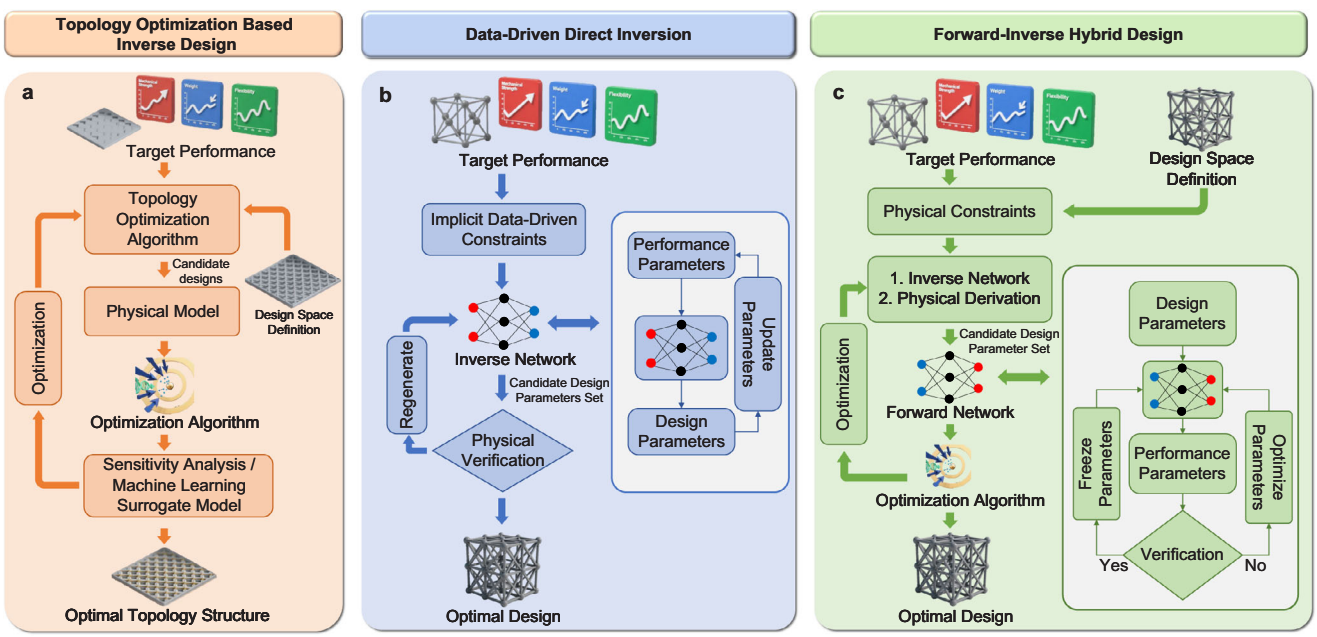

FIGURE 3 | Three inverse design processes. (a) The typical process of topology optimization based inverse design. (b) The typical process of data-driven direct inverse design. (c) The typical process of forward-inverse hybrid design.

distribution, thereby enabling precise inverse design. However, topology optimization typically suffers from high computational cost due to repeated large-scale numerical simulations, and its scalability becomes a limiting factor in high-resolution 3D or multi-physics coupled problems. Moreover, it is less suitable in regimes where governing physics is uncertain or where differentiable formulations are unavailable. For instance, Hammond et al. [178] employed photonic topology optimization for the inverse design of photonic devices. They imposed constraints on material properties using the Lorentz–Drude model and restricted the dielectric response of intermediate densities through material constitutive relations, ensuring physical consistency. Additionally, Han et al. [162] developed an inverse design framework based on the heat diffusion equation to generate 3D sequential metamaterials with extreme stiffness. By treating candidate microstructures as heat sources and adjusting the non-uniform thermal diffusion coefficient field, they generated dynamic temperature fields, from which continuous microstructure sequences were extracted via isothermal surfaces.

Machine learning serves as an acceleration tool in topology optimization inverse design to address efficiency bottlenecks in large-scale and high-complexity problems. While surrogate-assisted topology optimization improves computational

efficiency, approximation errors introduced by learned sensitivity models may accumulate during iterative updates, potentially leading to suboptimal or physically inconsistent solutions if not carefully validated. Chi et al. [179] integrated machine learning models into a general topology optimization framework, where a deep neural network (DNN) was trained to learn the mapping from design variables and coarse-network strain information to sensitivities, replacing traditional FEM-based sensitivity solutions. For the 3D cantilever beam design problem, the standard method took 25,455 s, while the ML framework required only 6,069 s. Furthermore, Kudela et al. [176] developed an inverse design approach integrating deep learning models with GA to optimize the topological configuration of phononic crystals. This method efficiently generated optimal geometries guided by target performance metrics, such as bandgap characteristics (Figure 4a). Numerous case studies demonstrate that the surrogate model significantly enhances design efficiency and consistently produces topologies with tailored bandgap properties. Another approach to enhancing efficiency in topology optimization via ML is directly establishing mappings between coarse and fine structures [180]. For instance, Napier et al. [180] employed an ANN to conduct topological optimization, where initial designs generated by conventional topology optimization algorithms were fed into a trained ANN model. Experiments showed that although compliance and volume errors increased slightly, this method saved approximately 85% of the time, reduced fuzzy transition layers, and produced clearer boundaries.

Machine learning can also directly generate structures [182] and expand datasets when data quantity or quality is insufficient [98]. This is because existing methods often fail to ensure complete boundary consistency of microstructures, leading to insufficient connectivity and compromised mechanical performance. Feng et al. [98] noted that even with data diversity expanded via shape perturbation and filtering, the dataset struggled to cover the full range of elastic moduli in microstructure design. They trained a diffusion model to generate high-quality novel samples and adjusted the dataset through active learning strategies, effectively enhancing the coverage of the elastic tensor space. The trained diffusion model produced microstructures with extremely high quality, achieving an R^2 of 0.994 and a boundary matching degree of 0.998 with target values.

2.4.2 | Data-Driven Direct Inverse Design

The core concept of a data-driven direct inverse design approach lies in constructing an end-to-end inverse solver that directly establishes a mapping from target performance to design parameters [73, 76, 115, 148]. Compared to forward-inverse hybrid approaches and topology optimization-based inverse design, this method avoid the need for time-consuming iterative optimization and numerical computations. However, this efficiency gain is achieved at the cost of heavy dependence on large, high-quality labeled datasets. In data-scarce or poorly characterized physical systems, purely data-driven inverse solvers may exhibit unstable generalization, mode collapse (in generative settings), or non-physical outputs. It operates on the premise that a sufficiently trained model can learn the intrinsic, complex mapping relationships from massive datasets and directly generate structures satisfying the target performance. Such a premise implicitly assumes adequate coverage of the design space; when extrapolation beyond the training distribution is required, direct inverse models often fail due to ill-posedness or non-uniqueness of the inverse mapping. The core workflow of this framework is illustrated in Figure 3b. The specific implementation methods primarily fall into three categories: direct mapping/supervised inversion, direct generation via generative models, and latent space optimization.

Direct Mapping/Supervised Inversion refers to using supervised learning algorithms to directly learn the mapping from performance to design. Once trained, the model can rapidly output design parameters based on performance requirements without intermediate optimization steps. For instance, Shi et al. [73] employed a combination of CNN, autoencoder, and optimized SVM to perform inverse design of metasurface structures. By leveraging the structure-performance correspondence within the dataset, the thoroughly trained model learned the intrinsic relationship between them, enabling direct generation of the metasurface structure matrix from target electromagnetic performance. CST simulations confirmed that its reflection coefficients closely matched the targets. Additionally, He et al. [148] developed and trained a neural network to directly generate metasurface structural parameters based on target properties. Testing showed the model could accurately produce the required arrangement radii within a target bandgap width range in just 0.05 s.

The direct generative modeling approach emphasizes the use of conditional generative models to produce designs from performance specifications. These models learn the distribution of the design space and generate novel, diverse design samples. This method is not only suitable for creative or exploratory tasks, but conditional generative models can also effectively incorporate performance constraints to create designs that meet requirements. For example, Bastek and Kochmann [76] addressed the lack of physical interpretability in direct mapping for metamaterial design. They innovatively employed a diffusion model to learn the mapping from a target stress-strain curve to the full-field stress distribution. The final structure satisfying the target nonlinear mechanical response was then extracted directly by analyzing the displacement field. This two-step process effectively functions as an inverse network for direct mapping (Figure 4b), likewise eliminating the need for explicit optimization or iterative tuning. Validation on 100 randomly generated designs showed a resulting response error of 6.98% in finite element verification.

Latent space optimization addresses the inherent limitations of generative models, such as incomplete representations and information loss in the latent space, by employing optimization algorithms to refine the design process. This approach involves three key steps: first, mapping designs to a low-dimensional latent space via generative models; second, performing optimization within this latent space using methods such as gradient descent, Bayesian optimization, evolutionary algorithms, or reinforcement learning; and finally, decoding the optimized latent representations into physical designs. For instance, Peng et al. [183] integrated a generative architecture design with a multi-objective active learning loop, forming a framework capable of generating microstructure materials with bone-matching elastic

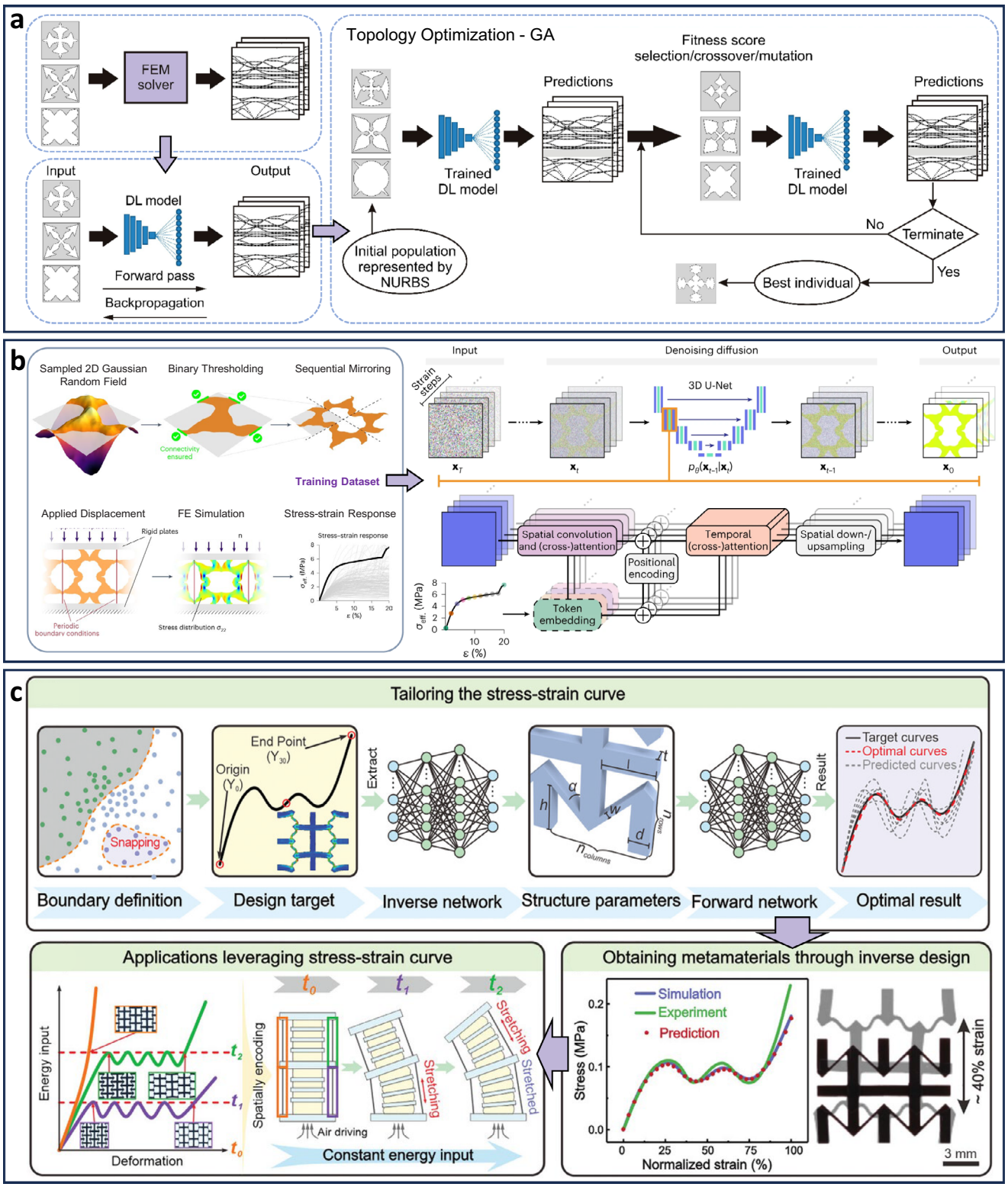

FIGURE 4 | Illustrations of three inverse design processes. (a) An inverse design framework integrating deep learning models with GA for optimizing the topology of phononic crystals. It involves using the FEM to acquire a labeled dataset, training a deep learning model, and subsequently coupling the trained model with a genetic algorithm for rapid topological optimization of phononic crystal structures (Reproduced with permission [176]. Copyright 2023, Elsevier.) (b) The process begins with dataset generation for model training, involving random sampling, mirroring, and FEM to obtain compressive strain data. A fully-trained diffusion model iteratively reconstructs a full-field stress distribution sequence from high-speed noise. The final binary structure is then extracted and directly output by analyzing the displacement field derived from the generated stress distribution (Reproduced with permission [76]. Copyright 2023, Springer Nature.) (c) A forward-inverse hybrid design framework. This approach first generates fracture-resistant mechanical metamaterials with ideal stress-strain curves via FEM-based machine learning, followed by a comparison and analysis of the simulated, experimental, and predicted stress-strain responses, and concludes with application-oriented experimental validation (Reproduced with permission [181]. Copyright 2024, Wiley-VCH).

modulus. The former employed a 3D convolutional autoencoder as the generative model, where an encoder mapped high-dimensional porosity matrices ($3 \times 3 \times 3$) into 8-dimensional latent vectors, and a decoder reconstructed the original porosity matrices from these vectors. The latter component performed multi-objective active learning optimization within the latent space, efficiently searching for design points that satisfy both constraints and optimization objectives while iteratively refining the model using FEM feedback. The optimized latent vectors were subsequently decoded into porosity matrices, which finally guided the geometric generation of Gyroid triply periodic minimal surface structures.

Notably, in the data-driven direct inverse design, both the efficiency and accuracy are largely determined by the performance of the inverse solver. This creates a fundamental trade-off: while data-driven direct inversion offers superior inference speed and scalability once trained, it sacrifices physical interpretability and may struggle in safety-critical or regulation-sensitive applications where explicit constraint satisfaction is mandatory. Therefore, its effective training becomes a critical step in this process. This primarily involves two aspects: one is how to optimize the inverse solver during training. For example, Shi et al. [73] used the Artificial Bee Colony (ABC) algorithm to automatically optimize the kernel parameters and penalty factors of the SVM during model training, effectively reducing errors caused by manual parameter tuning. The other aspect requires sufficient high-quality training datasets. For example, Gao et al. [115] established a comprehensive acoustic sink database (79,730 entries) within the 0–5 kHz frequency range using the transfer matrix method. The dataset was uniformly distributed and covered a broad range of acoustic performance. When inputting a 5,000-dimensional acoustic absorption curve into the model, it directly predicted the corresponding geometric parameters and the errors were all less than ± 0.2.

2.4.3 | Forward-Inverse Hybrid Design

The core logic of forward-inverse joint inverse design lies in the alternating iteration of forward prediction and inverse inference (Figure 3c), achieving closed-loop optimization between design parameters and target performance [97, 101, 141, 171, 181, 184, 185]. Distinct from traditional data-driven direct inverse design, this framework not only incorporates a forward performance prediction mechanism to guide structural updates but also integrates multiple machine learning strategies to enhance design efficiency and realizability. By explicitly retaining a forward validation loop, hybrid frameworks improve physical reliability and mitigate inverse non-uniqueness; however, they reintroduce iterative optimization overhead, resulting in intermediate computational cost between topology optimization and direct inversion. Based on this concept, current mainstream implementation pathways can be categorized into three types. These variants differ in their balance between gradient availability, model complexity, and exploration capability, making them suitable for different scales of design spaces and levels of physics knowledge. First, coupling forward surrogate models with external optimization algorithms or inverse models. Second, incorporating physics-informed and differentiable methods to enable end-to-end gradient propagation. Third, formulating the design process as a sequential decision-making problem and optimizing strategies through reinforcement learning.

The core of integrating forward surrogate models with inverse models or optimization methods lies in employing surrogate models (e.g., feedforward neural networks [10, 97, 101, 171, 181, 185], residual networks [8, 141], kernel ridge regression [184]) for rapid performance prediction, combined with inverse models (e.g., generative models) to produce optimal designs or optimization algorithms (e.g., genetic algorithms, Bayesian optimization) to search for optimal solutions. For example, Ha et al. [97] established a tandem framework of a forward neural network and an inverse generative network to design structural parameters that meet target stress-strain curves. The generative model generated candidate design parameters from the target curves, while the forward model replaced conventional simulations, enabling the mechanical behavior of candidate designs to be evaluated within seconds. Similarly, Chai et al. [181] established an ML pipeline comprising inverse and forward networks for inverse designing flexible mechanical metamaterials with specific stress-strain responses (Figure 4c). The inverse network generated multiple candidate parameters, and the forward network predicted their performances to select the optimal solution with minimal error, improving overall efficiency by 50%. Furthermore, the integration of forward surrogate models with optimization methods also demonstrates broad applicability. For example, Jin et al. [8] combined a forward prediction model (ResNet) with genetic algorithms for inverse designing complex 4D-printed structures. The forward model accurately mapped material distribution to structural deformation, enabling efficient iterative optimization via evolutionary algorithms. Additionally, Hossain et al. [186] employed a supervised learning model to establish interpretable mathematical relationships between the creep rupture of superalloys and key parameters such as stress, temperature, chemical composition, and stoichiometry. By further integrating an evolutionary algorithm, they inversely identified the optimal chemical compositions under given stress–temperature conditions, effectively enhancing the creep life of Alloy 617.

Physics-informed and differentiable approaches emphasize embedding physical principles or differentiable simulations into machine learning models to enhance physical consistency and optimization efficiency. Such methods are particularly advantageous in data-scarce yet physically well-understood systems, where governing equations are available but experimental data are limited. By transforming conventional "black-box" neural networks into physically interpretable "white-box" or "grey-box" frameworks, the entire optimization process becomes continuous and differentiable, enabling gradient-based optimization through backpropagation. This allows efficient computation of gradients of loss functions with respect to design parameters. For high-dimensional design spaces, gradient-based optimization algorithms significantly outperform gradient-free methods in computational efficiency. Nevertheless, their performance deteriorates when governing equations are incomplete, highly stiff, or computationally expensive to differentiate, limiting applicability in poorly characterized or strongly discontinuous systems. Besides, conventional PINNs often struggle with convergence due to data biases, particularly

in photonic material design. To address this, the Multiscale Physics-Informed Neural Network (MscalePINN) has been introduced, offering enhanced capability in capturing multiscale information. For instance, Rigant et al. [187] successfully employed MscalePINN as a solver, where multiple sub-networks processed input signals at different frequencies. This approach accurately and efficiently reconstructed the effective permittivity distribution, thereby advancing the design of photonic materials with disordered ensemble structures.

Sequential decision-based methods typically employ reinforcement learning to dynamically adjust design parameters through environmental interaction, enabling effective solutions for multi-objective trade-offs and dynamic optimization. This approach constitutes a stepwise decision-making process rather than a one-shot mapping or optimization. Within this framework, the design object is treated as an "environment," modifications to design parameters are regarded as "actions," and environmental feedback provides "rewards" to evaluate design performance. While reinforcement learning excels in sequential and multi-objective decision problems, it typically requires extensive exploration and large numbers of environment interactions, making it computationally expensive and potentially unstable in high-dimensional continuous design spaces. The ultimate goal is for the agent to learn a policy that maximizes cumulative rewards through multi-step decisions. For instance, Li et al. [132] integrated the DQN and PPO algorithms, optimizing the Q–factor via a reward function, ultimately designing a photonic crystal laser cavity whose performance surpassed that achieved by human expert manual optimization by nearly four times.

3 | Adaptive Strategies of Inverse Design

In Section 2, we review the evolution of inverse design technologies and summarize the machine models, methodologies, optimization algorithms, and mainstream strategies employed in inverse design. Subsequently, we discuss the selection criteria for appropriate models and optimization methods under varying conditions, with a focus on addressing challenges such as limited data availability and high-dimensional parameter spaces. By synthesizing commonly used approaches, we aim to provide readers with practical design insights and solutions (Figure 5).

3.1 | Sufficient Data with Low-Dimensional Parameters

When sufficient and well-distributed data are available alongside a low-dimensional parametric structure of the design target, the inverse network can be adequately trained to enhance model complexity and generate precise design parameters. For instance, in acoustics research, Zhang et al. [142] trained a multilayer ANN inverse model using a dataset of 20,000 structure-acoustic performance pairs. Although the parameter dimensionality was not extremely low, the training set comprehensively covered diverse parameter combinations. The well-trained inverse model generated 500 structural designs in only 4 s. Moreover, the extensive data improved the model's extrapolation capability: even when tested beyond the training domain, it maintained high predictive accuracy (with 99.6% of samples achieving MSE < 0.0001) and spontaneously generated designs with superior performance.

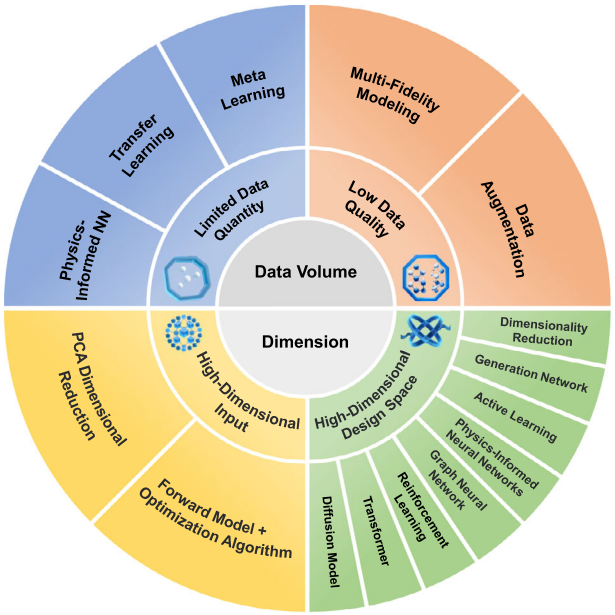

FIGURE 5 | Problems encountered in inverse design and the corresponding solutions.

3.2 | Scarcity in Data Volume

In ML-based inverse design, two common scenarios of data scarcity are often encountered: insufficiency in data quantity and deficiencies in data quality. Insufficient data quantity primarily refers to an inadequate total number of samples for model training or a shortage of data samples in the target domain. On the other hand, deficiencies in data quality pertain to issues in the accuracy, completeness, or signal-to-noise ratio of existing data-such as excessive noise, mislabeling, or incomplete key feature information, which results in a scarcity of high-fidelity data. Another manifestation of poor data quality is low diversity, characterized by homogeneous data. Currently, in ML-driven inverse design, several strategies can effectively address these challenges (Figure 6). In the following sections, we will delve into these strategies in detail.

3.2.1 | Limited Data Quantity

In practical research, data scarcity is a common challenge, including insufficient data in the target domain and a lack of labeled data. The issue of limited data in the target domain arises from difficulties in real-world data acquisition, which compromises the generalization ability of trained models in the target domain. Regarding data labeling, the need for time-consuming and costly numerical simulations to annotate large-scale unlabeled data has motivated research into training effective models with reduced reliance on labeled data. In such data-scarce scenarios, meta-learning, transfer learning, and physics-informed neural networks have been employed to address these challenges (Figure 6).

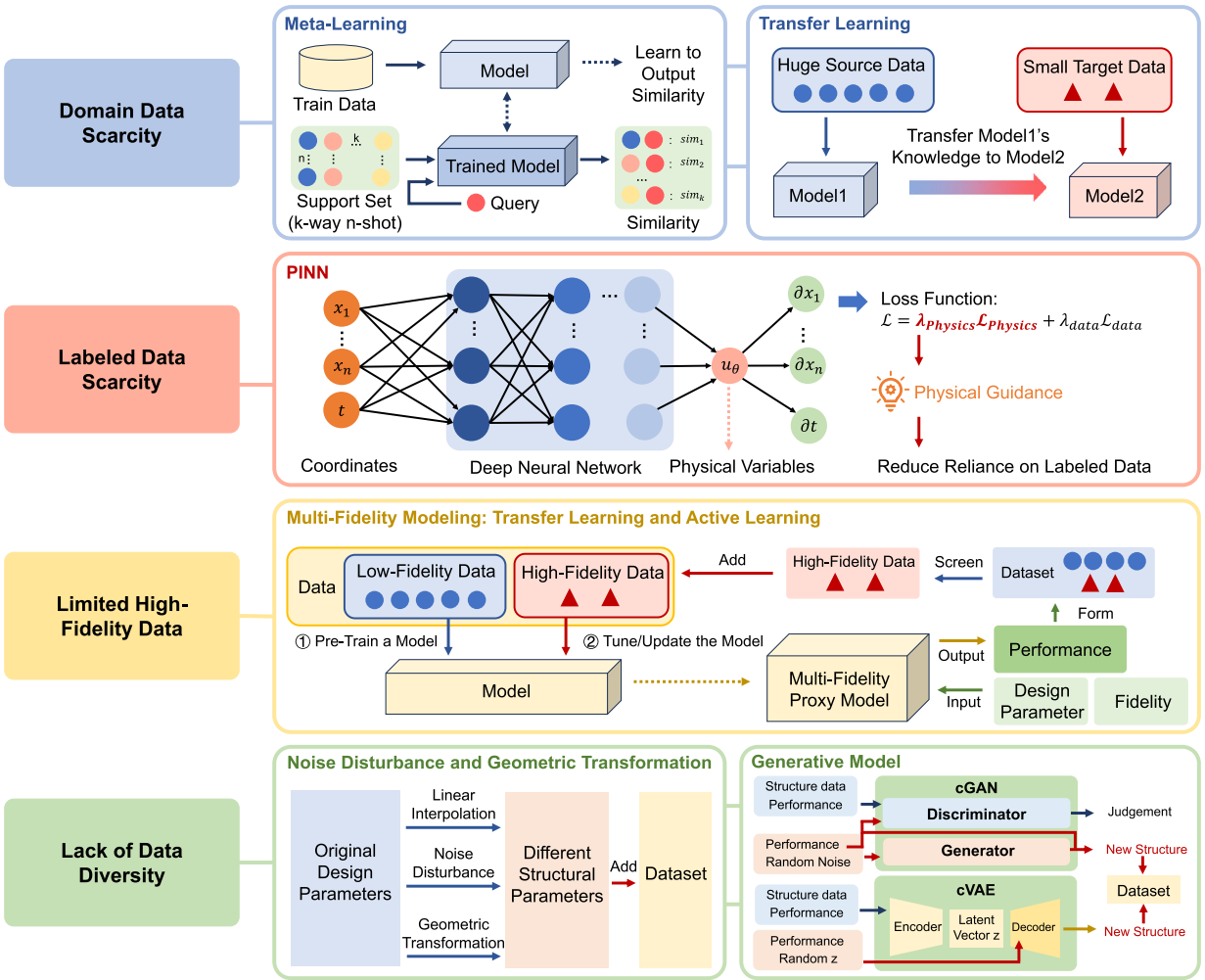

FIGURE 6 | The blue and red regions correspond to the two scenarios of insufficient data quantity and their respective resolution strategies. When data in the target domain is scarce, meta-learning and transfer learning can be employed; whereas for limited labeled data, PINNs offer a viable solution. The yellow and green areas represent the two manifestations of deficient data quality and corresponding mitigation approaches. In cases where high-fidelity data is insufficient, multi-fidelity modeling serves as an effective strategy; for inadequate data coverage, data augmentation techniques—including noise injection, geometric transformations, and generative models—can be applied.

3.2.1.1 | Meta-Learning. Meta-learning involves acquiring cross-task general knowledge from multiple related tasks, with the core objective of enabling models to learn the "method of learning" from data, thereby enhancing learning efficiency and adaptability to new tasks. As Figure 6 illustrated, the objective of meta-learning is to acquire a universal "similarity comparison" or "rapid adaptation" mechanism. When classifying new tasks, the model can effectively process them with limited samples by leveraging previously acquired methodological principles. In essence, meta-learning optimizes the model's "adaptation process" rather than directly transferring specific knowledge [188]. Morrison and Ma [143] investigated the tuning effects of meta-learning on machine learning optimizers for nanophotonic inverse design tasks. Their meta-learning strategy aimed to enable optimizers to learn how to adjust hyperparameters (e.g., learning rate) during iterations to better address the current task. After systematically comparing 24 optimizers, they found that meta-learning significantly improved performance for specific optimizers: AdaGrad and RMSProp showed an average desired performance improvement of 0.05–0.1 in mode separators and 0.1–0.2 in wavelength multiplexer, approaching the level of Adam. In the context of small sample sizes, Ma et al. [189] proposed an inverse design approach for composite materials incorporating meta-learning strategies, which optimized the dielectric properties of additive-manufactured polymer composites by integrating material composition, structural design, and process parameters. The study combined theoretical models with machine learning (few-shot learning combined with model-agnostic meta-learning algorithm) to achieve precise predictions of dielectric constant and loss tangent. By leveraging meta-learning to initialize model parameters, the approach enabled the model to rapidly adapt to new structure-process combinations within 5–10 samples per task. The model demonstrated strong generalization capability on the test set, achieving an R^2 of 0.986 for dielectric constant and 0.976 for loss tangent.

3.2.1.2 | Transfer Learning. Unlike meta-learning, transfer learning addresses the issue of insufficient data in the target domain by leveraging knowledge from the source domain [144]. As Figure 6 illustrated, transferring the parameters from the source model (Model 1), obtained by solving the source task, into the target model (Model 2) makes it possible to effectively

address the target task without requiring extensive data. Currently, transfer learning has emerged as a new framework in deep learning-based machine learning [104, 144, 149, 152, 153, 163], enabling pre-trained models to share experiences and parameters with new tasks, thus eliminating the need for extensive retraining with massive additional data. Zhu et al. [149] highlighted that traditional deep learning methods require enormous datasets to achieve high accuracy in meta-atom phase prediction tasks; otherwise, models severely overfit, with accuracy remaining around only 10%. They employed a transfer learning strategy using a pre-trained GoogLeNet-Inception-V3 model, drastically reducing data requirements (from the conventional tens of millions to 20,000) to directly establish an accurate mapping from phase distributions to metasurface structural parameters. Given a desired 2D phase profile, this approach automatically generated the entire pattern of functional metasurfaces rapidly, achieving an accuracy of 89%. In the optical field, where data collection for optical materials is costly, transfer learning strategies are widely adopted [104, 144, 163]. Dong et al. [163], when inversely designing composite metal oxide optical materials, noted that certain element groups in their database had only 51 samples. They transferred the parameters of a fully trained model1 to an architecturally identical model2, then fine-tuned the parameters by continuing training on the small dataset specific to the target elemental combination. This adapted the model2 to the characteristics of the target domain. Experiments demonstrated that the model using transfer learning ($R^2 = 0.9947$) demonstrated superior performance compared to the model without transfer learning ($R^2 = 0.9295$).

3.2.1.3 | PINNs. To address the issue of insufficient labeled data, another approach is to explicitly incorporate physical equations to reduce reliance on them. In data-scarce but physically well-understood systems, physics-constrained optimization may be more suitable than purely data-driven models. By integrating governing equations into the learning process, models do not need to infer fundamental physical laws from limited data but instead inherit a feasible solution space defined by established theoretical principles (Figure 6). Furthermore, when reliable governing equations are available, physical models themselves can serve as high-fidelity simulators to generate synthetic or pseudo-labeled data, thereby alleviating data scarcity while enhancing interpretability and convergence stability [35, 154–156, 190]. Wiecha et al. [35] pointed out that PINNs is a deep learning approach that solves PDEs by directly embedding physical equations into the loss function. Unlike traditional data-driven neural networks, PINNs do not require pre-generated large-scale training datasets. Instead, they are trained under constraints imposed by physical equations (such as the Helmholtz equation or wave equation), enabling high-precision modeling even with limited data. For example, in the design of optical invisibility cloaks [154], the network optimizes the dielectric permittivity distribution to satisfy the wave equation solutions under specific boundary conditions. Lu et al.'s [156] hard-constraint PINNs eliminated the need for massive datasets generated by traditional numerical solvers. By directly embedding physical equations (e.g., PDE residuals, volume constraints) as loss functions during training, hard-constraint PINNs demonstrated performance comparable to traditional numerical methods. In their optical holography experiments for light field distribution, without relying on labeled data, the optimized objective values ranged from 0.0517 to 0.0528, with losses reduced to the order of 10^{-5}.

3.2.2 | Low Data Quality

Another manifestation of data inadequacy lies in quality deficits, characterized by a lack of high-fidelity data and insufficient data diversity. Regarding data accuracy, high-precision data are typically obtained from high-accuracy experimental instruments or high-fidelity numerical simulations, whereas low-fidelity data often originate from historical databases or rapid approximate models. These two types of data exhibit systematic deviations. The research challenge stems from the high cost associated with acquiring high-fidelity data [149], making the effective utilization of low-fidelity data crucial. In terms of inadequate data coverage, trained models tend to exhibit limited generalization capability [191] and poor extrapolation performance [192], which represents a critical issue that must be addressed. In such data quality-constrained scenarios, multi-fidelity modeling and data augmentation strategies have been employed to mitigate and resolve these challenges (Figure 6).

3.2.2.1 | Multi-Fidelity Modeling Approaches. Multi-fidelity modeling, a technique commonly used to handle heterogeneous data, aims to reduce computational costs and enhance model performance through collaborative optimization of low-cost low-fidelity data and high-accuracy high-fidelity data. This method typically employs multi-fidelity models combined with transfer learning and active learning strategies in the design workflow (Figure 6). Specifically, the low-fidelity model is used to perform a global exploration of the entire design space, quickly screening multiple promising candidate designs. Subsequently, the high-fidelity model is activated only in the vicinity of these promising candidates for local refinement and validation. In fields characterized by complex microstructures, such as lattice material design and photonic material design, high-fidelity simulations are often time-consuming and expensive, whereas low-fidelity models can be trained rapidly. Multi-fidelity modeling thus effectively addresses the scarcity of high-fidelity data relative to the abundance of low-fidelity data. For example, Grbčić et al. [166] adopted a multi-fidelity ensemble framework for the inverse design of photonic surfaces, which incorporated a low-fidelity model for rapid screening of the potential solution space and a high-fidelity model for fine optimization in promising regions. This integrated approach not only significantly reduces the overall computational burden but also demonstrates superior performance in terms of both root mean square error (RMSE) and design novelty compared to single-fidelity models and deep learning generative models.

3.2.2.2 | Data Augmentation. Physics-based numerical simulations provide an effective approach for dataset expansion. Table 1 summarizes common numerical calculation methods, among which FDTD, FEM, and FIT are most widely applied in inverse design. These methods have been integrated into professional simulation tools, including multi-physics platforms (COMSOL Multiphysics, ANSYS), electromagnetic simulation tools (Lumerical FDTD, CST Studio Suite), and structural analysis software (Abaqus, LS-DYNA) [130, 149]. Although simulation tools can effectively compensate for the shortage of

experimental data, they suffer from high computational costs and time consumption, often failing to fully cover the design space and carrying risks of discrepancies with experimental results. To enhance data generation efficiency, data augmentation methods are required, including generating new data through noise perturbation and geometric transformation based on existing datasets; using generative models to create targeted new data consistent with physical laws; and applying active learning to select the most informative data points.

In machine learning, noise perturbation refers to a technique that generates new samples with statistical variability by adding random perturbations to original data. This technique essentially simulates real-world phenomena such as sensor errors, illumination fluctuations, or environmental disturbances through controlled random corruption [193]. Geometric transformations generate new samples with variations in viewpoint, pose, or scale by applying affine or non-rigid deformations to the spatial structure of data [181, 194]. It simulates physical phenomena like changes in observation angle or object deformation. For instance, in clinical chest X-ray image processing [195], moderate geometric variations efficiently simulate clinically plausible minor positioning or equipment angle deviations, yielding new image data. Images are common data in topology optimization design. Regarding image data augmentation, Wang et al. [193] categorized three modes: individual, multiple, and population augmentation. In material design, individual augmentation is predominantly employed, modifying pixel values or spatial structures through techniques such as pixel erasure and geometric transformations. For instance, in the inverse design of 2D compliant mechanisms, Forte et al. [194] employed geometric transformations for individual augmentation. The initial samples generated via FEM were augmented through rotation and mirroring, resulting in 180,000 data points. The neural network trained on this augmented data achieves 89.2% binary design accuracy in testing.

However, conventional noise perturbation and geometric transformation techniques exhibit limitations. Simple noise addition and transformations often fail to capture the complex data distribution of real-world tasks or introduce novel information and intricate features. Generative networks offer distinct advantages in addressing these issues. Specifically, conditional generative networks-such as cGANs [100, 120, 121, 196, 197] and cVAEs [118, 197]-not only synthesize novel samples but also generate samples with specific attributes while ensuring authenticity (Figure 6). Jain et al. proposed three GAN variants [100]: deep convolutional GAN, auxiliary classifier GAN, and information-theoretic GAN. Utilizing auxiliary classifier GAN with class labels, they generated synthetic images labeled with six surface defect categories (e.g., inclusions, scratches), expanding the training set from 5,400 to 9,000 images. A CNN classifier trained on this augmented dataset achieves 92.78% accuracy, significantly outperforming one trained using traditional geometric augmentation (90.28%). To address the time-intensive nature of super-resolution fluorescence microscopy and limited observable polydisperse nanoparticles, Azad et al. [118] proposed selecting representative samples and training a deep generative model (cVAE). By incorporating temperature conditions into the latent space, their model generated microgel samples at arbitrary temperatures, covering ranges beyond the original experiments or supplementing statistical data. Extensive experimental evaluation confirmed that the generated microgel samples closely match actual data, and demonstrating extrapolation capability.

Generative models represent a viable choice when dealing with insufficient quantities of both existing and novel samples. However, for scenarios characterized by a large volume of samples with inadequate quality (i.e., heterogeneous information content), active learning strategies emerge as a superior solution [165, 198]. The core principle of active learning involves researchers predicting sample performance through simulations or forward predictive neural networks, followed by screening high-quality samples to augment the training dataset. Currently, active learning strategies are primarily categorized into three types: the pool-based scenario, stream-based scenario, and query synthesis scenario. In the pool-based scenario, specific strategies such as uncertainty sampling or diversity sampling are employed to select the most informative samples from an unlabeled data pool for annotation requests. The stream-based scenario involves data input as a continuous stream, where the model must make immediate decisions on whether to request annotation for each incoming sample, typically based on predefined thresholds to assess informativeness. In the query synthesis scenario, although an unlabeled data pool is also provided, the active learning strategy does not select samples from this pool for querying; instead, it generates new samples autonomously for annotation.

Kim et al. [165] proposed a materials design framework based on the query synthesis approach, leveraging GA and the forward-predictive capability of DNNs for data augmentation. Their method employed a hyper-heuristic GA to generate approximately 4×10^4 candidate microstructures. The optimal candidates were selected and replicated to form an augmented dataset. Experimental results demonstrated that under this active learning framework, adding only 366 new stiffness data points and 424 new strength data points sufficed to approach the global optimum. The optimized composite stiffness neared the theoretical limit.

3.3 | High-Dimensional Scenarios

In ML-based inverse design, two distinct high-dimensional scenarios are frequently encountered: high-dimensional inputs and high-dimensional design spaces. The distinction between them lies in that the former refers to the complexity of input data dimensions, whereas the latter denotes the complexity of parameters to be designed. Although both involve high-dimensional problems, their focal points differ: the former emphasizes the complexity of input features, with challenges primarily centered on enhancing model robustness and computational efficiency; the latter highlights the high dimensionality of design degrees of freedom, with difficulties arising from efficiently exploring optimal parameters.

3.3.1 | High-Dimensional Input

With the increasing complexity of requirements, researchers need to encode material or structural features/properties into high-dimensional vectors (such as composition, lattice parameters, topological characteristics, etc.) as inputs. However, these

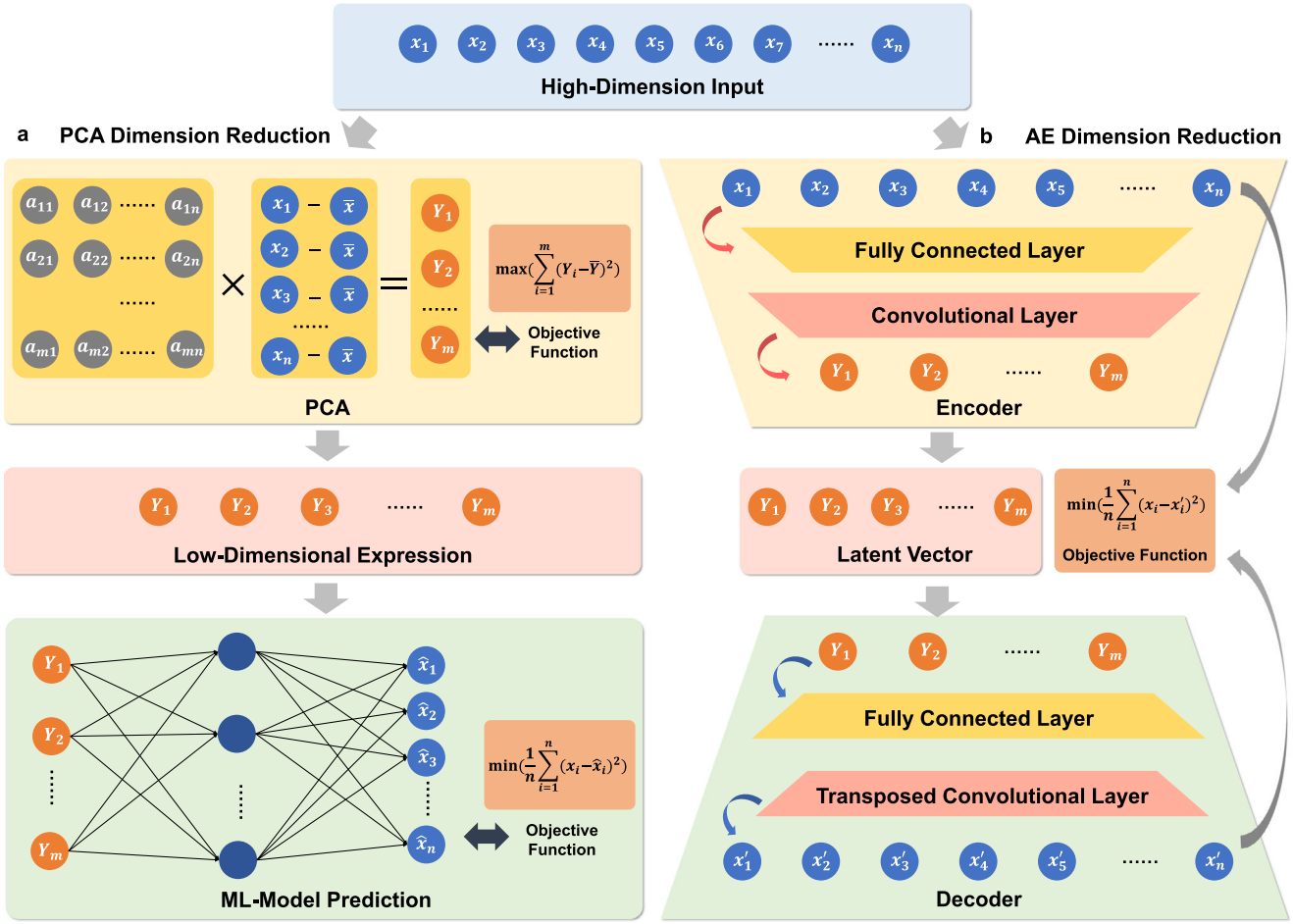

FIGURE 7 | A schematic illustration of dimensionality reduction for high-dimension input data using either PCA or an AE. (a) PCA-based dimension reduction for high-dimensional input data requires optimization guided by the objective function. (b) Dimension reduction of high-dimensional input data is achieved through AE.

high-dimensional inputs are often intractable, thus necessitating dimensionality reduction processing. Here, we summarize two dimensionality reduction techniques—principal component analysis (PCA) and Autoencoder (AE)—both of which effectively reduce data dimensionality and mitigate complexity while preserving essential information (Figure 7). Forward models, in contrast, do not face challenges with high-dimensional inputs during training: even when the dimension of design variables (inputs) far exceeds that of performance (outputs), a sufficiently trained forward model can still respond quickly.

3.3.1.1 | PCA Dimension Reduction. The core idea of PCA is to project the original high-dimensional data onto a new set of mutually orthogonal low-dimensional coordinate axes through a linear transformation [199]. By sorting eigenvalues in descending order and selecting the top principal components based on cumulative variance contribution ratio, the original data can be projected onto these selected components to obtain a low-dimensional representation, thereby achieving dimension reduction (Figure 7a). In inverse design, PCA enables data compression and simplification, effectively preserving the primary characteristics of the data, and plays a crucial role in handling high-dimensional input parameters. For example, in the work by Zhou et al. [200] on the inverse design of bulk metallic glasses using unsupervised generative models, supervised evaluation was incorporated to assess the glass-forming ability of the generated compositions-a strategy termed forward-inverse combined inverse design. Within this forward supervised evaluation framework, PCA and kernel smoothing function estimation were employed to visualize the distributions of both the original and generated data. The Wasserstein distance was then used to quantify the discrepancy between these distributions. Specifically, PCA effectively reduced the high-dimensional original literature data and generated data to a two-dimensional space, which not only facilitated clear visualization but also enabled robust quantitative assessment. Further, Wang et al. [125] applied PCA for dimensionality reduction on high-dimensional inputs while using diffusion models for the inverse design of energy-absorbing metamaterial microstructures. They successfully reduced the number of principal components from nearly 100 to 15, while still covering 99.98% of the variance. As a classical dimensionality reduction technique, PCA played a pivotal role in inverse design by effectively addressing the complexities arising from high-dimensional parameter inputs. It operated by projecting the original high-dimensional data into a lower-dimensional space through a linear transformation, thereby preserving the dominant data characteristics and significantly enhancing both the computational efficiency and predictive accuracy of the model.

3.3.1.2 | AE Dimension Reduction. AE and its variants (VAE, cVAE) can reduce the dimensionality of high-dimensional design parameters through their special encoder-decoder architectures (Figure 7b). For example, in the inverse design of metasurfaces, Naseri et al. [113] utilized a VAE to compress high-dimensional metasurface physical structures (such as scatterer shapes and interlayer coupling parameters) into a low-dimensional continuous latent space (8 dimensions). Within this latent space, PSO was employed to find the optimal latent variables. The optimized latent variables were then converted into physical structures via the decoder, outputting parameters such as scatterer shapes and interlayer dielectric thicknesses to obtain the physical design of the optimal electromagnetic metasurface.

Subsequently, researchers integrated conditional control into VAEs, using target properties as conditional variables fed alongside input data into the encoder and decoder. This enables finer control over the generation process [113, 157, 158, 164, 201–203]. For example, Tang et al. [201] proposed an adversarial conditional VAE (A-cVAE) model for inverse design of nanophotonic devices. Their model mapped the 400-dimensional parameter space of the device into a low-dimensional latent space via CVAE. By sampling latent variables and combining adversarial training with active learning, it generated novel designs achieving an average figure of merit of 0.901. In a similar vein, some studies have further extended VAE applications across domains. In absorber design, Li et al. [157] developed an enhanced cVAE for metamaterial absorber inverse design. Their encoder utilized 1D convolutional layers and residual blocks to extract local features from absorption spectra, sampling a 20-dimensional latent variable. The decoder reconstructed absorption spectra via fully connected layers and nonlinear activation, achieving high consistency between fabricated prototypes and simulations.

3.3.1.3 | Forward Model-Guided Optimization. Current research has explored inverse design using forward models with high-dimensional inputs [204, 205]. When the input dimension is much higher than the output dimension, forward models can still train reliable mapping relationships, though they face challenges in optimizing network parameters. The use of appropriate algorithms, such as backpropagation, can significantly enhance the efficiency of parameter optimization. In nanophotonic inverse design, when the number of parameters increases (e.g., involving 5 to 10 dielectric layers), traditional numerical optimization methods (such as interior-point methods) are prone to local minima and exhibit exponentially increasing computational complexity. To address this, Peurifoy et al. [204] directly trained a fully connected feedforward neural network to learn the complex mapping between the thickness of each shell layer in 8-layer shell nanophotons and their scattering spectra. The network took layer thicknesses as inputs and outputted candidate scattering spectra in the 400–800 wavelength range. Backpropagation algorithm was used to optimize input parameters until the minimum error with the target spectrum was achieved, solving the complex nonlinear mapping problem in nanophotonics.

3.3.2 | High-Dimensional Design Space

For complex inverse design problems, the challenge lies in the huge design space, which may involve continuous distributions of material compositions or topological diversity of structures (Figure 8: blue part). However, the information in initial training datasets often fails to encompass the input-output relationships across the entire design space. Even with sufficient experimental data, under increasingly complex experimental conditions, model complexity far exceeds data volume, leading to sparse data representation. For example, in chemistry, datasets typically range from tens of thousands to hundreds of thousands, yet they still fail to cover the enormous chemical design space [135]. The model is unable to adequately capture underlying patterns. It only remembers the noise in the training set or specific samples, but has extremely poor generalization ability for the performance of new targets. Methods employing forward modeling networks for inverse design also face certain issues: as demands grow more complex, the parameters of fully connected networks increase dramatically [10]. Therefore, addressing high-dimensional design spaces hinges on improving search efficiency, narrowing the search scope, and efficiently approximating target performance. In this section, we summarize several approaches (Figure 8), such as leveraging advanced optimization algorithms (e.g., NSGA-II) and utilizing active learning to enhance data coverage. Additionally, advanced neural network models, including GNNs, Diffusion Models, and Transfer Models, can effectively tackle complex high-dimensional design challenges.

3.3.2.1 | A Combined Generative-Predictive-Optimization Framework. As mentioned in Section 2.4.3, the forward-inverse hybrid design framework is now widely applied. Specifically, it establishes a closed-loop process of generation-prediction-optimization-feedback-regeneration. This enables the search to actively and adaptively focus on promising regions rather than relying on passive random trials. Moreover, the generative network can inherently embed fundamental physical constraints and symmetries, ensuring the physical feasibility of proposed designs. Thus, this framework is particularly suitable for complex problems within high-dimensional design spaces. Early on, facing the multi-component combinatorial space on the order of 10^{13} in inorganic material design, Dan et al. [135] proposed a model assisted by Wasserstein GANs (WGAN) and AEs. By integrating Adam optimization with the forward model ElemNet to predict the formation energy and bandgap of generated materials, this approach efficiently produced a large number of valid and novel samples. Experiments demonstrated that the chemical validity of the generated samples is 77 times higher than that of enumeration methods, with a novelty rate of 92.53% among 2 million generated samples. Based on the combination of the forward-inverse hybrid model and an optimization algorithm with extensive search performance, high-dimensional design space problems can be handled more effectively. Brzin and Brojan [124] tackled the large design space encompassing material, geometric, and actuation parameters for the inverse design of soft, deformable composite beams. They employed a GAN architecture combined with a forward simulator network, RMSprop optimization, and a joint loss function. This framework achieves RMSE between the deformed beams and target shapes (e.g., circle, wave) ranging from 0.65×10^{-3} to 6.47×10^{-3} mm^{-1}. Generating 10,000 design parameter sets required only 0.8 s.

3.3.2.2 | Active Learning Strategy. As previously noted, active learning strategies enhance dataset quality by proactively

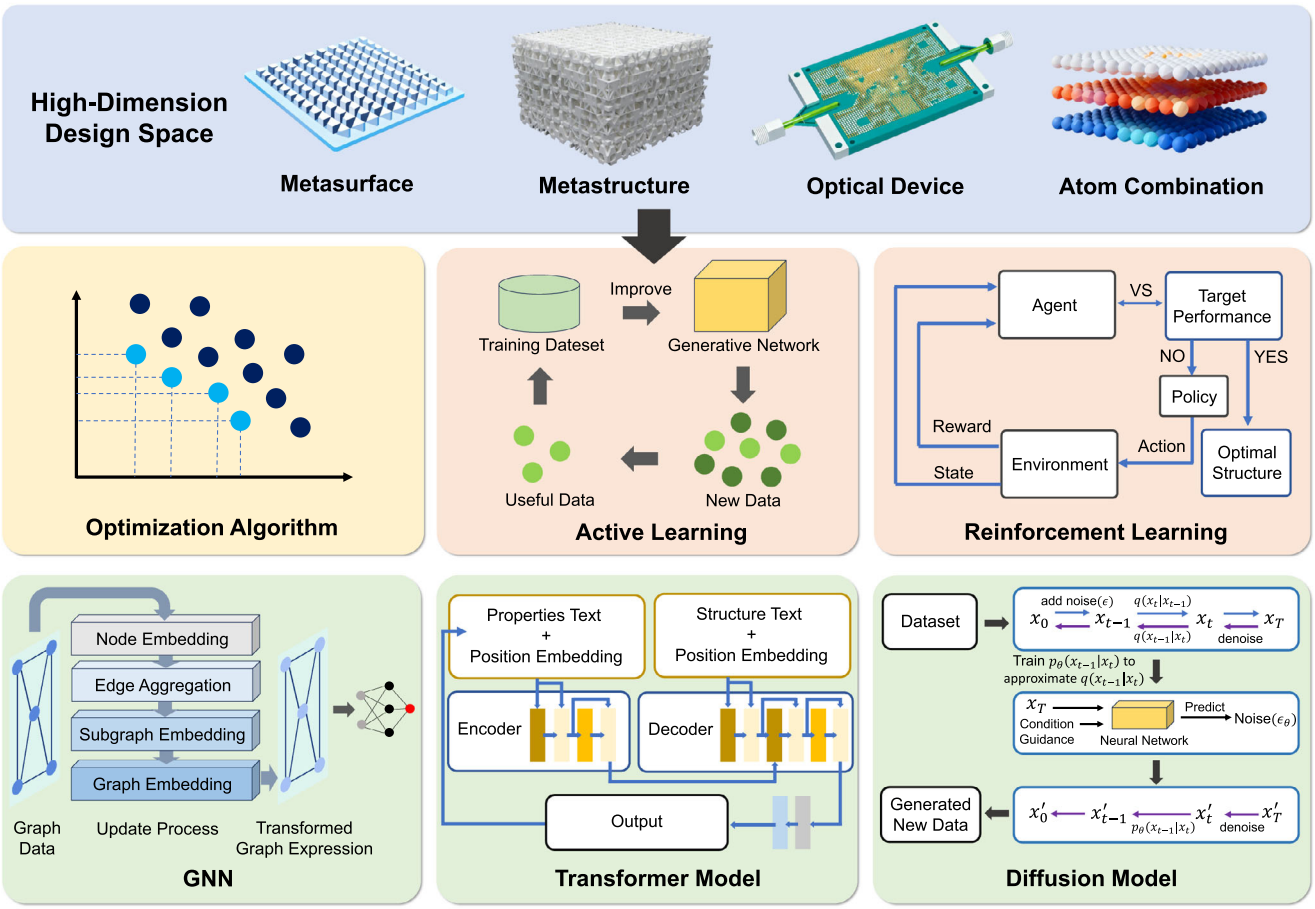

FIGURE 8 | Complex problems, such as those involving metasurface, metastructure, nano-optical device, and material atomic combination, often present challenges due to high dimension. These challenges can be effectively mitigated by employing optimization algorithms (e.g., NSGA-II), strategies like active and reinforcement learning, as well as models including GNN, Transformer model, and Diffusion model.

selecting high-value samples for annotation, primarily aimed at addressing the cost and time constraints of labeling training data within high-dimensional design spaces. For inverse design in such spaces, a third active learning approach involves generating samples via a generative network, subsequently filtering high-performance candidates from this pool. These selected samples are incorporated into subsequent training rounds (Figure 8), overcoming conventional data limitations and improving model generalization [103, 122, 201]. Nanophotonics exemplifies a field characterized by a high-dimensional design space. Early work by Tang et al. [201] highlighted the need for extensive training data when using cVAE for inverse design of nanopatterned integrated photonic devices. Traditional methods like Direct Binary Search yielded limited optimized data, insufficient for complex geometric parameters and broad optical responses, prompting their adoption of active learning. Their initial A-cVAE, trained on 15,000 samples, generated 1,000 continuous-variable hole-size patterns. High-performance samples were selected and added to the training set (totaling 16,000 samples), boosting model performance. Results showed the figure of merit improved from 0.888 (A-cVAE without active learning) to 0.901 (A-cVAE with active learning). Singh et al. [122] proposed an active learning-based framework to address the large-scale design space problem in nanophotonics. By iteratively labeling and expanding the training dataset, they trained models for subsequent inverse design. The experimental results showed that the model trained on the actively sampled dataset (44,000 samples) achieves a mean squared error (MSE) of 0.007 on a test set of 20,000 samples, which is significantly lower than the MSE of 0.011 obtained by the model trained on a randomly sampled dataset (200,000 samples).

3.3.2.3 | PINNs. As previously mentioned, PINNs reduce reliance on extensive labeled data by embedding physical laws. Concurrently, physical constraints decompose high-dimensional spaces into physics-governed low-dimensional manifolds or, combined with governing differential equations, provide directional guidance for the optimization process. These mechanisms enhance the feasibility of inverse design by stabilizing training within high-dimensional parameter spaces, narrowing the search domain, and preventing physically meaningless solutions [156, 206]. In metasurface design research, Xu et al. [206] also developed a physics-informed inverse design method for multi-bit programmable terahertz metasurfaces. Physics-guided learning first trained a residual MLP to establish a forward mapping from geometric to modal parameters, achieving convergence 2.5 times faster than conventional MLPs in high-dimensional parameter space. By incorporating physical constraints (e.g., periodicity and liquid crystal layer thickness) into the loss function, 500 high-quality candidate structures were generated within 10 s. Comparative MSE analysis demonstrated that the

physics-informed inverse design method achieves over a 50% reduction in error compared to a physics-agnostic Residual MLP.

3.3.2.4 | GNN. GNNs, with their efficient search performance and targeted search capabilities, are also well-suited for this high-dimensional design scenario. It models materials or structures as graph representations based on topological relationships (e.g., lattice structures), and updates graph data through a hierarchical abstraction process from local to global scales, effectively capturing both local and global features to facilitate subsequent predictive classification (Figure 8). For example, addressing the challenge of the enormous atomic configuration space in glass materials due to the disorder and high complexity of their amorphous structures, Wang and Zhang [116] used GNNs to directly target plastic resistance, screening for metastable structures with superior performance. This "performance-oriented" strategy avoided ineffective searches on irrelevant configurations, significantly narrowing the design space to be explored. Experiments demonstrated that the strong predictive performance of GNNs greatly enhances generalization ability, maintaining high accuracy (0.741) across different quenching rates.

3.3.2.5 | Reinforcement Learning. Reinforcement learning interacts directly with simulation environments to explore high-dimensional parameter spaces without requiring pre-training data. As the strategy learns from rewards obtained by executing specific actions in certain states (Figure 8), decisions are made in sequence using the Markov decision process. Li et al. [132] dynamically explored optimal solutions within the high-dimensional design space of photonic crystal laser cavities using deep RL (combining DQN and PPO algorithms). The DQN and PPO algorithms proved highly efficient for high-dimensional space exploration. DQN enhanced stability and avoided relearning through "experience replay", while PPO prevented training divergence by limiting the magnitude of policy updates. Through multiple training rounds, the policy network gradually optimized the design parameters. Results demonstrated that after 152 hours of training (versus 1.5 months for human experts), the designed long nanocavity achieves a Q-factor of 5.04×10^7. This represented a 17-fold improvement over the initial value and was nearly four times higher than the result (1.3×10^7) achieved through manual optimization by human experts.

3.3.2.6 | Transformer Model. The Transformer model, initially proposed by Vaswani et al. [207], abandons conventional recurrent and CNNs. It employs self-attention and multi-head attention mechanisms to achieve efficient parallel computation and long-range dependency modeling. In high-dimensional inverse design spaces, Transformers leverage encoder-decoder architectures with attention mechanisms to effectively address complex structural parameters through structured sequence representation, enhanced attention mechanisms, flexible architectural design, and efficient training strategies (Figure 8). This approach has established Transformers as state-of-the-art frameworks for inverse design in materials science and acoustics [77, 117, 161, 208].

For superconductor inverse design requiring exploration of infinite atomic configurations, Choudhary [77] developed AtomGPT, a Transformer-based pretrained model for generative atomic design. They converted material structures and properties from the JARVIS-DFT database into standardized textual descriptions via ChemNLP, enabling efficient exploration in high-dimensional text space. With minimal low-rank matrix fine-tuning and batch training using cross-entropy loss with AdamW optimizer, AtomGPT generated structure-compliant text. The results demonstrated that AtomGPT consistently yields lower RMSE for generated structures than Crystal Diffusional VAE (CDVAE) across various datasets.

Addressing vast chemical spaces in multi-property solid-state material design, Chen et al. proposed a generative Transformer framework [161]. Crystalline structures were encoded as SLICES (Simplified Line-Input Crystal-Encoding System) strings concatenated with target properties. The Transformer predicted subsequent tokens during training via Adam optimization, enabling property-specified structure generation. Generated structures exhibit exceptional diversity-spanning hexagonal, orthorhombic, monoclinic, and triclinic systems with 31 elements-demonstrating robust generalization.

Chen et al. [117] introduced a Transformer-based inverse design model for rapid development of multilayer micro-perforated panels with target sound absorption. Their framework encodes target spectra into latent features via Transformer encoders, while decoders autoregressively generate layer parameters through multi-head cross-attention. Bidirectional LSTMs validated spectral matching, enabling global optimization in high-dimensional parameter spaces. Even within a 60-dimensional high-dimensional design space, the model-designed micro-perforated panel demonstrated excellent sound absorption performance, achieving absorption coefficients of 98.03% at 500 Hz and 97.94% at 1,000 Hz.

3.3.2.7 | Diffusion Model. Diffusion models have demonstrated remarkable generative capacity in inverse design, owing to their ability to learn complex distributions within high-dimensional design spaces through a Markov chain process of forward noise addition and reverse denoising [209]. This enables efficient exploration of vast solution spaces. By incorporating conditional inputs (e.g., target properties, physical constraints) to guide the inverse generation process, they establish strong correlations between high-dimensional design parameters and target performance, mitigating local optima entrapment (Figure 8). Compared to GANs, diffusion models offer superior generation stability and sample diversity. They naturally handle one-to-many mapping problems, supporting the inverse derivation of diverse structural designs from performance targets. Particularly effective in complex, high-dimensional domains like materials and lattices [76, 98, 106, 125–129], they effectively balance generation precision with design space coverage. Conventional GANs exhibit instability in metasurface inverse design, primarily due to imbalanced adversarial training where one network dominates, leading to failure. Furthermore, methods like Wasserstein GANs and SLMGAN suffer from generating structurally ambiguous outputs-a consequence of unstable adversarial convergence. To address these limitations, Zhang et al. [128] proposed MetaDiffusion, a diffusion probabilistic model-based approach for metasurface inverse design. In the forward process, Gaussian noise was incrementally added to the original meta-atom structure x_0 via Markov transitions, ultimately yielding Gaussian noise x_T. For the inverse process, a neural network was trained to approximate

the denoising trajectory, learning to reconstruct the original structure from noise x_T. Post-training, the model iteratively generated target meta-atom structures x'_T starting from x_T. Experimental results demonstrated that diffusion models excel in high-dimensional design spaces, significantly outperforming other generative models.

Simultaneously, to address the susceptibility of GANs and VAEs to minor noise perturbations when designing microstructures for specified material responses, Vlassis and Sun [106] introduced a Denoising Diffusion Probabilistic Model. This model utilized embedded feature vectors of target properties to guide the diffusion generation process. Compared to GANs, the forward noise-adding and inverse gradual denoising diffusion process ensured enhanced training stability and greater performance scalability as data volume increases. From 2.112 generated candidate samples, a CNN filtered 512 high-accuracy samples within seconds. These samples exhibit finite element validation errors below 5% and successfully generated non-training set topologies (e.g., the letter "twin"), demonstrating the model's generalization capability in high-dimensional spaces. In the field of inverse design for lattice structure topology optimization, Zhang et al. [127] combined a diffusion model with a regression surrogate model to overcome the inefficiency and limited diversity of traditional topology optimization methods within complex, high-dimensional design spaces. During generation, the trained diffusion model incorporated target property conditions to produce geometric parameters. Gradients computed by the regression surrogate model were then used to adjust the generation direction, approximating the target properties. Consequently, the hybrid lattice structures generated by this diffusion model exhibit superior performance, with significantly enhanced generalization capabilities compared to the state-of-the-art IH-GAN model.

4 | Inverse Design of Functional Materials via Machine Learning

In section 3, we presented methodologies and strategies for ML-based inverse design in engineering problems, addressing data volume variations and two high-dimensional scenarios. This section provides a comprehensive overview of mainstream applications of ML-based inverse design for functional materials in engineering domains. These case studies demonstrate the effectiveness of the aforementioned methodologies and strategies across various fields and for different problems, offering readers clear design guidelines.

4.1 | Mechanical Engineering

Mechanical functional materials encompass the design, synthesis, analysis, and control of materials and structures with targeted mechanical or multifunctional properties. The growing demand for performance-driven design and novel functionalities renders traditional, iterative development approaches insufficient, often failing to achieve optimal material architectures. In contrast, machine learning-based inverse design strategies enable the efficient discovery and rational design of mechanical functional materials with specific, pre-defined performance requirements [210, 211].

4.1.1 | Energy Absorption

Mechanical materials with energy-absorbing properties are capable of effectively dissipating, storing, or transforming input mechanical energy through their specific microstructures or deformation mechanisms, thereby mitigating impacts or dampening vibrations [212–221]. Conventional design approaches for such materials exhibit inherent limitations [222]. First, topology optimization methods for novel energy-absorbing materials are constrained by multiple geometric parameters, leading to high design dimensionality. Second, difficulty in balancing multi-objective optimization trade-offs such as impact resistance and energy absorption performances. ML-based inverse design methods are increasingly employed to develop mechanical materials with tailored energy absorption properties, exemplified by re-entrant structures [212, 223], honeycombs [224–227], and shell-based lattice structures [10, 213, 228, 229].

To address the effects of multiple geometric parameters in the topology optimization of energy-absorbing materials, the forward-inverse hybrid design framework provides an effective solution, particularly through the integration of machine learning models with search algorithms. For instance, Chang et al. [223] proposed a machine learning model integrating a back-propagation neural network (BPNN) with a GA to inversely design mechanical metamaterials with prescribed Poisson's ratio. This approach efficiently addressed the problem arising from the complex nonlinear coupling between multiple geometric parameters and mechanical properties. The BPNN established an end-to-end forward mapping, and the optimal combination of parameters was rapidly identified through the framework, yielding a Poisson's ratio of 1.7105×10^{-10}. Notably, the resulting structure exhibits a pronounced zero Poisson's ratio effect under both tensile and compressive deformation. Similarly, Deng et al. [212] proposed an inverse design methodology that integrated neural networks with an evolution strategy to create mechanical metamaterials. To handle the high-dimensional geometric parameters, they first employed PCA to reduce the dimensionality of the stress-strain curves. Subsequently, a neural network was trained to achieve efficient parameter–property mapping (Figure 9a). After iterative optimization, the mechanical metamaterials generated by this framework exhibit excellent energy absorption performance (Figure 9b), with a maximum absorption efficiency of 94% (Figure 9c).

Regarding the challenge of balancing multi-objective optimization in the design of energy-absorbing mechanical materials, the use of improved multi-objective search algorithms offers an effective solution. For example, Li et al. [215] integrated ANN with GA for the inverse design of energy-absorbing metamaterial structures and multi-objective optimization. A fully trained ANN enabled the GA to perform iterative optimization (Figure 9d). This approach endowed the metamaterial architecture with enhanced plateau stress, stiffness, and reusability. The optimal geometric parameters were output once the MSE fell below a threshold, followed by the fabrication of physical structures via 3D printing (Figure 9e). In experimental tests assessing practical energy absorption and protective performance, the thermoplastic polyurethane structure successfully absorbed the impact energy, leaving the egg intact (Figure 9f).

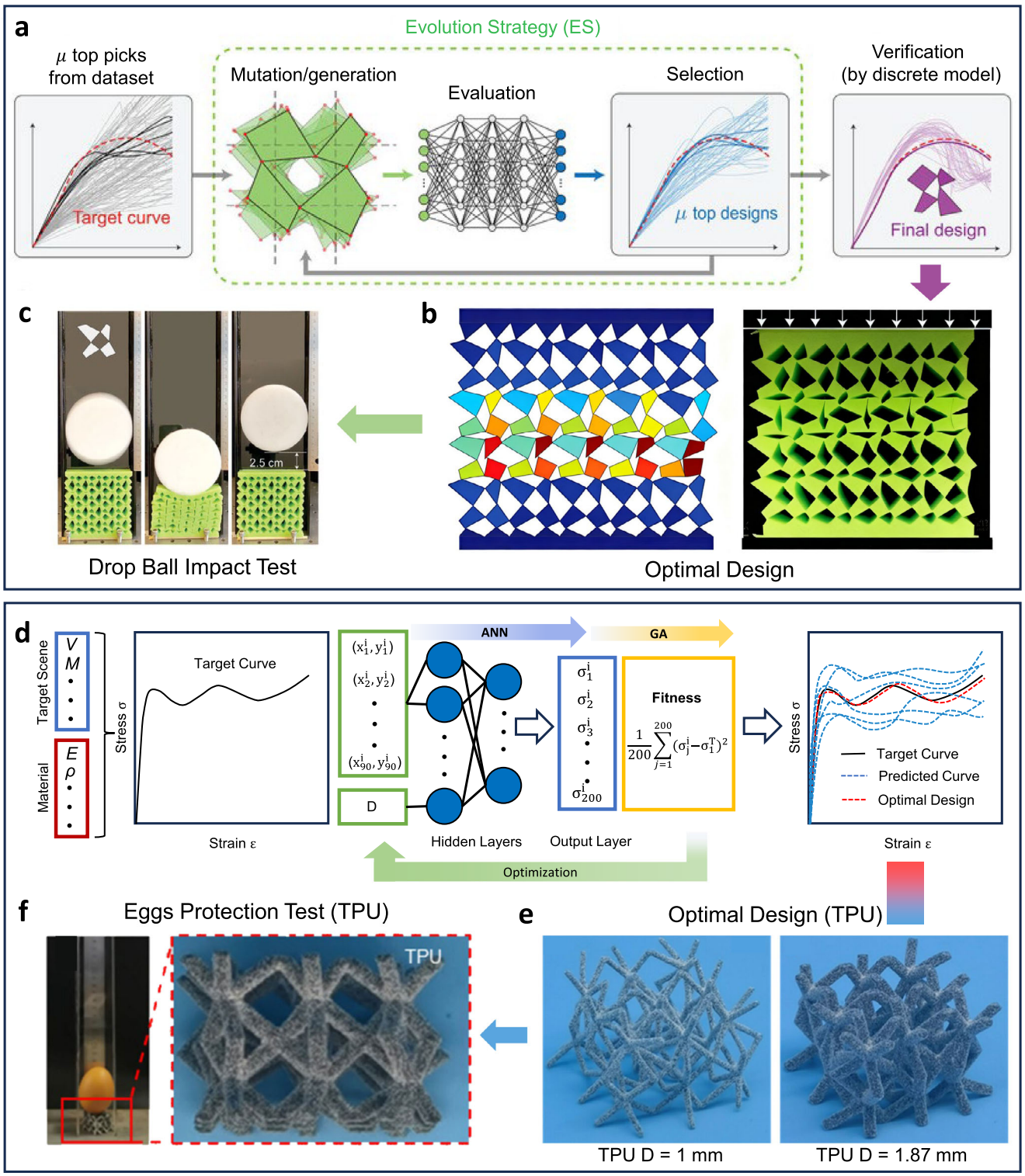

FIGURE 9 | Inverse design of structures with energy absorption. (a) The process of the proposed inverse design algorithm based on neural accelerated evolution strategy (Reproduced with permission [212]. Copyright 2022, Wiley-VCH.) (b) Optimized energy-absorbing structure (Structure iv) obtained via inverse design, showing numerical and experimental snapshots at a compressive strain of −0.1. Colors in the numerical snapshot represent local quadrilateral rotations (Reproduced with permission [212]. Copyright 2022, Wiley-VCH.) (c) Drop-weight impact test on Structure iv results in a rebound height of 2.5 cm, indicating an energy absorption efficiency of 94% (Reproduced with permission [212]. Copyright 2022, Wiley-VCH.) (d) Inverse design framework integrating ANN and GA. The GA generates multiple sets of geometric parameters, while the ANN predicts the stress response for each candidate design (Reproduced with permission [215]. Copyright 2025, American Chemical Society) (e) Fabricated specimen via ANN-GA-based inverse design, presenting a 3D-printed energy-absorbing structure made of thermoplastic polyurethane material (Reproduced with permission [215]. Copyright 2025, American Chemical Society) (f) Inverse-designed thermoplastic polyurethane lattice protective structure with a thickness of 1.8 mm successfully prevents egg damage in impact tests (Reproduced with permission [215]. Copyright 2025, American Chemical Society).

Overall, the forward-inverse hybrid design framework, particularly through the combination of forward predictive models and global search algorithms, proves to be suitable for the design of mechanical materials with energy-absorbing features. Data-driven machine learning models directly correlate structural parameters with target properties (e.g., specific Poisson's ratio, impact resistance, and high energy absorption), enabling efficient and rapid prediction. Combined with optimization algorithms (e.g., GA, NSGA-II), they efficiently handle multi-solution optimization and multi-objective trade-offs, enabling global optimal parameter searches. This significantly shortens the design cycle for complex energy-absorbing structures, allowing rapid inverse design of structures like re-entrant angles, petal-shaped honeycombs, and shell-based lattices.

4.1.2 | High-Strength Materials

As a key enabler for breakthroughs in the structural performance of engineering components, high-strength material systems primarily encompass categories such as advanced high-strength steels, reinforced composites, specialty alloys, and lattice metamaterials. These materials have demonstrated important roles in aerospace [230], automotive engineering [231, 232], and high-end equipment [233], with their core advantages lying in enhancing structural load-bearing efficiency and service safety through superior strength, stiffness, and damage tolerance. However, traditional design approaches still face several prominent limitations in the development of components using these high-strength materials [231, 234, 235]. First, for novel materials, the structure-property relationship is complex, and the design parameter space is high-dimensional and nonintuitive. Second, performance objectives such as high strength, high toughness, lightweight, and impact resistance are often mutually constraining, making it difficult for traditional methods to identify a globally optimal balance. Third, for traditional materials like alloys, the final properties are determined collectively by multiple elemental compositions and processing techniques such as heat treatment, whose interactions constitute a vast and discontinuous design space. In this context, ML-based inverse design offers a novel pathway for the multi-objective co-optimization of high-strength materials.

A powerful solution to address the challenges posed by the complex structure–property relationships, high-dimensional and non-intuitive design spaces of mechanical metamaterials is the integration of machine learning with evolutionary algorithms. Maurizi et al. [205] presented an inverse design method using ML and GA. The framework arranged fundamental truss units into macrostructures (Figure 10a). A DNN and GA iteratively searched the high-dimensional design space, yielding 12 high-performance candidate structures. Experimental results showed the ML-designed structures have 30%–90% higher buckling strength than conventional grid structures. In quasi-static compression tests on 3D-printed specimens (Figure 10b), the ML-designed structures exhibit approximately 15% higher average load-bearing capacity than sponge-inspired β-structures.

The trade-offs among multiple performance objectives—such as high strength, lightweight, and impact resistance—present another significant hurdle in novel mechanical materials. To navigate these conflicting goals, numerous studies have employed ML-based forward-inverse hybrid design frameworks with remarkable success. For instance, Challapalli et al. [236] proposed an inverse ML framework combining GANs and forward regression models. The entire process involved manufacturing datasets, machine learning inverse design, and additive manufacturing experimental verification (Figure 10c). After screening and iterative optimization, the generated lightweight lattice structures exhibit a 40%–120% increase in compressive strength compared to the original octet-truss sandwich structure, achieving both weight reduction and high strength. For composite lattice materials, Ha et al. [97] proposed an ML framework based on a forward-inverse co-design strategy for rapid development of lightweight, high-strength materials (Figure 10d). Inputting target compressive stress-strain curves and physical constraints allowed the model to rapidly generate candidate structures, predict mechanical responses, and select the optimum. Incorporating gradient parameters into the ML pipeline further enhanced the strength of the generated composite lattices. Drop tests showed reductions of approximately 30% in measured acceleration and approximately 25% in impact potential energy.

For traditional materials such as alloys, their final properties are determined collectively by multiple elemental compositions and processing techniques like heat treatment. Their interactions constitute a vast and discontinuous design space. To address the inefficiency of conventional design methods for high-strength alloys and the difficulty of balancing multiple elemental compositions, ML-based inverse design frameworks offer a new strategy for developing and optimizing high-strength alloys. First, machine learning models are utilized to assist in predicting the properties of alloy materials. For instance, Bhat et al. [237] developed a multi-objective ML-based inverse design method for Al alloys, rapidly predicting compositions and processing conditions meeting specific mechanical properties. A multi-objective random forest regressor simultaneously predicted properties. When targeting 600 MPa tensile strength, the model predicted 7 wt% Zn concentration, consistent with actual 7xxx series alloy trends. This ML-assisted optimization strategy is also applicable to the design of new alloys (e.g., Haynes 282 [238], Alloy 617 [186], gradient alloys [11]). For instance, Wang et al. [11] proposed a forward-inverse hybrid design framework to develop high-performance functionally graded alloys. The framework employed a GA to automatically identify the most critical feature combinations–from composition, phase constitution, and thermodynamic characteristics–for property prediction. A machine learning model was subsequently built for property prediction and composition optimization. The design results demonstrated that the framework successfully identified an alloy with an optimal combination of properties at a composition of 90 wt.% P91 and 10 wt.% 740H, achieving impressive yield and tensile strengths of 873 MPa and 1086 MPa, respectively. Second, generative models are directly employed to synthesize alloy materials. Kim et al. [239] employed a diffusion model in inverse designing 7xxx series Al alloys to achieve the desired ultimate tensile strength (UTS). Data preprocessing used UTS × EL (elongation) to balance strength and toughness. As noted previously, diffusion models demonstrated strong generative capabilities. Thus, the generated data sufficiently covered design spaces beyond the original domain. Results showed generated data closely matched

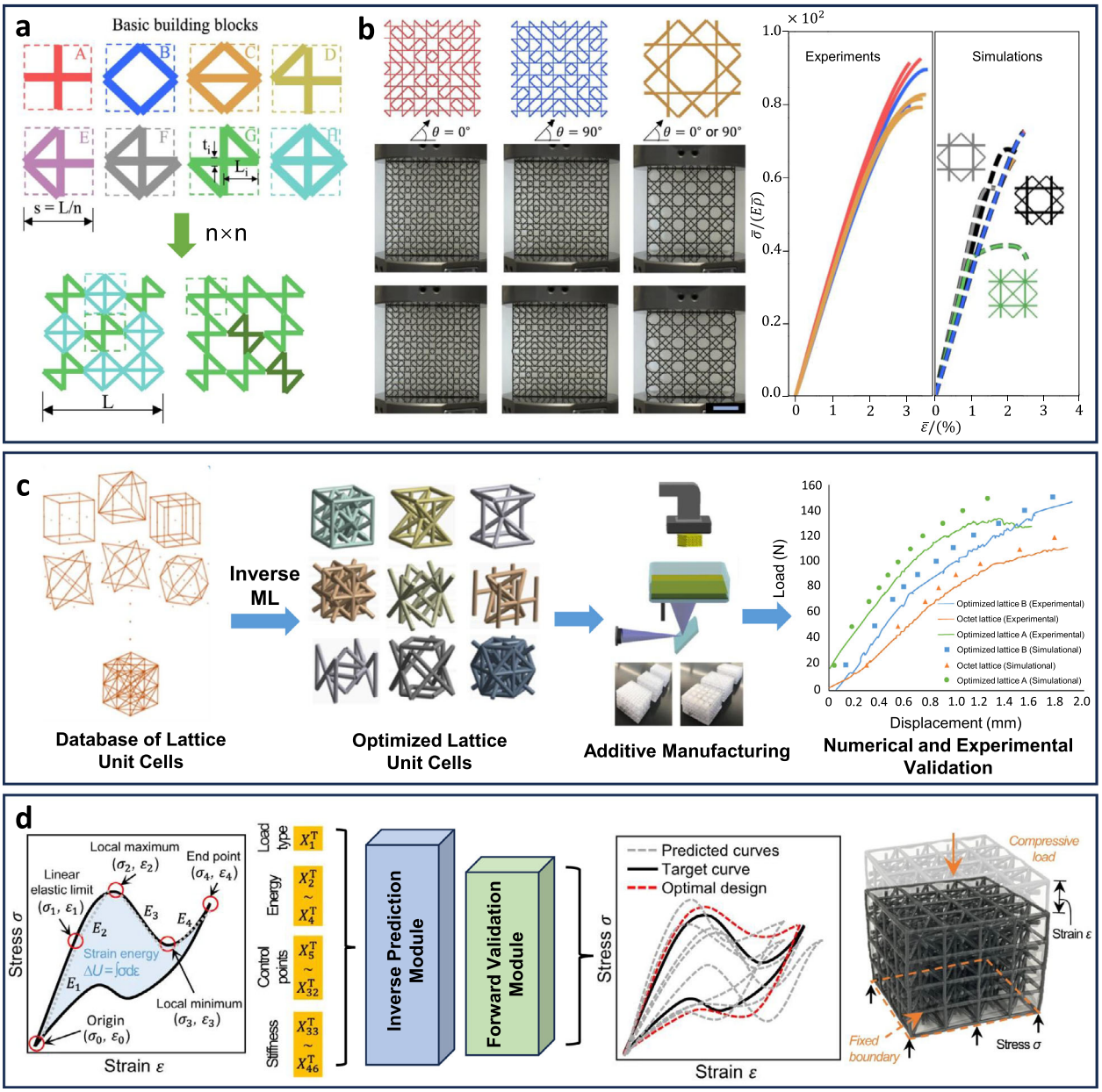

FIGURE 10 | Inverse design of structures with lightweight and high-strength characteristics. (a) Eight fundamental truss elements with distinct topologies/geometries assembled non-uniformly into larger units (Reproduced with permission [205]. Copyright 2022, Springer Nature.) (b) Architectures of ML-designed (red and blue) and sponge-inspired (yellow) structures. Deformation states of the three printed specimens at 3.3% strain. Normalized experimental and numerical stress-strain curves for symmetric inverse-designed, bioinspired, and conventional grid structures (Reproduced with permission [205]. Copyright 2022, Springer Nature.) (c) A Framework for Inverse Design of Lattice Unit Cells. Required properties are input into pre-trained GAN and regression models, yielding an optimal set of unit cells meeting specified constraints. Subsequent numerical and experimental validation demonstrates close alignment, confirming the practical feasibility of the ML-inversed lattice structures (Reproduced with permission [236]. Copyright 2021, Elsevier.) (d) Generative machine learning workflow for inverse design of composite lattice materials. Target uniaxial compression behavior, encoded as curve features, serves as input to the inverse prediction module generating candidate designs. These designs undergo forward validation to estimate their mechanical response. Each response is compared against target curves to identify the optimal design (Reproduced with permission [97]. Copyright 2023, Springer Nature).

the original data distribution, with the highest designed UTS reaching 784 MPa.

In summary, the core advantage of ML-based inverse design for high-strength structures lies in its ability to efficiently explore high-dimensional, complex material design spaces, achieving multi-objective optimization. The forward-inverse hybrid strategy encompasses approaches that combine generative models with forward prediction models, as well as those that integrate forward prediction models with global optimization algorithms. Another approach is the purely data-driven direct generation strategy, exemplified by diffusion models that autonomously

produce novel and non-intuitive material configurations. These approaches have been successfully applied to designing mechanical metamaterials and lightweight high-strength alloys, yielding substantial improvements in key metrics such as compressive strength, buckling resistance, recovery stress and load-bearing capacity, overcoming traditional limitations in performance trade-offs, cost control, empirical dependence, and manufacturability.

4.1.3 | Deployable Structures

Deployable structures represent a specialized category of engineering design, capable of transforming from a compact, folded state into a predetermined, stable functional configuration through controlled deployment motions. A key feature of such structures is their generally repeatable and controllable deployment process, often achieved via mechanical strategies such as kirigami and origami-inspired architectures [240–245]. However, the design methodologies for traditional deployable structures face several key challenges. First, the geometric patterns, material properties, and manufacturing parameters of kirigami/origami structures form a high-dimensional design space. Second, the mapping between the target three-dimensional geometries of deployable materials and their two-dimensional initial design parameters is highly nonlinear and non-intuitive. Currently, the machine learning-based framework for the inverse design of deployable structures not only effectively enables complex and innovative design requirements but also significantly enhances design efficiency.

To address the challenge of the ultrahigh-dimensional design space formed by the geometric patterns, material properties, and manufacturing parameters of kirigami/origami structural materials, a generative model-based design framework-such as VAEs and GANs-can be employed. Both types of generative models are capable of effectively handling high-dimensional design spaces. For instance, Ma et al. [246] employed a framework combining a VAE and Bayesian optimization for the inverse design of kirigami structures. The VAE mapped 64×64 binary images into a low-dimensional latent space, while Bayesian optimization iteratively searched for optimal parameters (Figure 11a). Experimental and simulation results for five target shapes (three of which are shown in Figure 11b) showed structural similarity index values around 0.9, confirming the reliability and feasibility of the method. Brzin et al. [247] proposed a GAN-based inverse design framework for self-folding soft kirigami composites. The framework consisted of three neural network components: a generator, a critic, and a simulator (Figure 11c). The latter two served as dual-loss constraints to ensure the physical feasibility of generated parameters. Faced with a high-dimensional parameter space (over 4096 dimensions), they reduced the search space by mirror symmetry. Subsequently, GAN collaboration was used to augment the dataset. Experimental results on inverse design for target shapes (Figure 11d) showed structural similarity generally above 0.86, demonstrating the method's feasibility and generalization capability.

Beyond the challenge of a high-dimensional parameter space, a more fundamental obstacle lies in establishing the highly nonlinear and non-intuitive mapping between a desired three-dimensional deployed geometry and its two-dimensional initial design parameters. A purely forward design approach is computationally prohibitive for rapid exploration. Consequently, a forward-inverse hybrid design framework has become a prevalent strategy in related fields, enabling a more direct and efficient pathway from target function to physical design. In the field of biomedicine, Truong-Quoc et al. [248] employed a DNA-origami-based GNN (DGNN) to generate DNA sequences that fold into a given target 3D shape. In this framework (Figure 11e), the DGNN rapidly predicted the three-dimensional equilibrium conformation (in about 1 s) for each mutant design. After iterative optimization, the final DNA origami design (Figure 11f) was obtained. Atomic force microscopy imaging confirmed that the DNA origami self-assembled into the expected helical structure, with peak positions matching predictions. In the aerospace sector, this framework is equally applicable for designing origami structures. Zhang et al. [249] proposed a ML-based inverse design method for deployable cylindrical composite shells used in solar sail structures. By combining a radial basis function neural network with a multi-island GA, their approach directly inferred geometric parameters from target performance (winding radius), avoiding blind trial-and-error iterations. The results demonstrated that the prototype's winding radius closely matched the target value, with an average error of only 4.65%.

In summary, within the field of deployable structures, the key advantage of ML-based inverse design lies in its ability to overcome the limitations of conventional methods. It efficiently handles high-dimensional parameter spaces and highly nonlinear problems by directly learning parameter distributions or establishing mappings between targets and design variables. This approach significantly reduces the need for blind trial-and-error and iterative optimization, thereby greatly enhancing design efficiency. Moreover, it excels in ensuring design accuracy, achieving close alignment with target configurations-whether for self-stretching shapes in kirigami composites or complex folded structures in origami-while maintaining errors at a low level.

4.1.4 | Adaptive Structures

Adaptive structural materials, capable of dynamically altering their shape, properties, or functions in response to external stimuli, are central to next-generation intelligent mechanical systems. 3D printing (additive manufacturing) provides a foundational platform for fabricating their complex architectures [250–256], while 4D printing further introduces a temporal dimension by incorporating stimuli-responsive materials (e.g., to light, heat, or magnetic fields), enabling predetermined shape morphing or functional evolution and thus serving as a key enabling technology for such adaptive structures [257–259]. These materials and structures demonstrate transformative potential in fields such as aerospace and soft robotics. However, conventional design approaches face significant limitations when applied to adaptive structures [260–262]. First, conventional approaches are often ineffective in handling the forward prediction of non–rectangular or irregular geometries–such as wrinkled surfaces, masks, or hand–shaped structures–where forward prediction using normal numerical calculation methods. Second, multi–material systems consist of numerous material units with distinct response properties, requiring simultaneous coordination of material distribution, geometric topology, and stimulus–response

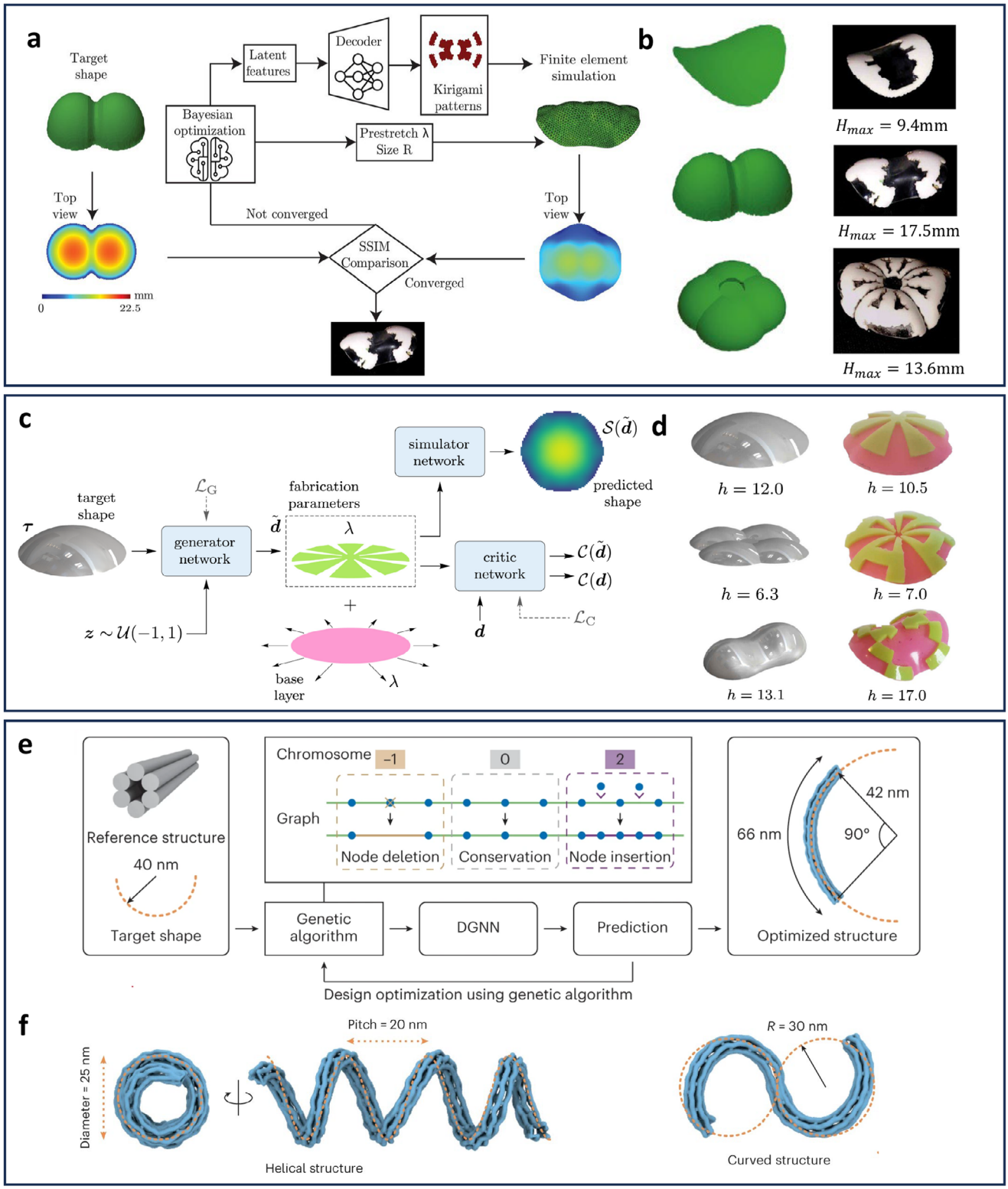

FIGURE 11 | Applications of machine learning-based inverse design in deployable structures. (a) Data-driven design and optimization pipeline for soft kirigami composites. A Bayesian optimization loop iteratively searches for the optimal combination of kirigami pattern variables, size, and pre-stretch (Reproduced with permission [246]. Copyright 2024, Wiley-VCH.) (b) 3D structures inversely designed using a framework integrating VAE and Bayesian optimization, showing representative shapes (pringle, peanut, and flower) (Reproduced with permission [246]. Copyright 2024 Wiley-VCH.) (c) Architecture of the inverse design framework based on Generator, Critic, and Simulator (Reproduced with permission [247]. Copyright 2025, Elsevier.) (d) Inverse design results for various target shapes, including dome, flower, and peanut shell (Reproduced with permission [247]. Copyright 2025, Elsevier.) (e) Inverse design and optimization workflow. The GA generates mutant designs from a reference structure by evaluating the error between predicted and target shapes. A DGNN predicts the conformation of each mutant at every iteration (Reproduced with permission [248]. Copyright 2024, Springer Nature) (f) Optimized DNA origami structures, illustrating a helical structure and a curved structure (Reproduced with permission [248]. Copyright 2024, Springer Nature).

parameters [263, 264]. This results in an extremely large search space, which complicates the optimization process. Within this context, ML-based inverse design offers a novel pathway to overcome these bottlenecks [265].

Addressing the limitation that traditional numerical methods face in handling non-rectangular shapes and high-dimensional design parameters within adaptive materials design. Sun et al. [266] proposed an inverse design framework integrating RNN and sequential subdomain optimization in the design of active composites. Subsequently, for active composites in 4D printing, voxel-based composites consist of multiple material units with distinct responsive properties. The distribution of these materials to achieve targeted shape morphing constitutes a complex optimization problem (Figure 12a), involving intricate data mapping and a significantly expanded design space. Sun et al. [141] further developed an inverse design strategy combining ML, GD, and EA (Figure 12b). ML-GD or ML-EA optimizes all voxels, while ML-EA further refines regions with large local errors. The inversely designed developable surfaces achieve highly matched voxel distributions. For non-uniform shapes, such as crumpled paper and masks, the inversely generated structures also exhibit high conformity with scanned targets. In addition, Jin et al. [8] introduced an ML-driven method combining ResNet and EA (Figure 12c). ResNet replaced FEA for forward prediction, directly forecasting complex hierarchical structure behavior. Experimental results demonstrated that EA-generated material distributions achieves high matching between simulated deformations and target curves in both fixed and random design domains. Successful opening/closing motion of a printed hand-shaped structure upon heating validates the method's practical feasibility (Figure 12d).

Multi-material systems integrate a vast array of material constituents, each exhibiting distinct stimulus-responsive characteristics. The design of such systems necessitates the simultaneous coordination of material distribution, geometrical topology, and stimulus-response parameters. As highlighted by Chen and Gu [103], the design space for rigid-flexible composite material systems can encompass up to 2^{128} design variables, illustrating the extraordinary complexity inherent in these systems. In response, they proposed a forward–inverse hybrid design framework based on a generative deep neural network (Figure 12e), allowing efficient discovery of material and structural configurations with superior adaptive properties (Figure 12f). Experimental results demonstrated that after multiple iterations, the maximum toughness of the composite system increased from 61.01 to 218.05. Another example is the design of hydrogel materials with autonomous deformation properties, Wang et al. [267] proposed the deep learning-progressive evolutionary algorithm framework (DL-PEA: Figure 12g). In this work, DL provides efficient and high-precision deformation prediction, while PEA employs an optimization strategy to swiftly search for optimal material distributions. Experimental validation via physical 4D printing demonstrated high consistency between actual and predicted deformations (Figure 12h), robustly confirming the feasibility and reliability of this machine learning-based inverse design framework.

In summary, within the design of adaptive structural materials, whether addressing performance prediction for non–rectangular and irregular geometries (e.g., wrinkled surfaces, masks, hand–shaped structures) or the simultaneous coordination of material distribution, geometric topology, and stimulus–responsive parameters, the forward–inverse hybrid design framework has proven to be highly effective. Case studies further demonstrate that such approaches enable inverse design that achieves target deformations or functionalities with high fidelity across various stimuli–responsive scenarios, including water–induced deformation and thermal actuation. These findings underscore that ML–based inverse design, with its integrated capabilities in forward prediction and inverse optimization, offers an efficient and reliable solution for meeting complex engineering requirements such as multi–stimuli responsiveness, multiscale structuring, and dynamic functional evolution.

4.2 | Energy Engineering

The global energy sector is undergoing a paradigm shift toward clean and low-carbon sources to address pressing concerns of energy security and environmental sustainability. While renewables such as solar, wind, and hydropower are rapidly displacing fossil fuels to curb oil dependence and carbon emissions, their large-scale integration faces persistent technical bottlenecks across the energy chain. These include limited conversion efficiency, insufficient storage capacity and safety issues, as well as grid instability caused by intermittent supply. Within this framework, ML offers a transformative pathway toward smart energy systems. ML supports data-driven discovery and design of high-performance energy functional materials, along with multi-objective optimization of complex system parameters, thereby improving overall efficiency and operational stability. For example, generative models and reinforcement learning can accelerate the development of novel photovoltaic materials, optimize wind farm layouts, predict battery lifespan, and enable real-time intelligent control of energy flows. Such approaches avoid traditional costly trial-and-error experiments and simulations, shortening research and development cycles and propelling renewable technologies toward higher performance and lower cost [268, 269].

4.2.1 | Energy Capture

Energy capture refers to harvesting ambient energies (e.g., mechanical vibration, thermal, light) and converting them into electricity, such as hybrid nanogenerators [270–272] and piezoelectric energy harvester [273, 274], etc. Energy capture devices are widely used in low-power electronics [270, 275] to replace batteries. However, significant challenges remain. First, critical factors lead to input dimension explosion, rendering conventional search methods ineffective. Second, precise multi-objective performance matching is difficult; for instance, complex trade-offs exist among parameters such as piezoelectric strain constant and Young's modulus, bandgap and formation energy, and light absorption and carrier recombination, hindering simultaneous optimization. Third, the energy conversion efficiency of energy harvesting materials is constrained by structural optical/electrical losses, including reflection losses in planar configurations, non-uniform absorption layer thickness, and carrier recombination. Fourth, these materials suffer from performance degradation under continuous thermal, optical, or electrical fields, failing to

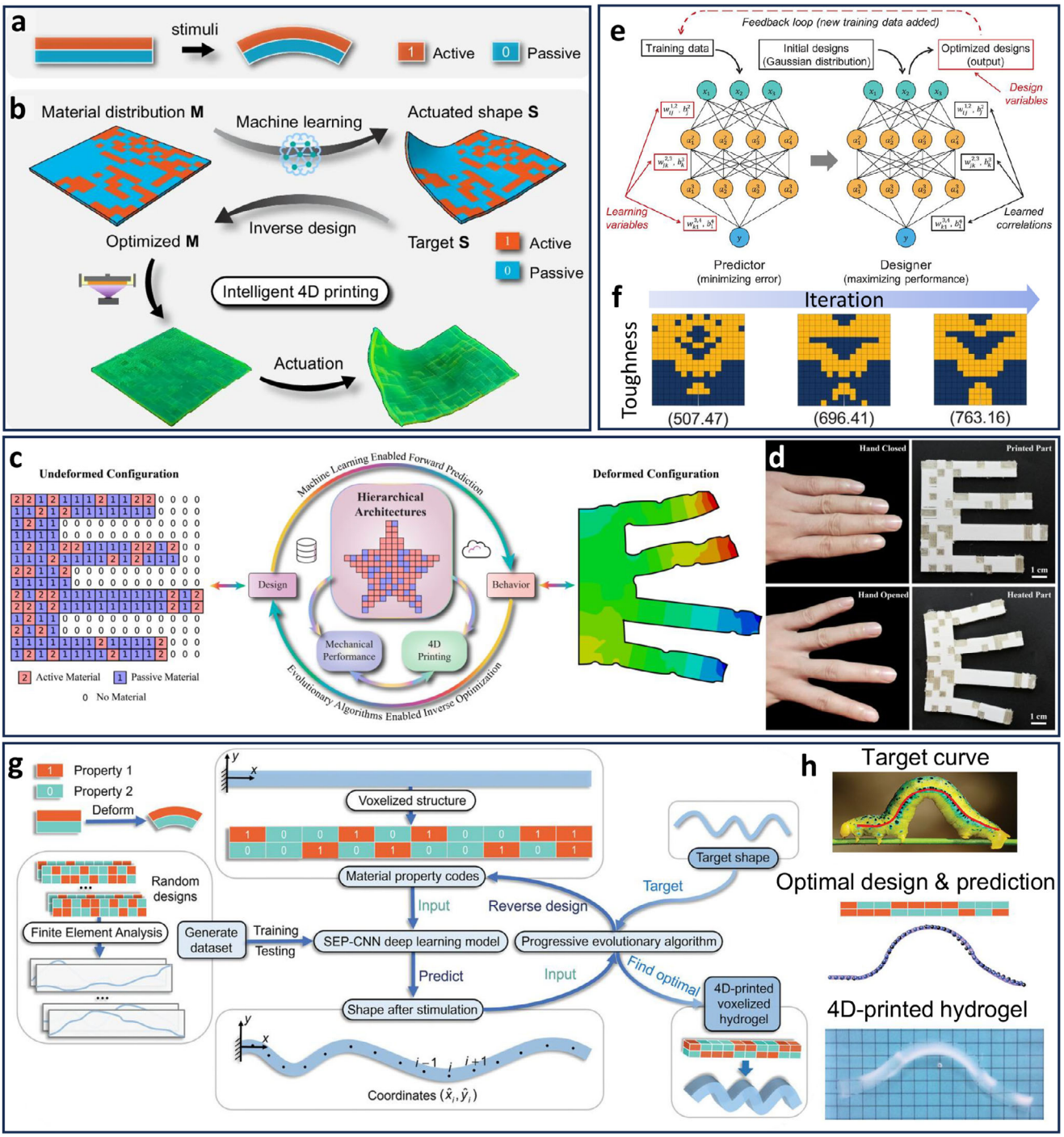

FIGURE 12 | Schematic of the inverse design process and corresponding outcomes in adaptive printing. (a) Overview of ML-driven voxel-level inverse design for a 4D-printed active composite plate (Reproduced with permission [141]. (Copyright 2024, Springer Nature.) (b) Forward shape prediction via machine learning and inverse design of material distribution via ML optimization, enabling voxel-level optimization for 4D printing of active composite plates (Reproduced with permission [141]. Copyright 2024, Springer Nature.) (c) Inverse optimization design flow for a 4D-printed hierarchical structure with a hand shape (Reproduced with permission [8]. Copyright 2024, Elsevier.) (d) Demonstration of the printed part after optimized material allocation (Reproduced with permission [8]. Copyright 2024, Elsevier.) (e) Framework of a generative deep neural network (Reproduced with permission [103]. Copyright 2020 Chen et al., Published by Wiley-VCH.) (f) Inverse design generated after three rounds of iteration (Reproduced with permission [103]. Copyright 2020 Chen et al., Published by Wiley-VCH.) (g) Schematic of rapid inverse design for 4D-printed voxelated composite structures (Reproduced with permission [267]. Copyright 2025, Wiley-VCH.) (h) Example of inverse design from a hand-drawn curve (Reproduced with permission [267]. Copyright 2025, Wiley-VCH).

meet service life requirements. Fifth, high-performance materials such as lead-based perovskites contain toxic elements, restricting their practical application and large-scale deployment. Consequently, machine learning has been introduced to overcome the bottlenecks in energy harvesting technology.

To address the challenge of input dimension explosion, deep learning frameworks have been introduced in this field. This approach is advantageous due to its capacity to manage high-dimensional inputs, enabling efficient inverse generation and performance matching. For instance, to tackle the high-dimensional input problem posed by metasurface patterns, Liu et al. [276] employed a CNN-GA-based inverse design framework to develop an adaptively tunable digitally coded metasurface. The CNN-GA effectively handles the dimensionality challenge, yielding a digitally coded metasurface capable of efficient electromagnetic energy harvesting. Additionally, Liu et al. utilized a radial basis function (RBF) neural network architecture to demonstrated the feasibility of replacing an optimized single multi-source system with a combined multi-source system for energy scavenging. In the case of input dimension explosion arising from multi-component materials, the integration of physics-informed models is essential to thoroughly analyze the influence of diverse material properties. Taking the triboelectric nanogenerator (TENG) as an example–a device that harvests ambient mechanical energy through contact electrification to power electronic systems–Jiao et al. [277] proposed a physics-informed AI-driven inverse design method to optimize TENG performance. By designing triboelectric conductive materials and metamaterials, and subsequently integrating material and structural designs via physics-informed AI, manufacturable TENG components are generated, leading to enhanced energy conversion efficiency and voltage stability.

Another significant challenge in the development of energy harvesting materials lies in precisely matching multiple performance targets, where generative models offer an effective solution by directly producing the corresponding structural parameters from given multi–objective specifications. For example, the c–VAE, through its encoder-decoder architecture, learns complex nonlinear mappings between performance goals and structural parameters within a low–dimensional latent space, thereby avoiding the inefficiency of conventional trial–and–error approaches. In the development of piezoelectric metamaterials, Liu et al. [138] introduced an ML–based inverse design framework and evaluated three deep learning models—cVAE, cGAN, and MLP—to inversely generate hybrid triple periodic minimal surface (H–TPMS) architectures. This enabled precise alignment of target piezoelectric strain constants and Young's moduli. Among the models, cVAE achieves the highest accuracy, attaining 98.92% matching precision for the piezoelectric constant, thereby ensuring efficient mechanical–to–electrical energy conversion in the designed H–TPMS. Notably, this forward-inverse hybrid design framework is also suitable to address this challenge, as it achieves precise matching by combining a forward model that maps structural parameters to material properties with an inverse algorithm for multi-objective optimization, thereby synergistically resolving conflicts among performance metrics. Cai et al. [278] proposed a design framework (Figure 13a) to address the challenge of simultaneously optimizing multiple performance metrics—such as bandgap, voltage, and current—where complex trade-offs often hinder synchronous improvement. The forward model established a mapping relationship among material composition, energy level alignment, and photovoltaic performance. In the inverse stage, GA and Bayesian optimization were employed to inversely search for the optimal Sn/Pb ratio. The framework ultimately predicted an optimal Sn ratio of 0.624, corresponding to a power conversion efficiency of 18.23%.

Beyond multi-objective matching, structural optical and electrical losses impose fundamental limitations on energy conversion efficiency. These losses–including reflection losses, non-uniform absorption layer thickness, and carrier recombination–necessitate meticulous structural optimization of energy harvesting materials. Perovskite crystal structures have emerged as promising electrode materials owing to their tunable composition and architecture, high electrical conductivity, and superior catalytic activity [12, 278–282]. Li et al. [12] employed a cascade neural network to inversely predict the pyramidal optical structure parameters of perovskite solar cells based on target power conversion efficiency (PCE) (Figure 13b). Their inverse-designed pyramidal architecture, compared to planar counterparts, enables multiple light reflections that substantially reduce reflection losses, thereby significantly enhancing PCE (Figures 13c and 13d). Experimentally, the pyramidal $FAPbI_3$ perovskite solar cell incorporating the optically optimized parameters achieves a PCE of 28.4%, approaching the theoretical limit of 33%.

Material durability under operational stress presents yet another critical consideration, as sustained thermal, optical, or electrical exposure typically degrades performance over time. Optimization of material composition or structure is therefore essential to mitigate such degradation. In perovskite materials, certain hole-transporting molecule (HTM) motifs—such as those incorporating triphenylamine, heterocycles, or fluorine substituents—exhibit the capability to passivate surface defects, thereby suppressing non–radiative recombination and reducing defect–assisted degradation under thermal or photoexcitation. In this context, Wu and Zhang [279] developed a closed–loop inverse design framework to inversely derive the optimal HTM structure from target performance specifications (Figure 13e). Through multiple iterative cycles, the optimized HTM yielded a substantial improvement in average PCE (Figure 13f), with a peak value of 26.2% (certified 25.9%). Furthermore, this architecture exhibits robust stability, retaining 80% of its initial performance after over 1,000 h of continuous illumination at 65°C.

Environmental concerns associated with high-performance materials, particularly the toxicity of lead-based perovskites, represent an equally important challenge that must be addressed for practical deployment. The primary strategy involves reducing the content of toxic elements, especially lead, while maintaining desirable photovoltaic properties. Kim et al. [282] adopted a B-site multi-alloying approach, partially substituting Pb with elements including Sn, Ge, Cd, Hg, and Zn to reconstitute the material composition. They developed an inverse design framework that integrates density functional theory (DFT) with ML. Within this framework, a crystal graph convolutional neural network takes unrelaxed crystal structures as input and predicts three key properties of the relaxed structures. Ultimately identifying two high-performance photovoltaic materials, $CsGe_{0.3125}Sn_{0.6875}I_3$ and $CsGe_{0.0625}Pb_{0.3125}Sn_{0.625}Br_3$, which effectively exhibit reduced

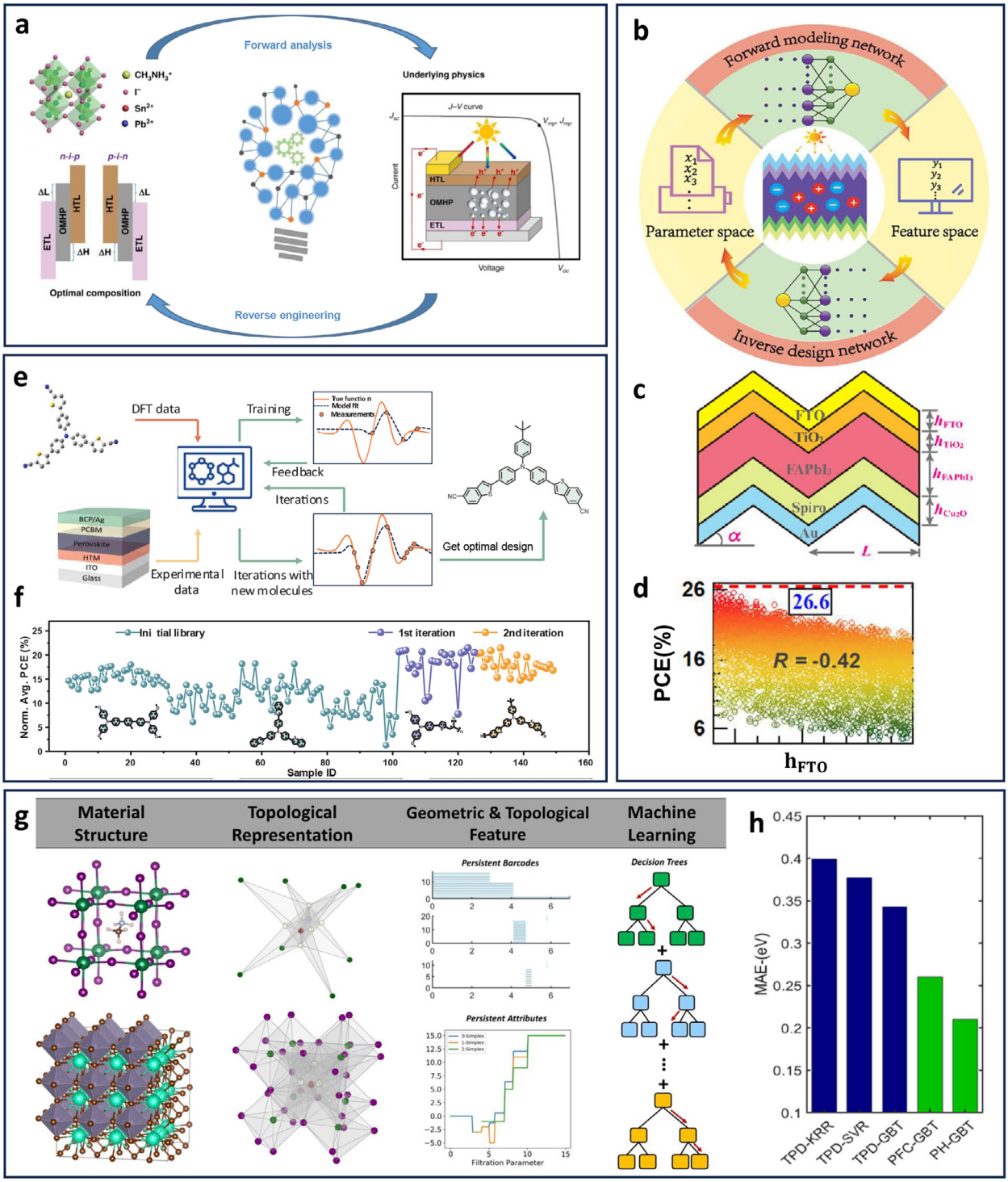

FIGURE 13 | Inverse design processes and results for energy capture materials. (a) A forward-inverse hybrid method for designing perovskite materials with multiple performance targets (Reproduced with permission [278]. Copyright 2022 Cai, Springer Nature.) (b) Integration of neural network models with high-throughput computational simulations, forming a framework for the inverse design (Reproduced with permission [12]. Copyright 2024, American Chemical Society.) (c) Structure and parameters of pyramid PSCs (Reproduced with permission [12]. Copyright 2024, American Chemical Society.) (d) Statistical PCE of pyramid PSCs under the h_{FTO} dimension (Reproduced with permission [12]. Copyright 2024, American Chemical Society.) (e) Descriptors of hole-transporting materials and device parameters were used to train the model (Reproduced with permission [279]. Copyright 2024, The American Association for the Advancement of Science.) (f) Two iteration rounds showing rising average PCE; optimal molecular structure achieving 26.23% PCE after multiple iterations (Reproduced with permission [279]. Copyright 2024, The American Association for the Advancement of Science.) (g) A model framework for the performance prediction and inverse design of lead-free substitute materials (Reproduced with permission [280]. Copyright 2022, Springer Nature.) (h) The PF-GBT model demonstrated consistently lower MAE values compared to traditional perovskite descriptor-based machine learning models (Reproduced with permission [280]. Copyright 2022, Springer Nature).

lead content. Furthermore, in the study of lead-free alternatives, Anand et al. [280] proposed a forward–inverse hybrid design framework based on persistent functions (Figure 13g). This framework integrated gradient boosting tree models to establish structure–property relationships, enabling high-accuracy prediction of bandgaps for lead-free substitute materials such as $CsGeX_3$. Experimental results demonstrated that the PH-GBT model (the model combined persistent functions-based features with gradient boosting tree models) achieves significantly lower mean absolute error (MAE) in bandgap prediction compared to traditional descriptor-based models (Figure 13h), validating the effectiveness of this approach for the efficient screening of lead-free perovskites.

In summary, ML-based inverse design demonstrates remarkable advantages and unique functionalities in the field of high-efficiency energy harvesting. Not only does it handle high-dimensional inputs and complex design spaces-as exemplified by the CNN-GA framework successfully processing binary-encoded matrices to achieve broadband and multi-angle efficient electromagnetic energy capture via self-adaptive metasurfaces-but it also integrates physical principles and design requirements to precisely match performance with structure. For instance, the cVAE model achieves 98.92% accuracy in matching piezoelectric constants for inverse generation of piezoelectric metamaterials, while physics-informed optimization of triboelectric nanogenerator significantly enhances energy conversion efficiency and voltage stability. Moreover, this approach considerably shortens development cycles; ANN-based design of solar absorbers reduces the process to hours, while simultaneously enhancing performance (e.g., perovskite solar cells approaching the theoretical PCE limit) and addressing practical issues such as toxicity and stability. This offers a novel and powerful design paradigm for advancing efficient and practical energy harvesting technologies.

4.2.2 | Energy Storage and Release

Power batteries hold a pivotal position in energy engineering. Distinguished from traditional lead-acid and nickel-cadmium batteries, their defining characteristics are rooted in new materials, novel chemical systems, and innovative structures, designed to meet the core demands of modern and future energy systems for high energy density, high power density, long cycle life, enhanced safety, and low cost. Currently, power batteries are widely used in industries like new energy vehicles and large-scale power grids [283]. However, their engineering applications face limitations [284, 285]. First, traditional homogeneous porous electrodes suffer from sluggish ion transport and substantial voltage drop at high charge rates. Second, the synergistic optimization of multi-objective electrochemical performance remains challenging, as energy storage materials must simultaneously satisfy multiple mutually constrained performance metrics. Third, crystal structure prediction and lattice stability regulation are hindered by the lack of prior structural knowledge in the development of novel cathode materials. ML-based inverse design methods are now being applied to power battery development [286], offering novel frameworks for energy storage and release technologies and significantly improving performance, as detailed below.

To address severe performance degradation in Li-ion batteries caused by slow ion transport in homogeneous porous electrodes and high voltage drops at high charging rates, the construction of novel electrode materials is imperative. Sui et al. [287] employed a deep learning-driven inverse design framework (Figure 14a) to develop a bio-inspired vascularized porous electrode. An ANN learned the parameter-performance mapping, enabling precise prediction of charging curves and identification of optimal structures based on requirements (Figure 14b). The experiment showed that at a current density of 3.2 C, the fully vascularized battery has a capacity increase of 66% compared to the homogeneous electrode. Due to low tortuosity and gradient porosity, the bi-vascular full cell achieves a pulse charging time of 22.98 s and higher capacity than a conventional uniform cell (Figure 14c). Due to low tortuosity and gradient porosity, the double vascular full-cell battery exhibits greater capacity compared to conventional uniform batteries.

The design of multi-objective energy storage materials necessitates the simultaneous satisfaction of multiple mutually constrained performance metrics–such as capacity, voltage, and induced charge. However, the synergistic optimization of multi-objective electrochemical performance remains a significant challenge. To address this issue, Li et al. [289] proposed an ML inverse design framework to derive MXene chemical compositions from target electrochemical properties (capacity, voltage, induced charge). Multi-objective random forest regression predicted the properties, while multi-objective random forest classification output the compositions. This method embedded highly active ions while filtering out low-contribution elements. The designed Li_2M_2C and Mg_2M_2C (M = Sc, Ti, Cr) significantly outperform conventional graphite anodes. Further, Duquesnoy et al. [288] developed an ML-assisted inverse design framework (Figure 14d) for optimizing Li-ion battery electrode manufacturing. By integrating physics-based models for synthetic data generation, deterministic ML model, and multi-objective Bayesian optimization, the strategy derived optimal manufacturing conditions from target electrode performance. Quantitative results showed synchronized maximization of density (2.4456 g/cm^3) and active surface area (55.723%), enhancing volumetric energy density. The multi-objective strategy prevented sacrificing other metrics during single-property optimization (Figure 14e).

Regarding the challenges of blindness in crystal structure prediction and the difficulty in regulating lattice stability, an integrated design approach combining machine learning with search algorithms can be employed. For instance, Wang et al. [290] employed a framework combining a forward model, PSO, and universal structure predictor-evolutionary xtallography. The evolutionary xtallography predicts globally stable crystal structures from composition, eliminating experimental blindness. Results showed smaller lattice parameter differences in Li/Ni@Ce-NCM than Ce-NCM, indicating that moderate Li/Ni mixing suppresses anisotropic lattice disorder, causing lattice expansion, thereby stabilizing the lattice. The developed Ce-NCM material achieves a Li^+ diffusion rate nearly 80 times higher than the target value.

In summary, within the field of energy storage and release structure optimization, the core advantage of ML-based inverse design lies in its breakthrough beyond the limitations of traditional "parameter trial-and-error" approaches. By establishing

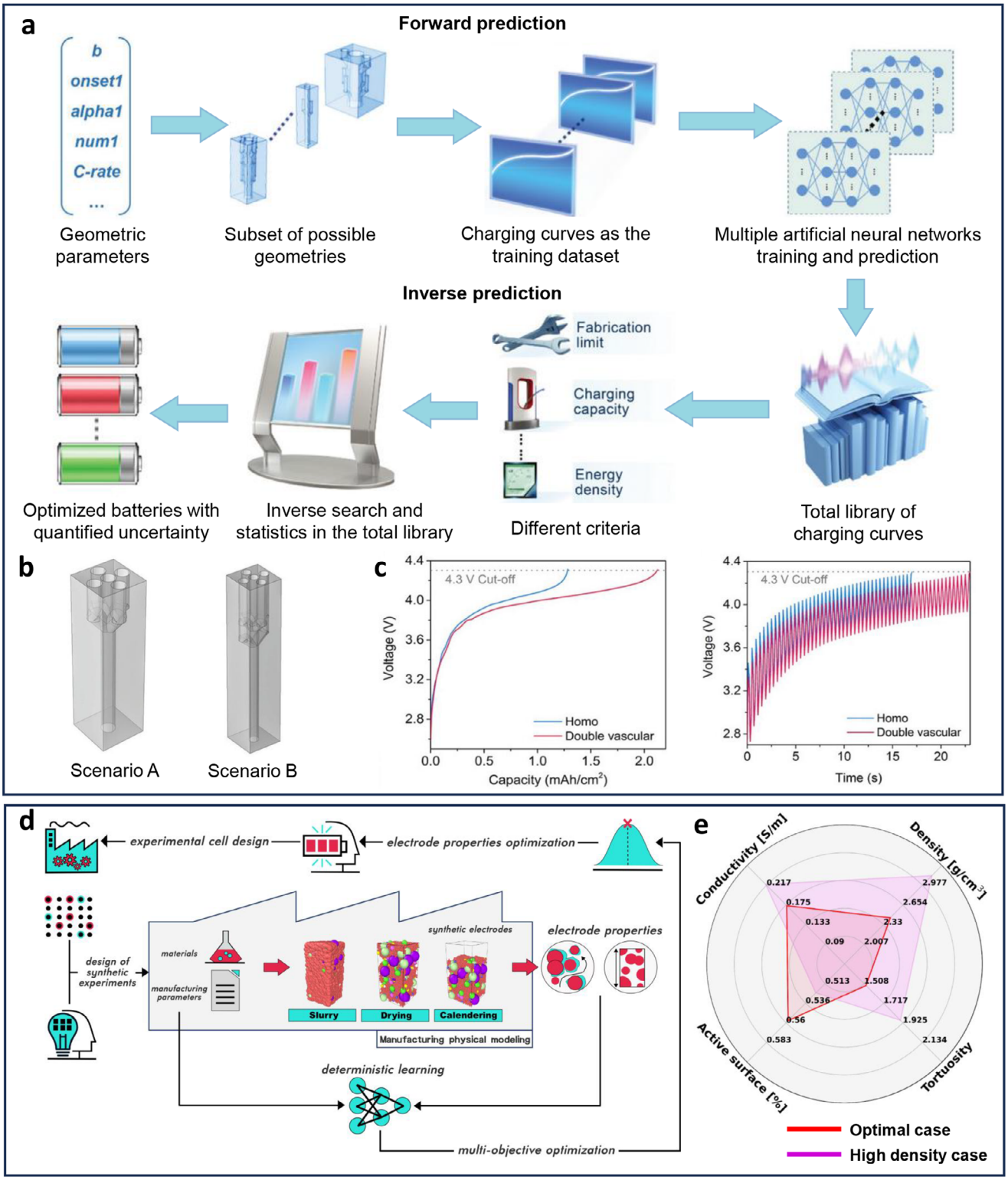

FIGURE 14 | Inverse design process and results for structures with energy storage/release characteristics. (a) Workflow integrating forward deep learning prediction with inverse design optimization (Reproduced with permission [287]. Copyright 2021, Wiley-VCH.) (b) Optimized geometries for Scenario A and B (Reproduced with permission [287]. Copyright 2021, Wiley-VCH.) (c) Charging curve comparison between the double vascular full-cell battery structure and U.S. Advanced Battery Consortium targets, alongside high-rate pulse charging profiles (Reproduced with permission [287]. Copyright 2021, Wiley-VCH.) (d) Schematic of deterministic-assisted multi-objective electrode optimization (Reproduced with permission [288]. Copyright 2023, Duquesnoy et al., Published by Elsevier.) (e) Radar chart comparing optimized electrode performance against extreme cases (high-density case shown) from the synthetic dataset (Reproduced with permission [288]. Copyright 2023, Elsevier).

accurate mapping models between performance and parameters, it enables direct derivation of optimal structures/parameters from target properties, significantly enhancing design efficiency and accuracy. Furthermore, this method exhibits robust multi-objective optimization capabilities, simultaneously balancing key indicators, thereby avoiding the trade-off issues inherent in single-objective optimization. Evidently, ML-driven inverse design not only facilitates innovative design of complex architectures but also allows precise inference of material compositions and manufacturing processes. It can even integrate with crystal structure prediction tools to achieve targeted modulation of material microstructures.

4.3 | Acoustic Engineering

In the field of acoustic functional materials, the precise manipulation of sound propagation paths, efficient absorption of acoustic energy, and effective blocking of harmful sound waves remain fundamental challenges. ML-based inverse design has emerged as a powerful paradigm for the efficient and precise development of acoustic structures tailored to specific performance requirements. This perspective elaborates on the application of ML-driven inverse design across three key areas: sound propagation, sound absorption, and sound blocking, highlighting its transformative potential for creating multifunctional acoustic materials.

4.3.1 | Sound Propagation

In engineering, sound propagation refers to the physical process of energy transfer by acoustic waves through gaseous, liquid, or solid media. The design of materials for controlling acoustic wave propagation faces several challenges. First, the global correlation between complex geometric features and acoustic performance is difficult to model. Second, the material fabrication process imposes stringent requirements on extreme physical parameters, which are challenging to achieve with existing manufacturing techniques. Therefore, researchers are developing novel materials for controlling acoustic wave propagation through inverse design frameworks based on machine learning, such as wide-bandgap acoustic topological devices [291], phononic crystals [292–295], lattice metamaterials [296, 297], and acoustic cloaks [298].

The challenge of modeling global correlations between complex geometrical features and acoustic properties stems from the inherent difficulty in establishing intuitive mappings between intricate configurations and bandgap characteristics. This limitation of traditional methods necessitates the development of forward models that can construct end-to-end mappings from complex configurations to bandgap characteristics, thereby enabling the inverse design of acoustic materials. Establishing such direct relationships is crucial for advancing the rational design of acoustic metamaterials with tailored bandgap properties. For example, Li et al. [291] employed a bidirectional ANN for the inverse design of wide-bandgap acoustic topological devices. The forward model directly outputs the bandgap width in an end-to-end manner, while the inverse model outputs the optimal radius for a target bandgap width. Results demonstrated that the inversely designed radius significantly enhances the unit cell's bandgap width. Finally, an acoustic splitter was designed using this boundary state mode, exhibiting stable propagation even with introduced defects and disordered structures. In addition, to address the mapping challenge between acoustic metamaterial configurations and bandgap characteristics, Chen et al. [299] proposed a new framework (Figure 15a). A forward prediction model was established using random forests to map design variables (e.g., geometric parameters) to acoustic responses (e.g., bandgap existence). By analyzing the tree structure, a likelihood function for target satisfaction was then constructed, and new designs were subsequently generated by sampling from this likelihood distribution via Markov chain Monte Carlo methods. Experimental results demonstrated that, with a sampling threshold of 0.6, 100% of the generated designs satisfied the target requirements. Moreover, the generated designs exhibit diversity in both geometry and frequency response (Figure 15b), covering the feasible design space more broadly than those obtained through GA. Furthermore, Wan et al. [294] proposed an AE-DNN hybrid architecture for inversely designing complex 2D phononic crystals with irregular scatterers, enabling bandgap tuning and Dirac dispersion. Plane waves maintained waveform integrity while propagating through the PC structure, preserving wavefront coherence even with inserted obstacles, verifying the zero-refractive-index property.

Manufacturing challenges present another significant obstacle, arising from stringent fabrication processes and extreme physical parameter requirements. Conventional transformation acoustics typically relies on heterogeneous, anisotropic, and extreme-parameter materials, which are difficult to realize in practice. In the design optimization of acoustic cloaks, approaches based on gradient [300] or topology optimization [301, 302] have demonstrated limited effectiveness. By contrast, ML–based inverse design provides a viable strategy to alleviate this issue. For example, Ahmed et al. [298] proposed an inverse design framework using deterministic and probabilistic deep learning models for broadband acoustic cloaks (Figure 15c). They first modeled a four-layer concentric core–shell structure. Subsequently, a fully connected neural network was established and trained for forward prediction, followed by inverse model design. They employed isotropic homogeneous material layers without requiring negative refractive indices, near-zero moduli, or anisotropic parameters. All design parameters are positive real numbers, thus enabling direct implementation using conventional acoustic materials. Finite element analysis confirmed that the field distribution with the cloak resembled that without any object, validating the cloak's performance across a broad spectrum.

In summary, in the field of acoustic engineering, ML–based inverse design has yielded differentiated framework strategies to tackle distinct bottlenecks. To address the challenges of complex configurations and the lack of configuration–performance mapping, forward models are employed to establish an end–to–end mapping between the architectures of acoustic materials and their acoustic properties. For the difficulty of fabricating devices with extreme parameters, machine learning models are further adopted to explore feasible material alternatives to unconventional parameters, thus endowing acoustic materials with manufacturability. These ML–enabled design frameworks

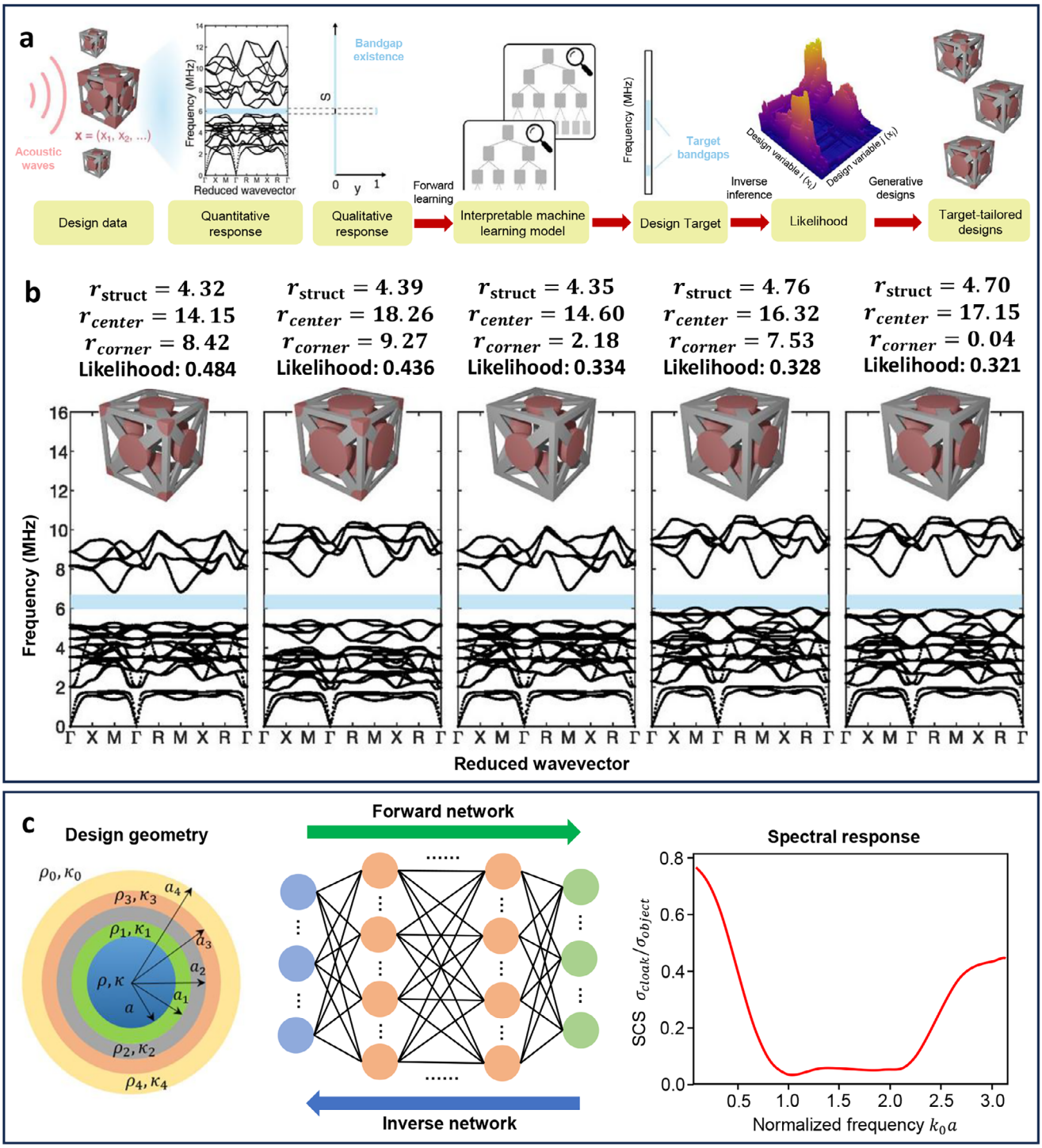

FIGURE 15 | Schematic of the inverse design process for sound propagation structures and corresponding results. (a) A framework terms random-forest-based interpretable generative inverse design (Reproduced with permission [299]. Copyright 2024, Wiley-VCH.) (b) Geometric parameters of five designed structures and their corresponding dispersion relations; these designs are the most likely to satisfy the specified target bandgap. Among them, only the fourth design fails to meet a small portion of the target bandgap, while the others fulfill the requirements (Reproduced with permission [299]. Copyright 2024, Wiley-VCH.) (c) Deep learning network framework for the inverse design of an acoustic invisibility cloak. Schematic of a core-shell acoustic cloak and its spectral response (Reproduced with permission [298]. Copyright 2021, American Physical Society).

have evolved inverse design from single–performance prediction to the collaborative solution of multiple constraints, providing a generalized technical route for the engineering implementation of frontier acoustic technologies.

4.3.2 | Sound Absorption

Sound absorption refers to the process of capturing sound energy via specific materials, structures, or devices, converting it into

other energy forms to reduce reflection and transmission. Its core functions include mitigating environmental noise pollution [303, 304], improving indoor acoustic environments [305], and protecting equipment and structures [306]. Current conventional approaches to sound-absorbing structure design face the following challenges [307, 308]. First, traditional design processes are constrained by material constitutive models, posing challenges in efficiently realizing compact, low-frequency, and high-performance sound-absorbing structures. Second, conventional design methods lack global search capability in multi-objective optimization, making them prone to falling into local optima. ML-based inverse design offers innovative breakthroughs for creating sound-absorbing materials. Current researches include: cavity-type metamaterials [142, 309], porous absorbers [310], resonant absorbers [311], acoustic coatings [312], composite structures [117, 313–315], and metasurfaces [316].

The inherent limitation of traditional design framework, which are strictly bound by material constitutive laws, presents a significant bottleneck in the development of compact, low-frequency, and high-performance sound-absorbing metastructures. Overcoming this physical constraint necessitates the exploration of novel acoustic material configurations and compositions. ML-based inverse design frameworks have emerged as a powerful tool to bypass these limitations, enabling the efficient discovery of non-intuitive geometries. In the study of artificial porous sound-absorbing materials, Yan et al. [310] proposed a DNN forward prediction and GA inverse optimization architecture to design Multi-order Coiled-up Channels lined with Porous Material (MCCPM). In the frequency range of 300–900 Hz, each resonant chamber contributes a distinct absorption peak. Through the synergistic interaction between porous materials and multi-order resonant cavities, enhanced dissipation is achieved. At the peak frequency, enhanced viscous thermal dissipation occurs within both the narrow necks and coiled channels. The average sound absorption coefficient of the inversely designed MCCPM reaches 0.81, significantly outperforming traditional foam or micro-perforated panels. Furthermore, Cheng et al. [313] integrated porous materials with Helmholtz resonators. Utilizing a DNN and an optimized deep autoencoder model, they achieved inverse generation of structural geometries from target acoustic properties. The inversely designed unit structure enabled broadband filtering. Xiao et al. [316] addressed the inverse design of a metasurface absorber comprising nine parallel Helmholtz resonators. To further optimize performance, they integrated an autoencoder-like network with a probabilistic model. This model generates multiple re-optimized solutions when fed initial predicted parameters. Results demonstrated absorption bandwidth expansion from 300 to 530 Hz. Finite element simulations confirmed an MAE below 3.75% within the target frequency band for the optimized absorber.

Beyond the discovery of novel configurations, a critical challenge lies in the multi-objective nature of practical absorber design, which must simultaneously optimize for sound absorption bandwidth, lightweight construction, and structural compactness. Conventional methods often lack the global search capability required for such tasks, frequently converging on local optima. This issue demands forward-inverse integrated frameworks coupled with swarm intelligence algorithms for global optimization. An illustrative example is the work of Zhou et al. [314], who composited porous materials with double-layer microperforated panels. Their bidirectional framework, combining forward prediction and inverse generation networks, enabled mapping between structural parameters and absorption curves (Figure 16a). NSGA-II multi-objective optimization facilitated global search for Pareto-optimal solutions, avoiding local optima while balancing absorption and lightweight design (Figure 16b). The results showed that, compared with the original structure, the average sound absorption coefficient of the optimized structure has increased by 4.84%, and the total mass has decreased by 18.98% (Figure 16c). Mahesh et al. [315] developed a hybrid absorber by combining a microperforated panel with four Helmholtz resonators featuring bent necks. An invertible convolutional autoencoder network was set to inversely design broadband low-frequency absorbers. Invertible convolutional autoencoder network used only one-third of the parameters of conventional DNNs, achieving $< 4\%$ average error between predicted and target spectra. The microperforated panel outperformed traditional multilayer structures in 200–315 Hz absorption with 30% thickness reduction. On the other hand, addressing the synergistic optimization of sound absorption and energy absorption in shell-based lattice metamaterials, Hu et al. [228] proposed a forward-inverse hybrid design framework that integrated K-nearest neighbors (KNN), an ANN, and the NSGA-II. In this framework, the ANN modeled the complex structure–multi-objective property relationships (Figure 16d), while NSGA-II searched for Pareto-optimal solutions in the global design space (Figure 16e), thereby avoiding the limitation of traditional methods that tend to become trapped in local optima. Experimental results demonstrated that the optimal structure demonstrated an energy absorption capacity of 16.431 MJ/m^3, with sound absorption coefficients of 0.975 at 1,400 Hz and 0.806 at 1,600 Hz (Figure 16f).

In summary, in the field of sound-absorbing structure design, ML-based inverse design has broken through many limitations of traditional design methods while possessing strong multi-objective optimization capabilities. Specifically, inverse design based on machine learning can achieve end-to-end models that directly infer structural parameters from target acoustic performance. Furthermore, through a forward-inverse hybrid framework, it can efficiently search for optimal solutions in high-dimensional parameter spaces. By integrating various optimization algorithms, it enables the rapid design of novel sound-absorbing structures that are difficult to achieve through traditional trial-and-error methods, thereby realizing multi-objective optimization.

4.3.3 | Sound Blocking

Sound insulation refers to blocking sound transmission paths through physical structures or materials. Unlike sound absorption, its core mechanism involves reflection and blocking to impede sound penetration across interfaces. Conventional materials and designs face limitations [317, 318]. First, traditional sound insulation materials rely on increasing thickness or density to effectively block low-frequency sound waves, leading to cumbersome structures and high costs. Second, conventional approaches often sacrifice multi-physics collaborative optimization capabilities—such as mechanical load-bearing and thermal management—in the pursuit of acoustic performance. ML-based

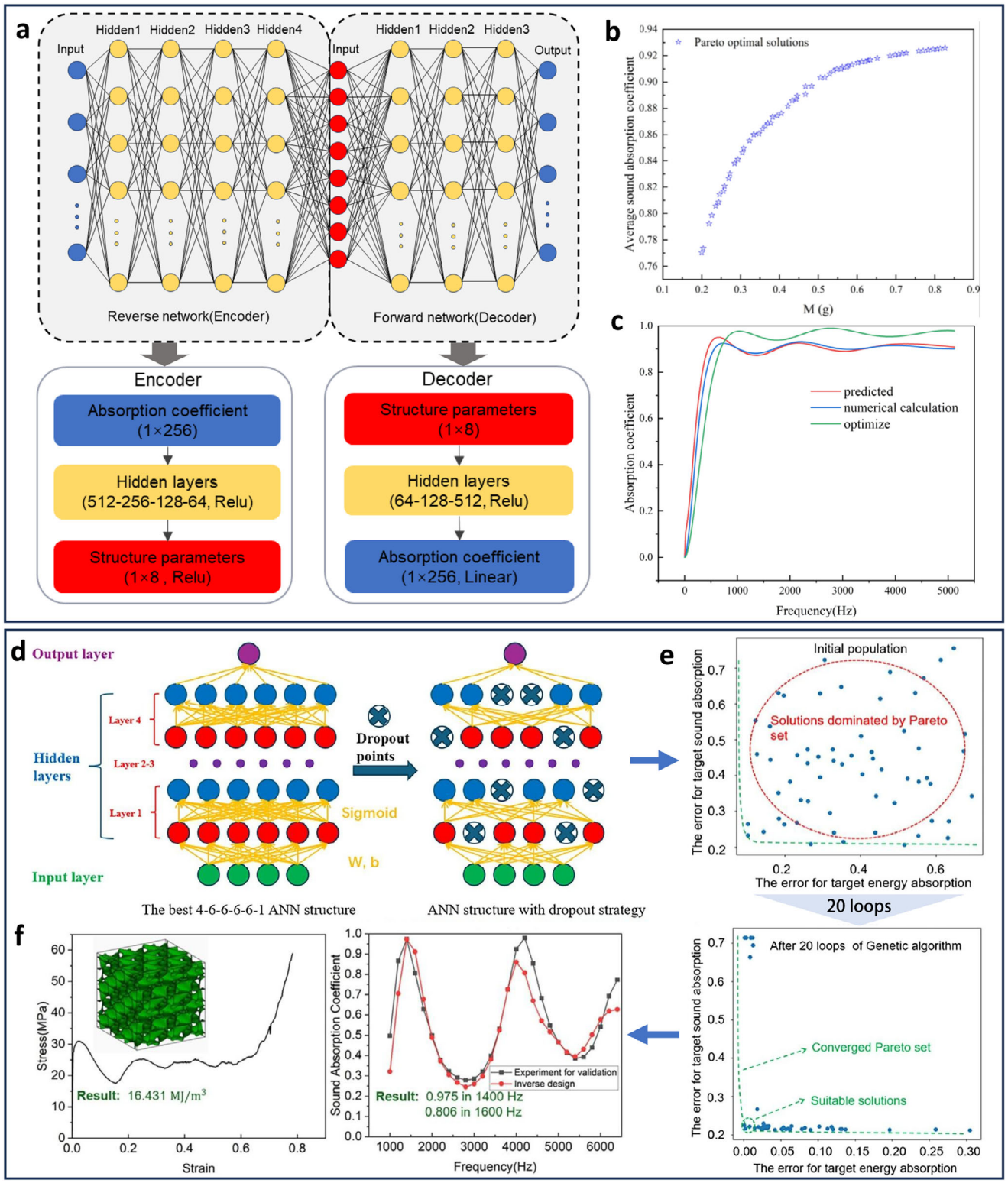

FIGURE 16 | Inverse design workflow and schematic results for sound-absorbing structures. (a) DNN framework model. Including the inverse network structure model and the forward network structure model (Reproduced with permission [314]. Copyright 2025, Springer Nature.) (b) The Pareto optimal solution set (Reproduced with permission [314]. Copyright 2025 Zhou et al., Published by Springer Nature.) (c) Comparison of the sound absorption coefficient of the optimized structure with the original structure (Reproduced with permission [314]. Copyright 2025, Springer Nature.) (d) A ANN model for predicting energy absorption capacity, and the updated ANN model after introducing the dropout strategy to prevent overfitting issues (Reproduced with permission [228]. Copyright 2024, Taylor & Francis.) (e) The initial population and the distribution of data points after 20 loops (Reproduced with permission [228]. Copyright 2024, Taylor & Francis.) (f) The most suitable shell-based lattice metamaterial for this multi-objective optimization problem, as it shows high energy absorption capacity and a respectable sound absorption coefficient in 1,400 Hz (0.975) (Reproduced with permission [228]. Copyright 2024, Taylor & Francis).

inverse design now offers breakthroughs for sound-insulating material structures, including cavity-based metamaterials [319], multilayered composites [320], and Helmholtz resonators [321].

To improve low-frequency insulation, Song et al. [320] proposed a deep learning-based inverse design for laminated plate metamaterials (LPAMs), stacking constrained-layer acoustic metamaterials and absorbers (e.g., foam). This framework includes an inverse design module and a post-processing module (Figure 17a). Based on three typical case studies, the inverse design framework was employed to develop single-layer, double-layer, and triple-layer LPAMs, respectively. The results demonstrated that all inversely designed structures meet the required specifications. The sound transmission loss (STL) of both single-layer and double-layer LPAMs showed strong agreement with the target STL, while the STL of the triple-layer LPAM exceeds the target values across most frequency bands. These findings collectively validated the effectiveness and practical utility of the comprehensive inverse design system for LPAMs. Sun et al. [321] employed a DNN to map acoustic targets (e.g., STL at specific frequencies) to equivalent electrical parameters. These equivalent electrical parameters were converted to geometric parameters via lumped-parameter technique, enabling efficient, lightweight two-order Helmholtz resonators. Within this inverse framework, inputting target STL spectra outputs normalized equivalent electrical parameters. The structure achieves high low-frequency (150–300 Hz) STL (18–25 dB peak) via resonance, with a centimeter-scale thickness enabling significant weight reduction. Similarly, Fan et al. [322] constructed an end-to-end model for the direct mapping from target broadband scattering spectra to the structural parameters of lightweight multilayer core-shell configurations. They employed deterministic and probabilistic inverse neural networks to directly generate the geometric and material parameters satisfying the requirements for broadband superscattering (Figure 17b and 17c). Mechanistically, they demonstrated that the designed structure achieves near-unity scattering responses across multiple scattering orders (Figure 17d). Experimentally, the resulting superscatterer enables efficient sound insulation with transmission below 10% over a normalized frequency range of 0.856 to 1.404, corresponding to a relative bandwidth of 48.9%, and a reflection efficiency as high as 99.94% (Figure 17e).

Another critical requirement in practical applications is the synergistic optimization of multi-performance attributes. Zhang et al. [319] proposed a forward-inverse hybrid design framework for the design of multi-gradient cavity acoustic metamaterials (MCAM). The modular, repeating units mitigate defect sensitivity, while the hollow structure ensures lightweight and high-frequency insulation. An inverse design framework (DNN+PSO) enhanced the broadband noise reduction capability, optimizing MCAM using STL as the objective function, while balancing acoustic, mechanical, and thermal performances. Impedance tube tests confirmed a 10.6–17.4 dB average STL improvement over existing structures.

In summary, ML-based inverse design demonstrates notable advantages and unique functionalities in sound-insulating structures or materials design. Compared to conventional approaches, it overcomes the limitations of traditional materials in low-frequency noise isolation, achieving high transmission loss in frequency ranges such as 150–300 Hz through mechanisms like resonance effects, while also addressing the challenge of balancing multiple performance criteria. The ML-enabled framework facilitates efficient inverse optimization by combining DNNs with optimization algorithms, rapidly tailoring structures with objectives such as transmission loss, thereby substantially enhancing noise reduction performance.

4.4 | Thermal Engineering

Thermal transport, the spontaneous migration of thermal energy from high- to low-temperature regions, requires precise regulation. This has become a central challenge for modern high-power-density, miniaturized, and extreme-condition engineering systems (e.g., chip cooling [323–325], battery thermal management [326–328], efficient heat engines [329–331]) to achieve performance breakthroughs and ensure safe operation. However, traditional design method faces several bottlenecks: First, the need to balance multiple performance metrics that are often conflicting, such as the synergistic tailoring of thermal conductivity and radiative spectrum. Second, the limitation of traditional thermal metamaterials, which suffer from functional fixedness and are ill-suited for dynamically changing environments. Third, the design of temperature field is intrinsically high-dimensional, owing to its strong dependence on both heat source locations and the spatial configuration of materials. To address these challenges, ML-based inverse design has emerged as a revolutionary paradigm for the development of thermal functional materials. Current frontier research primarily focuses on three directions: the design of thermal metamaterials [332–334], materials for radiative regulation [185, 334], and the co-design of multifunctional composites and thermal layouts [190, 335].

The design of thermal functional materials often presents a multi-objective optimization challenge. For instance, enhancing the thermal conductivity of a material must be balanced with the precise control of its radiative properties within specific wavelength bands, all while ensuring no degradation in its overall thermal management efficiency. To address such optimization problems in thermal functional materials, Garcia-Esteban et al. [332] proposed a neural network-based inverse design framework incorporating transfer learning. By flexibly defining the loss function and leveraging efficient backpropagation optimization, the neural network can rapidly identify optimal solutions that satisfy multiple objectives within the complex design space of thermal metamaterials. The optimized 8-layer hyperbolic metamaterial achieves an enhanced thermal conductivity of up to 1.31×10^5 $W/(m^2 \cdot K)$, enhancing heat transfer performance while enabling tailored radiation control within specific wavelength bands and maintaining overall thermal management efficiency. In other aspects, considerations such as the trade-off between color generation and radiative cooling performance also warrant attention. Guan et al. [185] developed an ML-assisted inverse method for designing transmissive colored radiative cooling films. This provides flexibility in balancing cooling and coloration. A memetic algorithm optimized the top radiative layer, while a joint forward-inverse network designed the bottom color filter (Figure 18a). The optimized top layer exhibits enhanced robustness, maintaining transmittance > 90% at incident angles $\leq 70°$ (Figure 18b). The transmissive colored radiative cooling film

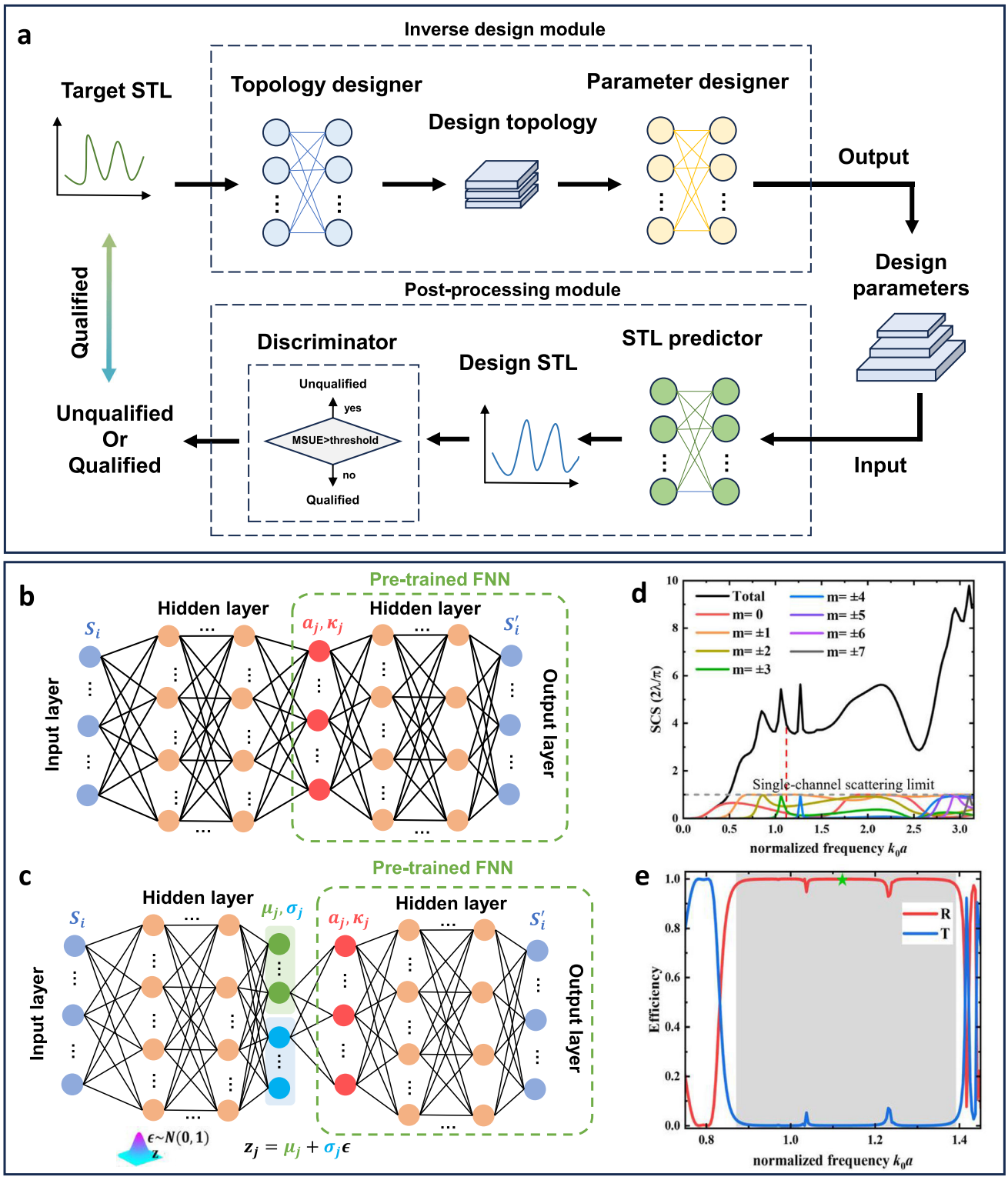

FIGURE 17 | Inverse design processes and results for sound-blocking structures. (a) Inverse design module to output the topology and parameters of LPAMs according target STL. Then discriminate the unqualified LPAM by the post-processing module [320]. (b) A deterministic inverse design model that concatenates a pretrained forward neural network as a decoder predicts spectral responses (Reproduced with permission [322]. Copyright 2026, Wiley-VCH.) (c) Probabilistic inverse design model, where the design parameter space is transformed into a latent space with a standard Gaussian distribution (Reproduced with permission [322]. Copyright 2026, Wiley-VCH.) (d) The scattering amplitude spectra of a specific superscattering configuration obtained through inverse design, shown across different scattering orders (Reproduced with permission [322]. Copyright 2026, Wiley-VCH.) (e) The transmission efficiency spectrum ultimately obtained after optimizing the inter-scatterer spacing and periodicity using an optimization algorithm (Reproduced with permission [322]. Copyright 2026, Wiley-VCH).

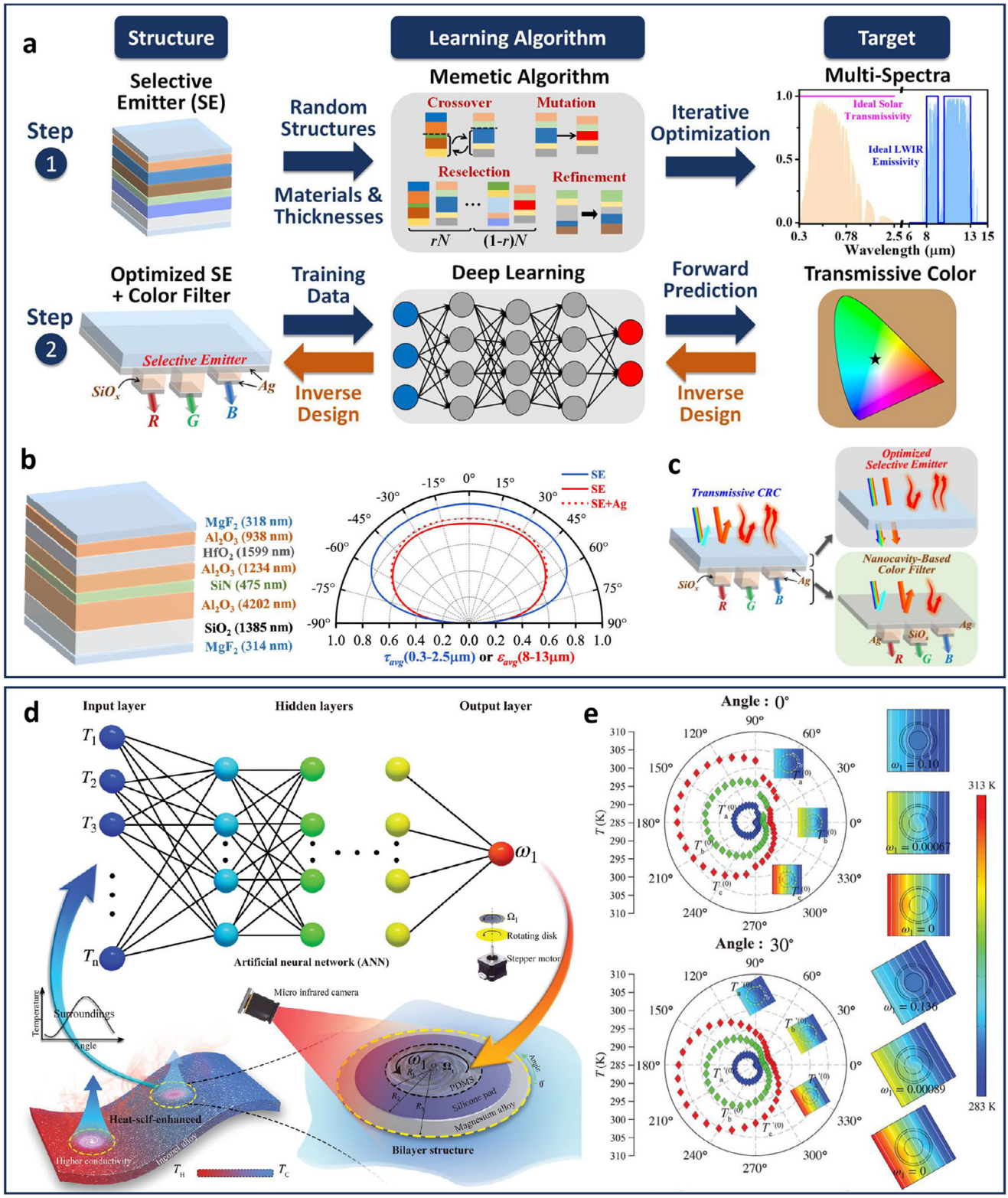

FIGURE 18 | Inverse design process and results for structures with heat transfer characteristics. (a) Overall design workflow for transmissive colored radiative cooling films (Reproduced with permission [185]. Copyright 2023, American Chemical Society.) (b) Schematic of the optimized selective emitter (SE) (showing layer materials/thickness) and polar plots of spectrally averaged solar transmittance (blue, solid), SE long-wavelength infrared emissivity (red, solid), and SE+Ag emissivity (red, dashed) versus incident angle (Reproduced with permission [185]. Copyright 2023, American Chemical Society.) (c) Schematic of the transmissive colored radiative cooling film comprising a top SE and bottom Ag − SiO_x − Ag nanocavity-based color filter (Reproduced with permission [185]. Copyright 2023, American Chemical Society.) (d) Schematic of the deep learning-assisted active metamaterial (Reproduced with permission [336]. Copyright 2023, Wiley-VCH.) (e) Simulated response of the thermal-enhanced diffusion metamaterial; stable core zone temperature gradient under rotating external thermal field (Reproduced with permission [336]. Copyright 2023, Wiley-VCH).

selectively transmits specific colors while reflecting infrared and unused visible light, minimizing heat absorption (Figure 18c).

Furthermore, most conventional thermal metamaterials are typically designed with fixed structures and operating conditions, rendering their functionalities locked-in post-fabrication and incapable of dynamic adjustment in response to environmental variations (e.g., fluctuations in ambient temperature or changes in heat source direction). To address this limitation, Jin et al. [336] proposed a closed-loop intelligent system integrating an infrared camera, a pre-trained neural network, a stepper motor, and a bilayer thermal material. In this system, the infrared camera captures real-time ambient temperature data around the metamaterial and inputs it into the pre-trained neural network, which rapidly computes the optimal rotational speed for the central rotating component. Subsequently, the stepper motor actuates the rotation of the core component, thereby modulating the effective thermal conductivity and enabling automatic regulation of the temperature gradient within the central region (Figure 18d). This mechanism empowers the thermal material to adaptively respond to changing environmental temperatures, maintaining stable thermal performance (Figure 18e).

The pathways and efficiencies of heat transfer are highly dependent on the location of heat sources and the spatial configuration of materials. However, addressing this issue often proves challenging to resolve through intuition or conventional physical models, particularly within high-dimensional combinatorial design spaces, where the search process becomes exceptionally time-consuming. To overcome this problem, Sun et al. [190] proposed the show attend and read model (SAR)-heat source layout inverse design framework, transforming heat source layout inverse design into an image-to-sequence prediction problem. Using temperature field images as input, SAR directly outputs discrete heat source location sequences. The framework achieves 100% prediction accuracy under temperature constraints. For material configuration, Yang et al. [335] proposed an inverse design framework for composite layouts based on a transfer learning strategy. The framework is capable of outputting the layout of a composite plate-heat source system according to the desired temperature or stress field. By leveraging transfer learning, the approach achieves 100% accuracy in heat source prediction and 99.98% accuracy in composite plate constituent prediction with only a limited amount of data. The results demonstrated that the average time required for the inverse design of material layouts is significantly reduced to 0.0284 s.

In summary, the ML-based inverse design framework offers a methodology that transcends traditional paradigms in the field of thermal engineering. Confronted with the complex design challenges of thermal metamaterials and functional thermal systems, this framework not only effectively addresses issues intractable for conventional methods–such as navigating high-dimensional parameter spaces and achieving multi-objective synergistic optimization–thereby enabling the simultaneous realization of enhanced thermal conductivity, radiative modulation, and color functionality. More importantly, by endowing materials with environmental perception and dynamic response capabilities, it overcomes the inherent limitation of traditional thermal metamaterials whose functionalities are fixed and unable to adapt to dynamic environments. Furthermore, concerning the non-intuitive, high-dimensional design problem involving heat source placement and material configuration, this inverse design framework transforms the design process from iterative, trial-and-error physical experimentation to data-driven, performance-oriented optimization.

4.5 | Optical Engineering

Optical functional materials are pivotal to advancing modern technology, underpinning innovations in communications, precision manufacturing, medical diagnostics and therapy, as well as consumer electronics and display systems. The drive toward higher performance and miniaturization in optical materials encounters considerable challenges. First, the design space for optical structures is typically defined by a vast number of geometric parameters. Conventional search and optimization algorithms often require numerous iterations, rendering them highly inefficient. Second, the relationship between optical response and geometric structure frequently exhibits a many-to-one mapping, meaning multiple distinct structures can yield identical spectral or functional characteristics, introducing uncertainty into the inverse design process. Third, optical design must satisfy physical laws (e.g., Maxwell's equations) and fabrication constraints. Ignoring these limitations may result in generated structures that cannot be practically fabricated or that fail to perform as intended. Currently, ML-enabled inverse design presents a transformative opportunity for engineering complex optical systems and tailoring functional material properties [337–348].

The traditional search and optimization methods are relatively inefficient when tasked with exploring the complex design space of optical structures, necessitating the adoption of machine learning techniques such as surrogate modeling or direct generative approaches. For instance, Peurifoy et al. [204] employed an ANN for both light scattering simulation and inverse design of multilayer nanoparticles. Their inverse design framework comprised two stages: an ANN predicting scattering spectra from layer thickness inputs, followed by gradient descent for rapid convergence to optimal geometries. This achieves precise single-wavelength narrowband and broadband scattering, outperforming standard gradient-free optimization methods by orders of magnitude in speed. In addition, Tang et al. [201] introduced an A-cVAE for designing a nanopatterned power splitter, incorporating an adversarial block to isolate latent variables from conditional parameters. An active learning strategy addressed limited data coverage, enhancing model generalizability. An average improvement of approximately 5% in the total transmission efficiency was achieved for devices generated by A-cVAE; moreover, as this generative model requires no additional electromagnetic simulations, new designs can be generated almost instantaneously.

Another significant challenge in the inverse design of optical materials is the many-to-one mapping problem, where multiple structural configurations yield similar optical responses. To address this, generative models and bidirectional networks have been employed to learn the complex relationships between optical responses and structural parameters. For example, So et al. [349] introduced a forward-inverse network for designing core-shell nanoparticles. The model mastered the complex relationship between spectral responses and structural parameters, rather

than learning a simple one-to-one mapping. The experimental results demonstrated that even when provided with identical or similar target spectra, the model is capable of generating diverse and valid designs. When tasked with achieving spectrally isolated magnetic dipole resonances or the spectral overlap of electric and magnetic dipole resonances, the model successfully identified multiple structural solutions that satisfy the underlying physical constraints. For three-dimensional optical metamaterials, which inherently exhibit a many-to-one mapping, Ma et al. [130] proposed a generative model-based design framework (Figure 19a). In this approach, the deep generative model consists of three sub-models: a recognition model, a forward prediction model, and a generative model (Figure 19b). Following semi-supervised training, a generated structure was retained only if the spectral error between its simulated response and the target spectrum was less than 0.2. Experimental validation demonstrated that, whether targeting specific reflection spectra in metamaterials or designing chiral mirrors, the model consistently generated a variety of geometrically distinct designs, all of which produced simulated spectra in excellent agreement with the target.

Ensuring that designed optical structures comply with physical laws and fabrication constraints is equally critical. To this end, researchers have explicitly incorporated physical information and geometric limitations into the design pipeline. For example, Liu et al. [351] introduced a neural network-based inverse design framework comprising three components (a simulator, generator, and critic) to design metasurfaces with target spectral responses. This model guides the generator's exploration of feasible solution spaces by incorporating geometric and physical constraints via the critic, addressing the challenge of high-dimensional design freedom. Capable of handling multiple input spectra, this approach significantly reduces the workload for complex problems requiring multiple metasurfaces or graded structures. Another powerful strategy involves embedding physical constraints via reward functions in reinforcement learning. Park et al. [350] introduced physics-informed reinforcement learning (PIRL) for the design of one-dimensional metasurface beam deflectors (Figure 19c). In their approach, physics-informed pretraining was employed to guide the RL agent away from invalid regions of the design space. Subsequently, the RL framework incorporated minimum feature size constraints via the reward function, thereby enforcing fabrication feasibility. By leveraging deep Q-learning, the RL agent acquired the ability to pursue long-term rewards, endowing it with global optimization capabilities. Experimental results demonstrated that, compared to other optimization algorithms, PIRL achieves the fastest convergence and highest efficiency (Figure 19d), while simultaneously ensuring that the designed structures remained fabricable.

In summary, ML-based inverse design offers multidimensional solutions to core challenges in optical engineering: it substantially reduces computational costs by efficiently exploring high-dimensional design spaces, addresses the non-uniqueness inherent in inverse problems through generative models, satisfies multiple performance metrics simultaneously via multi-objective optimization frameworks, and ensures practical utility by incorporating physical and fabrication constraints. These advancements have not only propelled the development of cutting-edge fields such as nanophotonics, metamaterials, and quantum optics, but have also laid a solid foundation for the rapid and intelligent design of next-generation high-performance optical devices.

4.6 | Biomedical Engineering

Biomedical functional materials are intrinsically linked with numerous engineering disciplines, encompassing the development of novel pharmaceuticals, design of biomedical materials, fabrication of biosensors, and beyond. This field is dedicated to enhancing the precision, efficiency, and personalization of healthcare—spanning prevention, diagnosis, therapy, and rehabilitation—thereby playing a pivotal role in tackling contemporary medical challenges, prolonging life expectancy, and elevating life quality. In recent years, machine learning has infused new vitality into this field. Notably, inverse design strategies powered by ML are reshaping traditional approaches to medical material development, substantially accelerating research and development processes, and opening new pathways for the discovery and innovation of advanced functional materials.

4.6.1 | Novel Drugs

The goal of drug development is to discover novel molecules with specific chemical properties for disease treatment. Despite advances in computational tools, designing safe and effective novel molecular entities remains challenging. These challenges can be summarized into several pervasive core issues. First, the conventional drug discovery framework exhibits low exploration efficiency and success rates when confronted with the vast chemical space, resulting in limited innovation in the discovered compounds. Second, in structure-based drug design, a key challenge lies in designing small molecules capable of accurately recognizing and binding to specific protein targets while avoiding interactions with non-target proteins. Third, fragment-based drug discovery represents another important research pathway, but designing appropriate linkers to connect two or more molecular fragments presents significant difficulties. Currently, inverse design strategies based on machine learning have made substantial progress in drug molecular design, offering novel paradigms for pharmaceutical research and development [90].

The exploration of the vast chemical space remains a fundamental bottleneck in traditional drug discovery, necessitating a paradigm shift towards more efficient methodologies. In response, ML-based inverse design frameworks have emerged as powerful tools for de novo drug design. Numerous approaches have been developed to design new drug molecules, including RNNs [352–354], RL [355], and generative models such as VAEs [75, 352, 355, 356], GANs [357], diffusion models [358, 359]. A notable example of this framework's power is the work by Zhavoronkov et al. [355], who integrated the VAE generative model, reinforcement learning, and tensor factorization—a method termed generative tensorial reinforcement learning (Figure 20a)—to rapidly design novel DDR1 kinase inhibitors. They successfully mapped discrete molecular structures into a continuous latent space by training a VAE model on multiple datasets. RL was then applied within this latent space to explore new molecules, guided by three self-organizing maps acting as reward functions. Experimental validation demonstrated that two

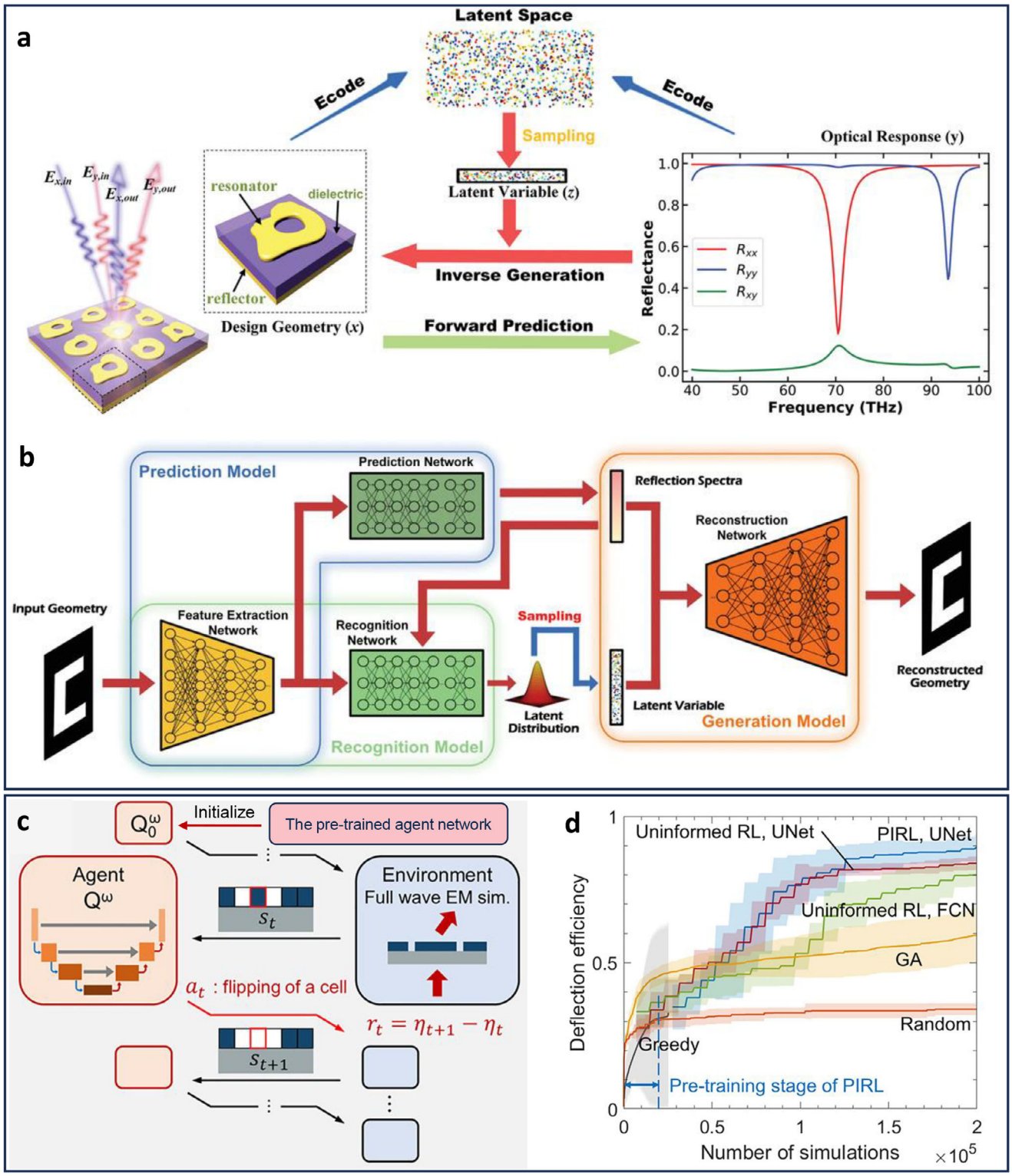

FIGURE 19 | The inverse design workflow and outcomes for optical materials. (a) The proposed deep generative model for metamaterial design and characterization. The metamaterial design and optical response are encoded into a latent space with a predefined prior distribution, from which the latent variables are sampled for inverse generation. The forward path is modeled as a deterministic prediction process (Reproduced with permission [130]. Copyright 2019, Wiley-VCH.) (b) Architecture of the proposed deep generative model. Three submodels, the recognition model, the prediction model, and the generation model, constitute the complete architecture (Reproduced with permission [130]. Copyright 2019, Wiley-VCH.) (c) Illustration of agent-environment interaction in reinforcement learning, including definitions of state, action, and reward. The agent network is initialized with a pre-trained network (Reproduced with permission [350]. Copyright 2024, De Gruyter.) (d) Performance comparison of physics-informed reinforcement learning with other algorithms: physics-informed reinforcement learning based on U-Net achieves the highest deflection efficiency (blue) (Reproduced with permission [350]. Copyright 2024, De Gruyter).

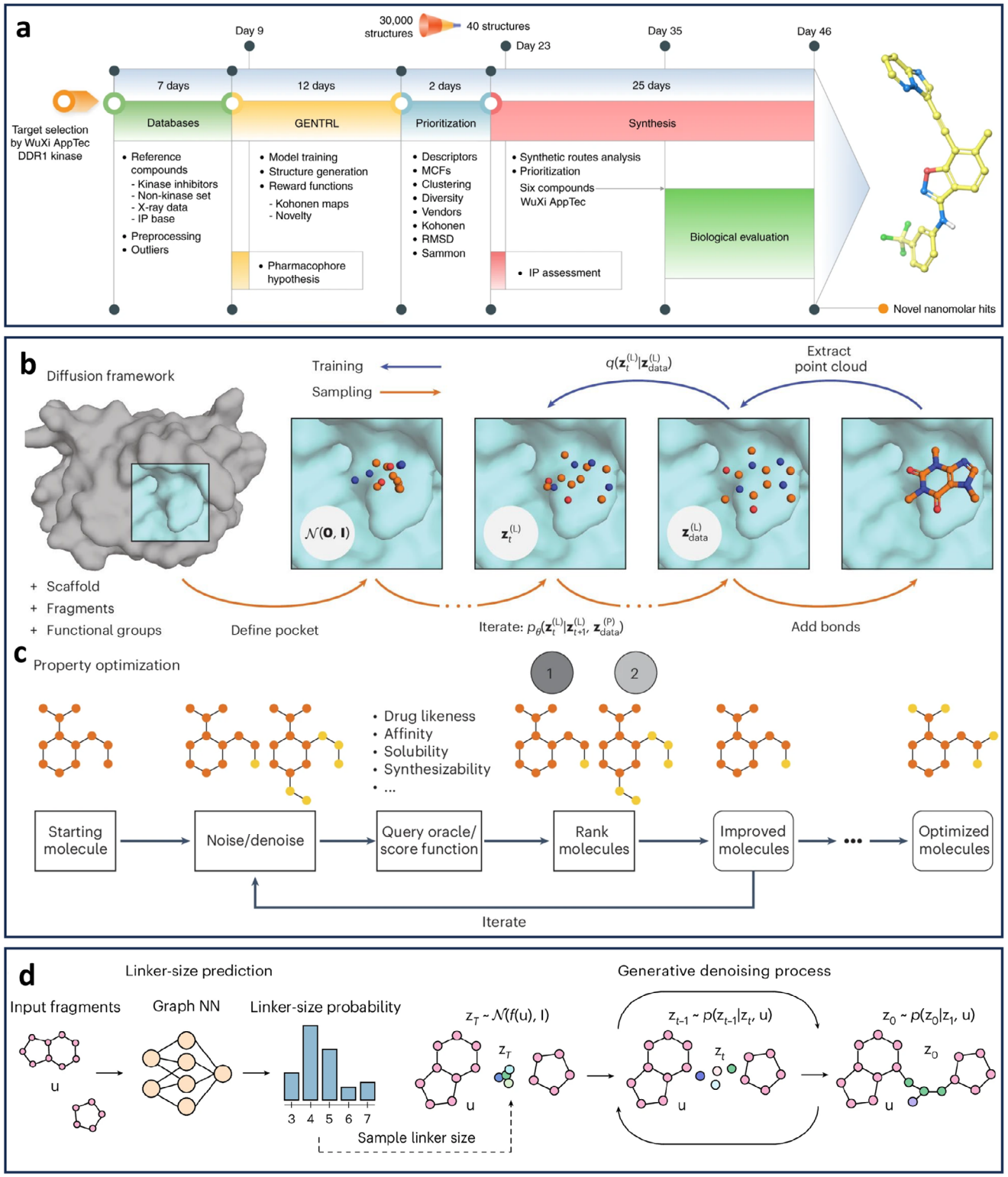

FIGURE 20 | An overview of the application of ML-based inverse design in drug development. (a) General workflow of Generative Tensorial Reinforcement Learning for candidate compound design (Reproduced with permission [355]. Copyright 2019, Springer Nature) (b) Framework and workflow of a diffusion model. Carbon, oxygen, and nitrogen atoms are represented in orange, red, and blue, respectively (Reproduced with permission [358]. Copyright 2024, Springer Nature.) (c) Application of minimal noise followed by a series of denoising steps to explore variations of the initial molecule. A new set of molecules is ranked by a predictor, and the process is repeated to select the highest-scoring candidates (Reproduced with permission [358]. Copyright 2024, Springer Nature.) (d) Molecular linker generation process. A GNN computes linking size probabilities for input fragments, and a fragment-conditioned equivariant diffusion model samples and denoises linker atoms (Reproduced with permission [359]. Copyright 2024, Springer Nature).

compounds exhibit potent inhibitory activity and high selectivity; for instance, Compound 1 exhibits significantly greater inhibitory activity against the DDR1 target than against DDR2. Notably, the entire process-from target identification to compound design, synthesis, and validation-was completed in only 46 days, significantly shorter than the traditional multi-year drug development cycle.

Addressing the challenge of inversely designing ligand molecules that bind with both high affinity and high selectivity to a specific protein target necessitates structure-based drug design, which in turn requires fully accounting for the three-dimensional structural constraints of the target protein. Schneuing et al. [358] introduced an equivariant diffusion model named DiffSBDD (Structure-Based Drug Design) (Figure 20b). They employed two protein pocket conditioning strategies and represented molecules as graphs to enhance computational efficiency. Additionally, by fixing certain atoms corresponding to known active substructures, the model generated the remaining structure. An iterative "noise-denoise" cycle coupled with a scoring function was used to select optimal molecules (Figure 20c). The experimental results demonstrated optimized kinase inhibitor specificity. The docking score for the target kinase increased, reflecting enhanced affinity, while that for the off-target kinase decreased, indicating improved specificity.

Furthermore, within the specific context of fragment-based drug discovery, a particularly intricate inverse design problem arises: the automated and intelligent linkage of multiple molecular fragments into complete, synthetically accessible drug candidates. This task is especially challenging as it must be performed under strict 3D steric and chemical compatibility constraints imposed by the target protein's binding site. ML-based inverse design paradigms are now providing innovative solutions to this precise challenge. To address this issue, Igashov et al. [359] developed DiffLinker for inverse molecular linker design. Given the 3D structures of multiple disjoint fragments, a GNN first predicts the probability distribution over linker atom counts. A denoising diffusion probabilistic model then iteratively refines the linker (Figure 20d). The final denoised linker atoms combine with the input fragments to form a full molecule. Experimental results showed that this method not only efficiently designs linkers but also overcomes limitations of conventional approaches—such as being restricted to connecting two fragments, inability to autonomously determine linker atom count and attachment points, and disregard of 3D protein pocket constraints.

In summary, ML-based inverse design demonstrates significant advantages and unique functional characteristics in the field of novel drug development. In terms of advantages, it not only substantially shortens the research and development cycle but also significantly enhances efficiency and success rates. By enabling precise exploration of the chemical molecular design space, it effectively addresses the low screening efficiency and limited innovation associated with traditional methods in vast molecular spaces. Functionally, this design strategy centers on de novo drug design and leverages various neural network frameworks-such as RL, VAEs, and diffusion models-to directionally generate novel lead compounds with desired pharmacological and physicochemical properties. It overcomes many limitations of conventional approaches and exhibits superior performance in key metrics including synthetic accessibility and drug-likeness. These attributes establish machine learning-based inverse design as an efficient, precise, and innovative pathway for drug discovery.

4.6.2 | Medical Materials

In the field of biomedical engineering, medical materials refer to natural or synthetic substances used to diagnose, treat, repair, or replace human tissues and organs, or to enhance their functions. These typically include orthopedic implants, cardiovascular stents, artificial heart valves, and tissue scaffolds. The current traditional design methods present some issues: First, medical materials typically require a multi-objective performance encompassing mechanical strength, biocompatibility, and other properties, making design through trial and error inherently inefficient. Second, patient-specific variability renders mass production insufficient to meet clinical needs, as traditional methods struggle to rapidly generate personalized implants that conform to specific anatomical structures and mechanical environments. Third, certain application scenarios demand materials with special properties that are inherently challenging to achieve through conventional design, such as anisotropic mechanical behavior and shape memory deployability. In response to these challenges, ML-based inverse design exhibits unique advantages: starting from predefined performance targets, it inversely deduces the composition and structure of medical materials.

Medical materials are often required to simultaneously satisfy multiple, and frequently conflicting, performance indicators. For instance, orthopedic implants must possess an elastic modulus that closely matches that of natural bone to mitigate stress shielding, while also exhibiting sufficiently high yield strength to withstand physiological loads. To address this issue, Peng et al. [183] proposed an active learning approach that integrates generative models, 3D neural networks, and finite element simulations for the multi-objective optimization (elastic modulus, yield strength) of orthopedic implants (Figure 21a). After dimensionality reduction of the porosity matrix via an encoder, the design framework performs efficient exploration of complex architectures within the latent space. Subsequently, a decoder reconstructs the latent space vectors back into the original porosity matrix (Figure 21b). Results showed a nearly 20% increase in yield load and ultimate bearing capacity, indicating enhanced mechanical support.

Orthopedic implants are intended to be implanted into the human body to replace, support, or restore the function of bones or joints [362]. Due to significant variations in individual bone morphology, mass production alone is insufficient to meet the needs of all patients in clinical practice. This challenge necessitates the custom design of diverse orthopedic implants. To address this issue, Jia et al. [363] introduced an ML and topology optimization-based framework for inverse design of orthopedic implants, which not only enables rapid prediction of microstructure–property relationships but also facilitates the automatic generation of spatially varying frequency distributions. By inversely deducing microstructural parameters from stress targets, they successfully designed patient-specific femoral scaffolds. The inverse-designed scaffold restricted micromotion at

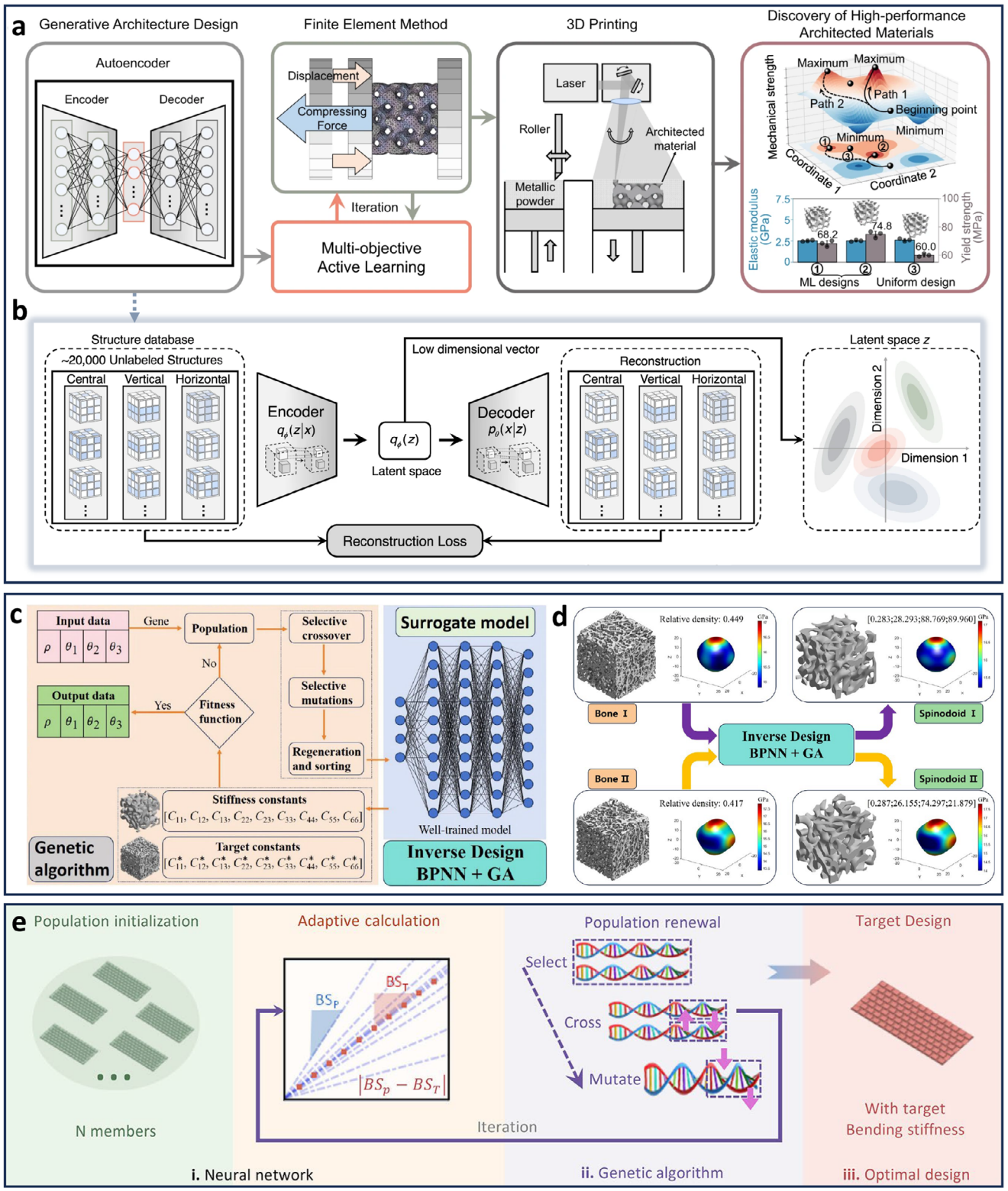

FIGURE 21 | An overview of the application of ML-based inverse design in medical materials. (a) The framework and workflow of generative architecture design and multi-objective active learning loop (Reproduced with permission [183]. Copyright 2023, Springer Nature.) (b) The generation model for the target scaffold. The encoder takes the scaffold porosity matrix as input, and the decoder can serve as a generator for proposing new scaffolds based on the learned latent sapce representation (Reproduced with permission [183]. Copyright 2023, Springer Nature.) (c) Inverse design workflow for scaffolds based on BP neural network and GA (Reproduced with permission [360]. Copyright 2025, Elsevier.) (d) Comparison of Young's modulus surfaces between Type I and II bones and spinodoid bone scaffolds (Reproduced with permission [360]. Copyright 2025, Elsevier.) (e) Machine learning-based inverse design process incorporating neural networks, evolutionary algorithms, and optimization design (Reproduced with permission [361]. Copyright 2025, American Chemical Society).

the fracture site to 0.3 mm, within the optimal range for bone regeneration (0.2–1.0 mm).

For medical materials with specially tailored complex properties, establishing a general design framework is essential to provide a correct design rationale for the development of novel medical materials exhibiting such properties. Forward-inverse hybrid design frameworks are widely applied in this field. For instance, Wang et al. [360] proposed an inverse design strategy for aperiodic porous structures (termed spinodoids) by integrating a forward prediction model (BPNN) with a GA (Figure 21c). The BPNN was embedded as a surrogate model within the GA to optimize the design parameters, minimizing the discrepancy between the nine target elastic constants of bone tissue and those predicted by the BPNN. The resulting spinodoid scaffolds (Type I and II) exhibit highly matched mechanical properties with the target bone. The spatial distribution of Young's modulus (Figure 21d) demonstrated close alignment between the scaffolds and natural bone, indicating comparable anisotropic behavior. Furthermore, in the design of medical thermal metamaterial implants, Jiao et al. [361] integrated a BP neural network with an evolutionary algorithm (Figure 21e) to automatically determine microstructural parameters with bending stiffness as the target. The BPNN, trained on experimental data, accurately predicted the relationship between parameters such as thickness and height and the resulting bending stiffness. Subsequently, the evolutionary algorithm iteratively optimized these parameters. In the porcine tracheal stent experiment, the resulting stent's strength increased by more than 421-fold, and its cross-sectional area increased by 223%, achieving a synergistic design of mechanical properties and shape memory functionality.

In summary, ML-based inverse design offers a systematic solution to the three core, long-standing challenges in the field of medical materials. To address the problem of multi-objective performance optimization, machine learning models, serving as efficient surrogates, can be integrated with active learning or evolutionary algorithms to rapidly search vast design spaces for optimal solutions that satisfy mutually conflicting performance indicators. In response to the demand for personalization, inverse design frameworks enable the derivation of microstructural parameters from patient-specific mechanical targets, facilitating the precise adaptation of implant morphology and performance. For the realization of specially tailored complex properties, machine learning establishes high-dimensional structure-property mappings via surrogate models. When combined with optimization algorithms, this approach can uncover configurations and properties unattainable through conventional methods, while simultaneously ensuring manufacturability.

4.6.3 | Medical Sensors

Sensors are characterized by their ability to convert target signals into readable outputs according to specific principles. Medical sensors, in particular, refer to devices specifically designed to measure, monitor, or diagnose physiological, biochemical, or physical parameters related to human health or disease states. These typically include physiological, biochemical, and physical parameter sensors, among others. Designing high-performance, reliable, and practical medical sensors is highly challenging. First, medical sensors often suffer from signal saturation and nonlinear response, leading to compromised measurement accuracy. Second, concerning sensor sensitivity, devices optimized through conventional methods still exhibit insufficient responsiveness to trace concentration variations. Third, the specificity and selectivity of medical sensors remain challenging, as traditional approaches are limited by their lack of precise predictive capabilities regarding complex molecular interactions. Currently, ML-based inverse design offers an innovative pathway to overcome these limitations.

In medical monitoring, flexible pressure sensors serve as core components for health tracking and tactile feedback, requiring highly linear responses across a broad pressure range. However, conventional devices often suffer from signal saturation due to structural limitations, leading to measurement distortion. To address this issue, Liu et al. [364] proposed an inverse design model based on machine learning. Their approach utilized a small dataset to train a model that predicts optimal geometric parameter combinations for iontronic microstructures in flexible pressure sensors, substantially enhancing design efficiency (Figure 22a). The results demonstrated that the sensor array designed using this model could output accurate total pressure regardless of object placement, without the need for calibration. This effectively achieves high linearity across a wide pressure range, thereby addressing the issue of signal saturation. (Figure 22b).

In biomedical detection, to address the challenge of insufficient sensor response to minute concentration changes, ML-based inverse design frameworks have been employed to efficiently and accurately traverse and optimize sensor structures. For instance, in malaria detection, Wekalao et al. [365] applied machine learning to the inverse design of terahertz metasurface biosensors. They trained an extreme Gradient Boosting (XGBoost) regression model to accurately and rapidly predict sensor absorption responses under various design parameter combinations. This model enabled efficient exploration of the vast design parameter space and identification of optimal configurations, ultimately facilitating the inverse design of a high-performance malaria sensor. It can detect minute changes in Plasmodium concentration, achieving a peak sensitivity of 429 $GHzRIU^{-1}$, a detection accuracy of 25.6, and a figure of merit of 10.989 RIU^{-1}.

In response to the challenges of low specificity and selectivity in biomedical sensors, it is essential to develop novel biosensors. For instance, in the detection of chiral enantiomers, Zhang et al. [119] proposed a deep learning-based inverse design strategy for chiral metasurface biosensors. A forward screening network (ResNet18) that rapidly evaluates whether the circular dichroism of a metasurface structure meets requirements (Figure 22c), and an inverse design network (cVAE) that generates metasurface structural images corresponding to a target circular dichroism response (Figure 22d). For experimental validation, the inversely designed structure closely matched the target in center frequency and lineshape (Figure 22e). In biosensing tests (Figure 22f), the sensor enabled discrimination between D/L-glutamic acid enantiomers at a concentration of 0.1 mg/mL, with a circular

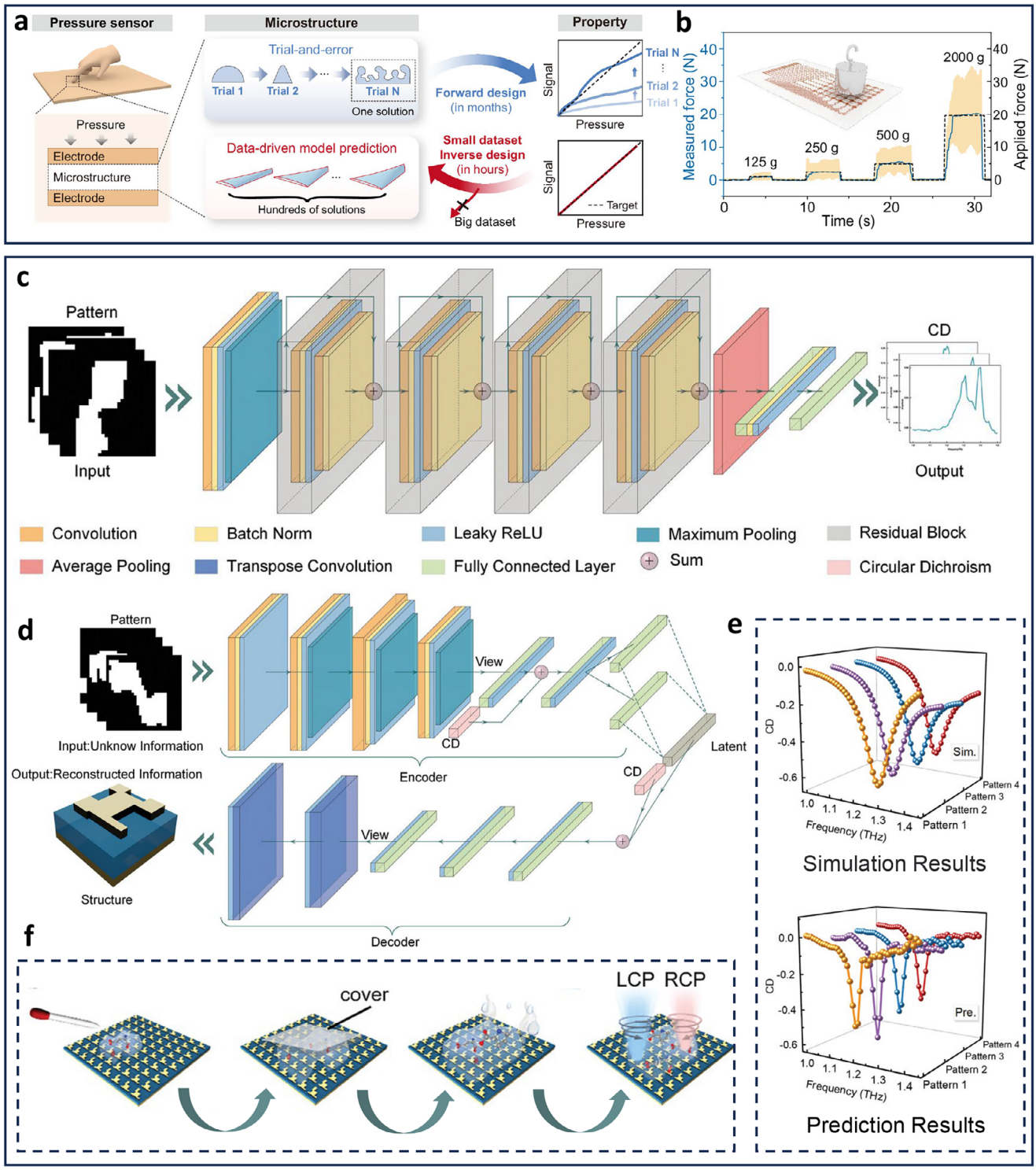

FIGURE 22 | An overview of the application of ML-based inverse design in medical sensors. (a) Schematic of the inverse design for a flexible pressure sensor. The left panel shows the common device structure of flexible pressure sensors. The right panel compares the time-consuming traditional forward design with the inverse design approach (Reproduced with permission [364]. Copyright 2024, PNAS.) (b) Sum of signals from all sensing units. The yellow region displays the amplified response range of all sensing units, with an amplification factor of 49 (i.e., the number of sensing units) (Reproduced with permission [364]. Copyright 2024, PNAS.) (c) Forward network based on the deep residual network ResNet18 (Reproduced with permission [119]. Copyright 2024, Wiley-VCH.) (d) Inverse network based on a conditional VAE (Reproduced with permission [119]. Copyright 2024, Wiley-VCH.) (e) FSN simulation results of the inversely designed metasurface and FSN prediction results of the inversely designed metasurface (Reproduced with permission [119]. Copyright 2024, Wiley-VCH.) (f) Inversely designed biosensor metasurface and schematic of the experimental procedure (Reproduced with permission [119]. Copyright 2024, Wiley-VCH).

dichroism value difference of approximately 0.05. The response exhibits concentration dependence, endowing the sensor with high specificity and selectivity.

In summary, ML-based inverse design has overcome the limitations of traditional approaches in the field of medical sensors. On one hand, models trained on small datasets or GANs effectively address the issue of insufficient sample availability. On the other hand, ML models enable rapid performance prediction for various parameter combinations and efficient exploration of the vast design space, significantly enhancing development efficiency. Functionally, ML-driven inverse design empowers medical sensors with superior performance and enhanced detection accuracy. It not only addresses specific shortcomings of conventional sensors-such as signal saturation and low sensitivity-but also improves their specificity and selectivity. For instance, inversely designed chiral metasurface biosensors can accurately distinguish D/L enantiomers, while terahertz metasurface biosensors detect minute changes in Plasmodium concentration. These advances substantially improve the practicality and reliability of medical sensors in applications such as health monitoring and disease diagnosis, offering an efficient and precise new pathway for developing high-performance medical sensors.

4.7 | Chemical Engineering

The essence of chemical functional materials lies in controlling energy transfer and chemical reactions across molecular, unit, and system scales. Translating laboratory innovations into practical applications not only generates material value but also drives the pursuit of cleaner, more efficient, and sustainable resource utilization to meet pressing global environmental and energy demands. In this review, we concentrate on two key areas: the design and optimization of catalytic materials, and the treatment of greenhouse gases. However, as sustainability goals grow increasingly complex, conventional design approaches-often reliant on trial-and-error and empirical knowledge-prove inefficient and costly for exploring novel materials and optimizing multifaceted systems. Therefore, machine learning-assisted inverse design offers significant potential for discovering and generating optimal material structures or process parameters to fulfill these objectives.

4.7.1 | Catalysts Design and Optimization

Catalysts play a central role in the chemical industry by enhancing reaction rates and process efficiency. Catalyst design relies on understanding structure–property relationships, such as how physicochemical characteristics influence activity, selectivity, and stability-to guide the development of novel catalysts. However, traditional methods suffer from the following limitations. First, the conventional trial-and-error approach is often constrained by existing knowledge frameworks, leading to limited innovation. Second, in high-dimensional complex chemical spaces, traditional methods struggle to conduct comprehensive searches, making it difficult to precisely identify the most promising catalysts. Third, catalyst design often requires balancing multiple performance indicators, such as high conversion rate and high selectivity, or high activity and long-term stability. Traditional single-objective optimization approaches fail to achieve the optimal trade-off among these multiple performance metrics. Inverse design, driven by target performance metrics and facilitated by machine learning, offers a promising alternative for deriving optimal material structures [366].

To reduce the heavy reliance of traditional catalyst development on empirical expertise, which restricts the ability to transcend established knowledge frameworks, researchers have employed neural networks to elucidate the relationships between material structures and catalytic properties. This approach enables the direct generation of novel material structures with targeted performance ranges and has demonstrated significant innovation. For instance, Kim et al. [367] proposed an improved GAN for the design of porous materials such as zeolites. Rather than modifying existing structures, they directed the model to generate new architectures directly from a target performance criterion–specifically, an adsorption heat in the range of 18–22 kJ/mol. This approach yielded six final structures, four of which fell within the desired target range. The results demonstrated that 4 out of the 6 generated candidates successfully achieve the targeted performance, offering a pioneering approach for directly "creating" catalysts based on desired properties. Building upon this concept, Mok and Back [368] introduced a Transformer-based machine learning model (CatGPT) for the inverse design of inorganic catalysts (Figure 23a). They encoded catalyst structures as strings, enabling the model to learn the "language" of catalyst structures. By inputting performance indicators such as target adsorbates, CatGPT directly "generates" novel catalyst structures in a manner analogous to writing a text. After fine-tuning on a small dataset, the ten structures generated by the model were all verified by DFT calculations to meet the high-activity criteria. Importantly, all these generated structures represent novel binary alloy combinations. In addition, Song et al. [369] proposed a framework termed "Material Generation with Efficient Global Chemical Space Search" (Figure 23b) for the design of electrocatalysts for CO_2 reduction (CO_2RR). This approach first employs a crystal diffusion variational autoencoder (CDVAE) to efficiently generate a diverse set of plausible catalyst surface structures from the latent space. Subsequently, a supervised GNN combined with a bird swarm algorithm accelerates the closed-loop search. Experimental results demonstrated that five alloys generated by this framework exhibit promising performance. Notably, both CuAl and Pd_5Sn_2 alloys achieve a Faradaic efficiency of approximately 90% for CO_2 electroreduction (Figure 23c and 23d), underscoring the framework's capability to discover high-performance catalysts within the vast chemical space. These works demonstrated that ML-based direct inverse generation frameworks have transcended conventional trial-and-error approaches, possessing unprecedented innovative capabilities.

The catalytic performance is not dictated by a single factor but arises from the complex coupling of multiple variables, including composition, structure, and external reaction conditions. Traditional approaches are prone to becoming trapped in local optima, thereby missing the globally optimal combinations. The integration of machine learning with optimization algorithms holds great promise in the design of chemical catalysts. For instance, Li et al. [370] addressed the optimization of catalysts for plastic waste pyrolysis by first employing a machine learning model (XGBoost) to learn from historical data, accurately

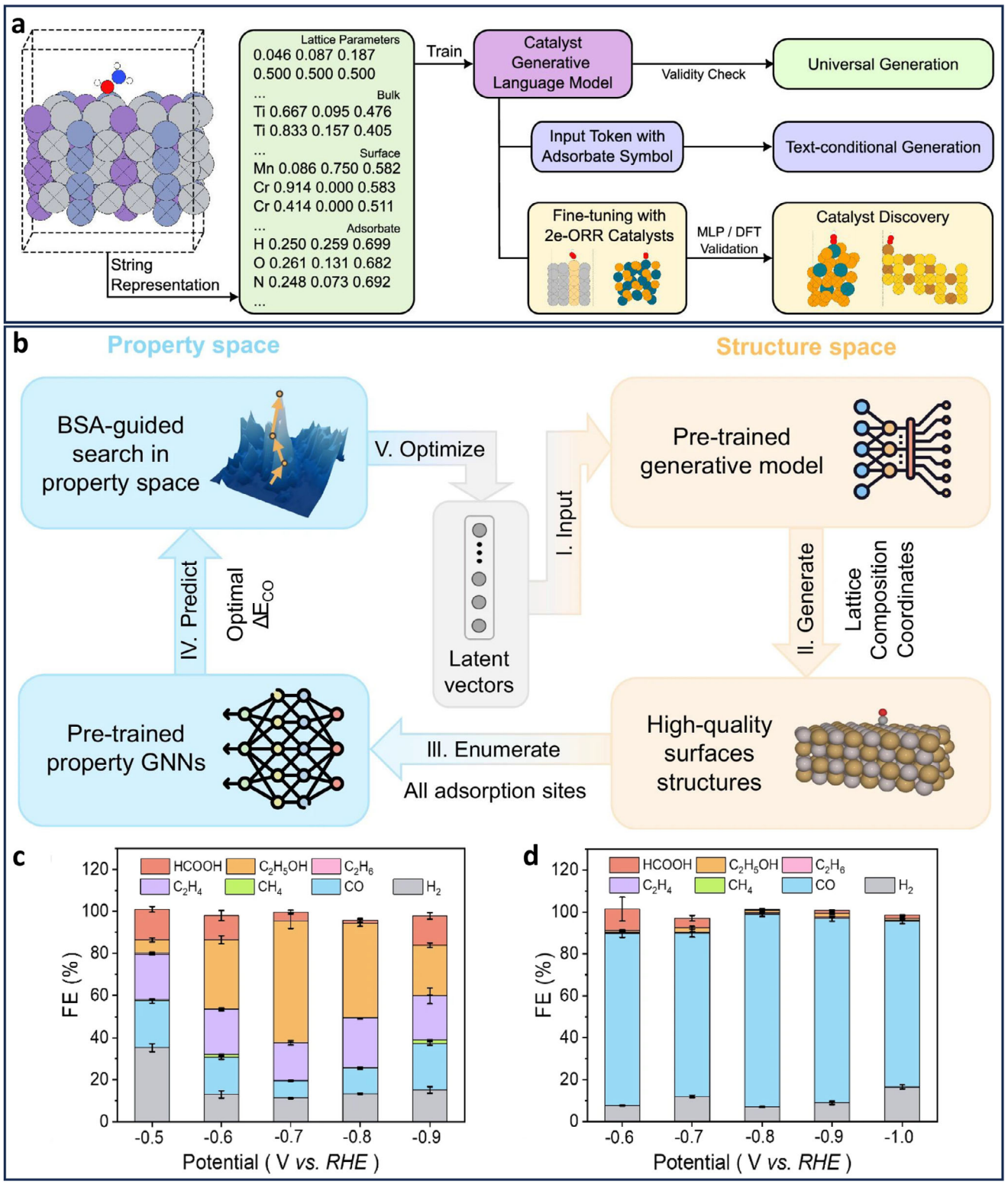

FIGURE 23 | The application of ML-based inverse design in catalysts design and optimization. (a) Workflow of the catalyst generation model, including training, fine-tuning, and evaluation (Reproduced with permission [368]. Copyright 2024, American Chemical Society.) (b) The closed-loop inverse design process, integrating CDVAE, supervised GNN, and bird swarm algorithm (Reproduced with permission [369]. Copyright 2025, Springer Nature.) (c) The faradaic efficiencies towards CO_2RR products under a range of applied potentials in 1 M KOH of CuAl alloys (Reproduced with permission [369]. Copyright 2025, Springer Nature.) (d) The faradaic efficiencies towards CO_2RR products under a range of applied potentials in 1 M KOH of Pd_5Sn_2 alloys (Reproduced with permission [369]. Copyright 2025, Springer Nature).

establishing the complex relationships among catalyst structure, reaction conditions, and catalytic efficiency. Subsequently, they integrated a PSO algorithm to inversely search for the optimal solution within the entire variable space. This strategy not only identified highly efficient catalysts but also reduced the reaction temperature by approximately 30% compared to conventional methods, significantly lowering energy consumption. This work demonstrated a synergistic optimization of both the catalyst and the reaction conditions. Similarly, Jiang et al. [371] adopted the strategy of combining predictive models with optimization algorithms in the design of inorganic catalysts for water treatment. They represented catalysts using four descriptors: cobalt atom count, metal diversity, oxygen atom count, and support type. After data collection, they trained a highly accurate AdaBoost model, which was combined with Sparrow Search Algorithm (SSA) to output optimal catalyst parameters. For instance, in experimental validation for norfloxacin degradation via a free radical mechanism, SSA recommended Co_3O_4, achieving a 97% removal rate.

The integration of forward predictive models with multi-objective optimization algorithms proves highly effective for achieving multi-objective optimization in catalyst design. For CO_2 conversion catalysis, Chandana et al. [372] proposed integrating a bayesian regularized artificial neural network with NSGA-II multi-objective optimization. This network served as a surrogate model, accurately predicting CO_2 conversion and lower olefin selectivity. Subsequently, NSGA-II was employed to simultaneously maximize these two performance metrics. The non-noble catalyst achieves 78.78% CO_2 conversion and 89.36% lower olefin selectivity, with yield increasing from 36.75% to 70.39%. The noble metal catalyst reached 73.78% conversion and 94.72% selectivity, with yield rising from 19.53% to 69.8%. These results demonstrated that the synergy between machine learning and optimization algorithms enables substantial simultaneous improvements across multiple key performance indicators.

In summary, for catalyst design and optimization, machine learning-based inverse design offers a fundamental advantage over traditional approaches reliant on expert experience and trial-and-error. It overcomes key limitations-such as handling multiple variables, long development cycles, and limited innovation-by efficiently deriving optimal catalyst structures and reaction conditions from target performance metrics, thereby significantly accelerating development and enhancing catalytic performance. Utilizing various models, including neural networks, GANs, and Transformers, combined with optimization algorithms (e.g., PSO, SSA, NSGA-II, bird swarm algorithm), this approach establishes a closed-loop workflow from performance objectives to structural design. It enables accurate learning of structure-property relationships and high-performance prediction, direct generation of novel catalyst structures with specified properties (e.g., CDVAE generating high-quality alloy surfaces, catalyst generative pretrained transformer producing unprecedented binary alloy combinations), and efficient navigation of vast chemical spaces to identify optimal solutions. These capabilities demonstrate the transformative potential and application value of machine learning-driven inverse design in catalyst research and development.

4.7.2 | Greenhouse Gas Treatment

The issue of greenhouse effect has become increasingly severe, emerging as a pressing global concern. In the field of chemistry, researching effective methods for handling greenhouse gases is of paramount importance. Current approaches primarily center on three stages: adsorption (capture), conversion (utilization), and sequestration. Currently, metal-organic frameworks (MOFs) are being widely applied in the adsorption of greenhouse gases owing to their high specific surface area, tunable pore structures, and chemical properties. However, traditional methods for designing MOFs have been challenging, particularly in precisely achieving structures that meet specific performance targets and in effectively conducting multi-objective optimization. In this context, the introduction of machine learning for inverse design in this field enables the efficient and accurate development of MOFs tailored to target requirements.

To address the demand for precise design of materials with specific target properties, machine learning-based inverse design has demonstrated powerful directional capabilities. For instance, Xin et al. [373] focused on machine learning-based inverse design of MOFs, but employed computational topology and natural language processing to automatically generate MOF structures and chemical descriptors. Machine learning models were then used for multi-objective performance prediction and screening. Ultimately, for various targets (e.g., CO_2 adsorption performance, CH_4 storage capacity, CO_2 catalytic conversion), this inverse design framework generated optimal MOFs that met the desired performance expectations.

In response to the need for multi-objective trade-offs, ML-based inverse design exhibits even more unique advantages. Park et al. [374] proposed using deep reinforcement learning for the inverse design of MOFs capable of directly capturing CO_2 from the air. Both the MOF generator and predictor architectures are based on transformer (Figure 24a and 24b), with a reward function evaluating the performance of generated MOFs. After three rounds of reinforcement learning iterations, the performance of the generated MOFs improved significantly. For instance, the CO_2 adsorption heat increased from 19.16 kJ/mol to 33.52 kJ/mol, and CO_2/H_2O selectivity rose from 1.74 to 4.14, demonstrating the success of this method in inverse designing target MOFs and effectively optimizing their performance. The newly generated dual-objective MOFs exhibit both high adsorption heat and high selectivity (Figure 24c). Furthermore, Cleeton and Sarkisov [114] employed a novel approach, deep dreaming strategies, to optimize the organic linkers of MOFs by backpropagating gradient information, driving the target properties toward predefined values. They represented the three components of MOFs (organic linkers, inorganic nodes, and topology) as strings, integrating LSTM, attention mechanisms, and MLP for prediction. Through gradient ascent, the input representations were iteratively refined to align the predicted properties with the target values (Figure 24d). In the multi-objective optimization of CO_2 adsorption heat and selectivity, the model successfully shifted the distribution toward higher adsorption heat and improved selectivity.

In summary, the dual challenges faced by traditional methods in designing MOFs–specifically, the difficulty in precisely achieving

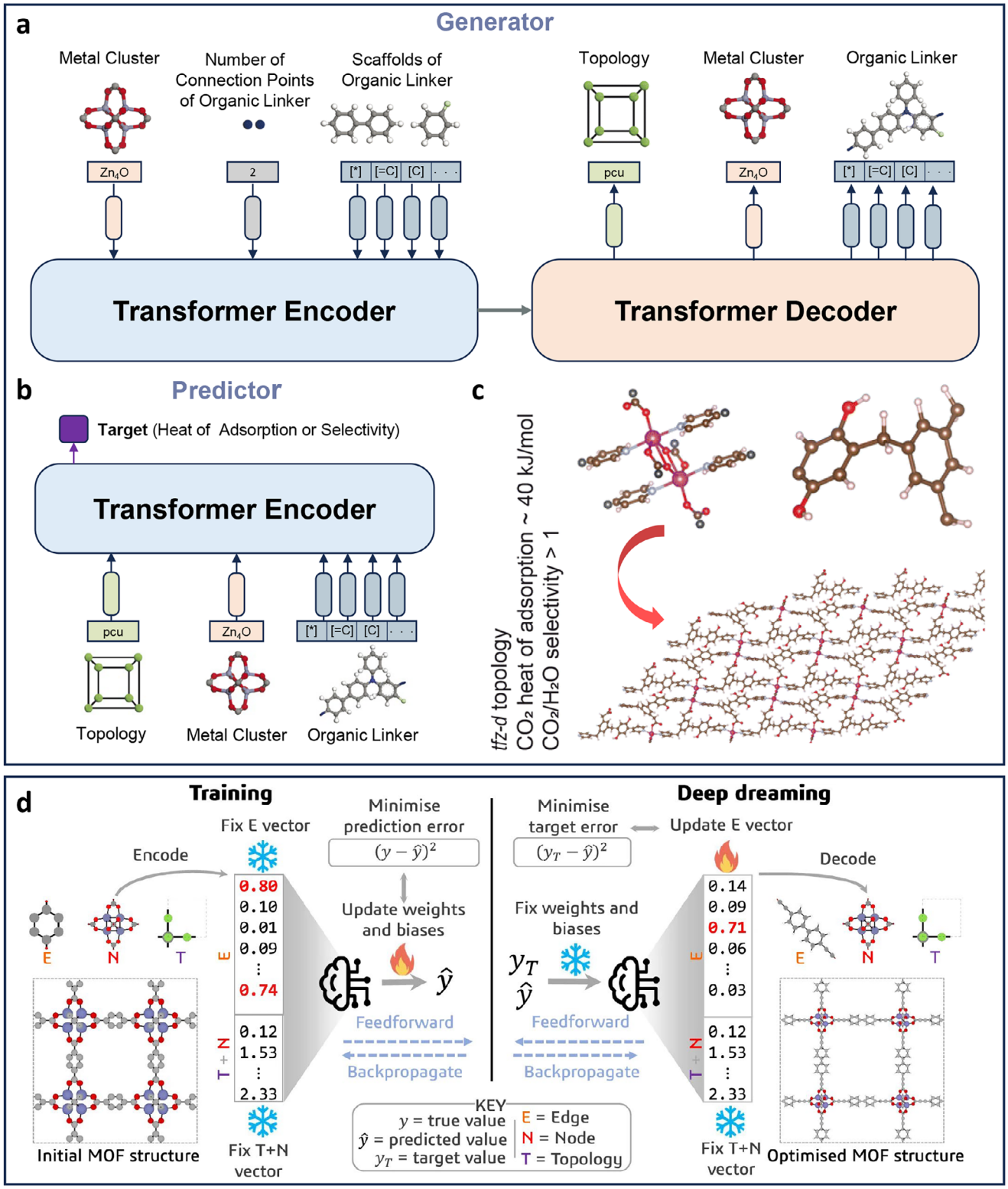

FIGURE 24 | An overview of the application of ML-based inverse design in greenhouse gas treatment. (a) Architecture of the generator, comprising a transformer encoder and decoder (Reproduced with permission [374]. Copyright 2024, Royal Society of Chemistry.) (b) The predictor, based on a transformer encoder, takes the generator's MOF representations as input and predicts target properties of interest (Reproduced with permission [374]. Copyright 2024, Royal Society of Chemistry.) (c) MOF structure generated by the inverse design framework, exhibiting high CO_2/H_2O selectivity (>1) and moderately high CO_2 adsorption heat (≈ 40 kJ $\cdot$ mol^{-1}) (Reproduced with permission [374]. Copyright 2024, Royal Society of Chemistry.) (d) Employing a deep dreaming approach for the inverse design of MOFs, the forward (training) phase involves an ML model learning to predict MOF properties by adjusting weights and biases through standard forward and backpropagation procedures. In the inverse (dreaming) phase, feedforward and backpropagation are similarly utilized to update edge encodings, thereby optimizing the MOF structure by minimizing the discrepancy between the predicted properties of the initial MOF and specified target properties (Reproduced with permission [114]. Copyright 2025, Springer Nature).

target-specific properties and the inability to conduct effective multi-objective optimization–are precisely the context in which machine learning-based inverse design proves its utility. By reframing the design problem as a search of structural space constrained by performance targets, inverse design not only efficiently generates customized materials that meet specific metrics but also identifies global optima amidst complex multi-objective trade-offs. This provides a practicable pathway for the on-demand development of high-performance materials in the field of greenhouse gas treatment.

4.8 | Other Applications

The ML-based inverse design framework has been widely applied in fields such as mechanical and energy engineering, and also demonstrates considerable research value and application potential in the domain of functional materials for civil and architectural engineering. As a fundamental sector closely tied to human productivity and daily life, civil and architectural engineering consistently emphasizes the safety, economy, durability, and functionality of structural materials. Introducing an ML-driven inverse design framework into this field can help overcome existing technical bottlenecks and create targeted pathways for innovation in functional material systems.

In civil and architectural engineering, there is a growing need to develop advanced functional materials that simultaneously meet multiple performance objectives, such as balancing mechanical strength, durability, cost efficiency, environmental sustainability, and vibration isolation [375]. Traditional material design approaches are often limited by empirical knowledge and iterative trial-and-error processes. Therefore, leveraging machine learning for the inverse design of construction-related functional materials presents a promising direction. Many inverse design paradigms from mechanical and acoustic engineering-such as energy-absorbing metamaterials, sound-absorbing porous media, and thermally insulating composites-can be adapted and extended to civil engineering applications. Nevertheless, numerous high-performance functional materials in this field remain unexplored. For example, Brzin and Brojan [124] integrated a GAN architecture into the inverse design of deformable soft composite beams, overcoming computational challenges in nonlinear multi-solution spaces. Their approach achieves a design speed of 0.8 s per 10,000 parameter sets with minimal shape deviation, demonstrating suitability for smart deployable structures in adaptive bridges or buildings. This case highlights the significant potential of ML-based inverse design in advancing functional materials for civil and architectural applications.

In summary, inverse design based on machine learning offers distinct advantages and functional capabilities in the development of civil engineering materials. Its strength lies in transcending the limitations of conventional design methodologies and knowledge systems, thereby substantially improving design efficiency and material performance. Functionally, it enables powerful multi-objective optimization-whether balancing strength, durability, cost, and environmental attributes of building materials, or tailoring acoustic, thermal, and mechanical responses for specific applications. Through ML techniques such as GANs and reinforcement learning, this framework can learn latent patterns from data and generate novel material solutions. These capabilities underscore its usability, importance, and broad application potential in tackling complex material design challenges across functional engineering domains.

5 | Challenges and Prospects

5.1 | Challenges

Despite the substantial progress in ML-driven inverse design, several unresolved bottlenecks continue to impede its translation from laboratory demonstrations to reliable real-world deployment and large-scale industrial adoption. These bottlenecks primarily arise from four interconnected issues: the persistent discrepancy between simulations and experimental observations, the prohibitive cost and infrastructure demands of data acquisition for complex systems, the lack of interpretability and certifiable physical consistency in ML models, and the substantial computational burden associated with training and deploying advanced architectures. Unless systematically addressed, these limitations restrict trust, reproducibility, certification, and integration into existing engineering workflows. This section therefore focuses on how these unresolved issues directly constrain practical deployment, reliability, and regulatory acceptance in real engineering environments.

One of the most pressing challenges is the inconsistency between simulation data used for model training and real-world experimental results. In practice, most ML-driven inverse design pipelines rely heavily on synthetic data generated from physics-based simulations, which, although controllable and scalable, inevitably idealize material behavior, boundary conditions, and fabrication tolerances. As a consequence, models that demonstrate high predictive accuracy in silico often suffer performance degradation when transferred to experimental or manufacturing settings. This simulation–experiment gap constitutes a fundamental deployment bottleneck: even minor discrepancies in material properties, geometric tolerances, or environmental noise can invalidate optimized designs, thereby undermining confidence in ML-generated solutions for high-precision domains such as functional materials, photonics, and aerospace components. In control-related applications, models trained under idealized assumptions may fail to maintain robustness under real-world disturbances, further limiting their readiness for safety-critical deployment.

The second major challenge is the prohibitive cost and infrastructure requirements associated with data generation and model training in complex, high-dimensional inverse design problems. For many functional material systems, generating sufficiently diverse and high-fidelity datasets requires extensive numerical simulations or expensive experimental campaigns, which are often beyond the reach of industrial timelines and budgets. This data bottleneck directly constrains the scalability of supervised and generative learning approaches in real-world settings. High-dimensional design spaces further exacerbate sample inefficiency and increase the risk of overfitting, limiting the reliability of learned inverse mappings. Although dimensionality reduction, transfer learning, and generative modeling provide partial mitigation, robust and industry-ready solutions for high-dimensional,

data-scarce environments remain largely unresolved. Furthermore, the substantial computational resources required to train and maintain high-capacity architectures (e.g., diffusion models or transformers) pose additional barriers to integration within existing industrial design pipelines, where computational efficiency, cost-effectiveness, and real-time responsiveness are essential.

Third, the interpretability and physical consistency of ML models represent critical bottlenecks for deployment in safety-critical, regulation-sensitive, or certification-intensive domains. Deep neural networks and other high-capacity models often operate as opaque black boxes, providing limited transparency regarding the causal or physics-governed relationships underlying the design–performance mapping. Such opacity hinders trust among domain experts, complicates model validation, and makes it challenging to satisfy regulatory or certification requirements that demand traceability and explainability. Moreover, without explicit physical constraints, ML-generated designs may violate conservation laws, manufacturability limits, or material feasibility constraints, which can render them unsuitable for direct fabrication. Although PINNs and constrained optimization frameworks have been proposed to mitigate these issues, their scalability, robustness, and compatibility with complex high-dimensional inverse design tasks remain insufficiently validated for widespread industrial adoption.

In response to the aforementioned challenges, three core solution pathways can be identified:

First, to address the discrepancies between simulation and experimental data while enhancing model trustworthiness, it is essential to develop learning frameworks that integrate physical principles with experimental validation. These frameworks embed physical laws (e.g., conservation laws, material constraints) directly into neural network architectures and establish experimental feedback mechanisms to ensure model outputs align with physical principles. Implementation approaches include: developing hybrid architectures that couple differentiable physics simulators with neural networks, constructing training loops incorporating real-time experimental validation, and formulating joint optimization objectives combining physical constraints with data-driven learning. Such frameworks not only improve model generalizability in real-world environments but also reduce reliance on massive datasets through physics-consistent regularization.

Second, to tackle data scarcity and high computational costs in high-dimensional design problems, a technical system emphasizing data-efficient utilization and knowledge transfer should be developed. This includes constructing foundational models via meta-learning for rapid adaptation to new tasks, employing multi-fidelity modeling to enable collaborative training across data of varying accuracy levels, and establishing cross-material/cross-scale feature transfer mechanisms. By excavating underlying patterns in design spaces, these methods significantly reduce dependence on large annotated datasets for specific scenarios, maintaining model performance under limited data conditions while alleviating computational burdens in high-dimensional optimization.

Third, to overcome model opacity and address complex engineering constraints, interactive design platforms integrating human expertise must be established. Such systems incorporate explainable AI techniques (e.g., attention mechanisms, symbolic reasoning) to transparentize design decision processes, develop real-time human-machine interfaces enabling domain experts to inject physical intuition and empirical rules, and create multi-objective trade-off analysis tools assisting engineers in navigating high-dimensional Pareto fronts. This human-AI symbiotic paradigm not only enhances the physical plausibility of model outputs but also strengthens credibility and practicality in engineering applications through visualized decision processes.

In summary, the continued advancement of ML-driven inverse design hinges on addressing its current limitations through interdisciplinary approaches that unify data-driven modeling, physical insight, and computational efficiency. By confronting these challenges, the field can progress toward creating intelligent, adaptive, and deployable design tools that transcend disciplinary boundaries and accelerate innovation across the engineering sciences.

5.2 | Prospects

The future of AI-driven inverse design will increasingly converge with predictive multiscale materials design, shifting from analyzing correlations to uncovering hierarchical physical principles across scales, thereby enabling the explainable and controllable creation of optimal structures from molecules to macroscale systems. Generative AI will actively invent novel materials and devices rather than just searching existing options. This transformation will be catalyzed by the integration of physics-based modeling, multiscale simulation, and collaborative AI ecosystems that reason across composition-structure-property-performance relationships beyond human intuition. Furthermore, the coupling of AI-driven inverse design with advanced manufacturing platforms–such as additive manufacturing and atomically precise fabrication–will establish tightly integrated design-to-manufacturing pipelines, enabling real-time design-verification-fabrication loops that dramatically shorten innovation cycles.

First, future inverse design will transcend the current black-box paradigm of input-output mapping. AI will move beyond merely learning complex correlations between the design space and performance targets, aiming instead to autonomously compress and abstract the underlying physical laws or chemical principles from massive design datasets. In this paradigm, inverse design systems will not only generate optimal structures but also extract transferable, multiscale design rules–bridging atomistic interactions, microstructural organization, and macroscopic functionality. Consequently, inverse design will evolve into a scientific discovery engine capable of revealing causal mechanisms that link molecular architecture to system-level performance, thereby transforming "materials by trial" into truly predictive "materials by design."

Second, with the maturation of generative AI, the core mechanism of inverse design will shift from screening for optimal solutions within a vast design space to actively and directionally creating unprecedented solutions. By leveraging generative

models (e.g., diffusion models, generative adversarial networks) in conjunction with quantum calculations, molecular dynamics, and continuum simulations, systems will be able to synthesize novel molecules, crystal structures, hierarchical composites, or metamaterial topologies that are consistent with physical constraints across scales. This will inaugurate a new era of "Generative Inverse Design," in which composition, microstructure, processing parameters, and structural architecture are co-optimized simultaneously, enabling on-demand creation of high-performance materials that are directly manufacturable.

Third, to overcome the limitations of human prior knowledge, future inverse design systems will adopt a multi-agent architecture. Within this ecosystem, AI agents specializing in distinct roles (e.g., atomistic simulation, microstructure modeling, process optimization, manufacturing feasibility assessment, and theoretical deduction) will collaboratively explore the design space across multiple physical scales. Such systems can iteratively propose hypotheses, validate them through embedded physics simulations, critique alternatives, and refine solutions in a closed-loop reasoning framework. By integrating scholarship, physical modeling, and data-driven inference, these multi-agent platforms may unlock materials and structures that transcend conventional intuition while remaining grounded in physical realizability.

Finally, the convergence of AI-driven inverse design with digital twins and intelligent manufacturing infrastructures will profoundly reshape the paradigm of materials innovation. Inverse design systems will increasingly be embedded within cyber–physical platforms, where digital twins continuously integrate real-time sensor data, simulation updates, and predictive models to guide material evolution throughout its life cycle. In this setting, inverse design ceases to function as an isolated computational module and instead becomes an active component of an intelligent design-to-manufacturing ecosystem. It can perceive the environment in real-time, generate candidate designs (e.g., new material molecules or optical structures), and perform preliminary performance simulations and screening locally. By coupling predictive modeling with additive manufacturing and in-situ monitoring, such closed-loop systems can drastically compress the iteration cycle from digital concept to physical realization. Moreover, distributed intelligent networks–spanning simulation platforms, manufacturing units, and experimental facilities–will collectively form an innovation ecosystem in which materials can be conceived, validated, fabricated, and refined in an integrated manner. This distributed yet coordinated intelligence may ultimately democratize advanced inverse design capabilities while maintaining the rigorous multiscale consistency required for industrial impact.

6 | Conclusions

This work presents a comprehensive and systematic review of machine learning–enabled inverse design, integrating fragmented advances across diverse functional material systems into a coherent methodological framework. By mapping the evolution from topology-optimization-based strategies to data-driven direct inversion and forward–inverse hybrid paradigms, and by analyzing how machine learning models and optimization algorithms adapt to variations in data availability, physical knowledge, and design-space dimensionality, this review clarifies not only the technical landscape but also the underlying principles shaping the field.

Across mechanical, acoustic, thermal, optical, energy-functional, biomedical, catalytic, and other emerging multifunctional materials, we observe that methodological choices are intrinsically coupled to physical mechanisms, combinatorial complexity, and data regimes. Mechanical and acoustic systems often integrate physics-based surrogates with global optimization to ensure structural reliability. Optical and photonic materials leverage deep generative models and differentiable optimization to navigate high-dimensional, wave-governed design spaces. Chemical and biomedical materials, characterized by vast compositional possibilities and limited labeled data, increasingly rely on conditional generation, active learning, Bayesian optimization, and transformer- or diffusion-based architectures. Meanwhile, physics-informed and differentiable frameworks offer particular advantages in data-scarce yet well-understood systems by embedding governing equations directly into the learning and optimization process.

Beyond methodological diversity, a deeper transformation is underway. Machine learning–enabled inverse design is progressively dissolving the traditional boundary between modeling, optimization, and realization. As physics-based simulation, data-driven intelligence, and advanced manufacturing technologies converge, inverse design is evolving from an iterative computational tool into an integrated design-to-manufacturing paradigm. In this emerging framework, target performance metrics serve as inputs, and the outputs increasingly approach physically consistent, fabrication-aware blueprints rather than abstract numerical solutions.

Future progress will likely be driven by three converging directions: tighter integration of physical constraints with generative AI, development of adaptive and interpretable models that balance data efficiency with scalability, and the establishment of closed-loop pipelines linking simulation, experiment, and autonomous optimization. Rather than replacing domain knowledge, machine learning acts as an amplifier of physical reasoning, enabling exploration of design regions that would remain inaccessible to intuition or brute-force enumeration.

Ultimately, ML-driven inverse design not only accelerates materials discovery but also redefines how functional materials are conceived, validated, and realized. By unifying data, physics, and computation within scalable optimization frameworks, it provides a foundation for predictive multiscale engineering–where material functionality is no longer searched for, but systematically constructed from specification to manufacturable implementation.

Acknowledgments

This work was funded by National Natural Science Foundation of China (Grant Nos. 52575130, 52422504), Guangdong Basic and Applied Basic Research Foundation, China (Grant No. 2026A1515010148), and Shenzhen Natural Science Fund (Grant No. JCYJ20230808105206013). W. L. acknowledges the support by Hong Kong Research Grants Council

(C4074-22G and STG5/E-103/24-R), Hong Kong Centre for Logistics Robotics of InnoHK, and The Chinese University of Hong Kong (Project No. 4055178). L. J. acknowledges the support by the Hong Kong Research Grants Council under the Hong Kong PhD Fellowship Scheme (No. PF21-60853). We also thank Chiara Daraio from the California Institute of Technology for her valuable insights and suggestions.

Conflicts of Interest

The authors declare no conflicts of interest.

Data Availability Statement

All data supporting the findings of this study are included within the article.

References

1. F. Wang, F. Luo, Y. Huang, X. Cao, and C. Yuan, "4D printing via multispeed fused deposition modeling," *Advanced Materials Technologies* 8, no. 2 (2023): 2201383.

2. Y. Tan and Y. Zhou, "Improved crashworthiness of sandwich wing structures by using negative Poisson's ratio honeycomb cores," *Thin-Walled Structures* 213 (2025): 113223.

3. Z. Zhang, K. Wang, B. A. Bednarcyk, L. Le Barbenchon, and Y. Chen, "Tailoring the architecture of fractal lattice metamaterials for tunable energy absorption," *Composites Part B: Engineering* 305 (2025): 112711.

4. H. Zhang, H. Zhu, H. Shi, and H. Fan, "Hierarchical truss-core sandwich cylinder: Additive manufacturing, testing and multi-elastoplastic-failure analyzing," *International Journal of Mechanical Sciences* 300 (2025): 110479.

5. R. Wang, C. Yuan, J. Cheng, et al., "Direct 4D printing of ceramics driven by hydrogel dehydration," *Nature Communications* 15, no. 1 (2024): 758.

6. Y. Liu, Z. Ding, and H. Lu, "Design principle in localized density coefficient of 3D-printing foamlike mechanical metamaterials toward a high-compression strain energy," *Advanced Engineering Materials* (2025): 2402525.

7. M. Jiang, W. Huang, Y. Zhang, et al., "Origami-inspired kagome honeycomb: an innovative design for preferable impact resistance," *Thin-Walled Structures* 215 (2025): 113521.

8. L. Jin, S. Yu, J. Cheng, et al., "Machine learning driven forward prediction and inverse design for 4D printed hierarchical architecture with arbitrary shapes," *Applied Materials Today* 40 (2024): 102373.

9. L. Jin, S. Yu, J. Cheng, et al., "Machine learning powered inverse design for strain fields of hierarchical architectures," *Composites Part B: Engineering* 299 (2025): 112372.

10. Y. Wang, Q. Zeng, J. Wang, Y. Li, and D. Fang, "Inverse design of shell-based mechanical metamaterial with customized loading curves based on machine learning and genetic algorithm," *Computer Methods in Applied Mechanics and Engineering* 401 (2022): 115571.

11. X. Wang, S. Sridar, M. Klecka, and W. Xiong, "Rapid data acquisition and machine learning-assisted composition design of functionally graded alloys via wire arc additive manufacturing," *npj Advanced Manufacturing* 2, no. 1 (2025): 17.

12. Z.-Z. Li, C. Guo, W. Lv, P. Huang, and Y. Zhang, "Machine learning-enabled optical architecture design of perovskite solar cells," *The Journal of Physical Chemistry Letters* 15, no. 14 (2024): 3835–3842.

13. M. W. Cho, S. H. Hwang, J.-Y. Jang, et al., "Beyond the limits of parametric design: Latent space exploration strategy enabling ultra-broadband acoustic metamaterials," *Engineering Applications of Artificial Intelligence* 133 (2024): 108595.

14. R. Deng, W. Liu, and L. Shi, "Inverse design in photonic crystals," *Nanophotonics* 13, no. 8 (2024): 1219–1237.

15. R. Shen, B. Hong, X. Ren, et al., "Recent progress on inverse design for integrated photonic devices: methodology and applications," *Journal of Nanophotonics* 18, no. 1 (2024): 010901–010901.

16. M. Mohammadnejad, A. Montazeri, E. Bahmanpour, and M. Mahnama, "Artificial neural networks for inverse design of a semi-auxetic metamaterial," *Thin-Walled Structures* 200 (2024): 111927.

17. D. Park, J. Lee, H. Lee, G. X. Gu, and S. Ryu, "Deep generative spatiotemporal learning for integrating fracture mechanics in composite materials: inverse design, discovery, and optimization," *Materials Horizons* 11, no. 13 (2024): 3048–3065.

18. X. Sun, L. Yue, L. Yu, et al., "Machine learning-evolutionary algorithm enabled design for 4D-printed active composite structures," *Advanced Functional Materials* 32, no. 10 (2022): 2109805.

19. T. Wu, M. Zhou, J. Zou, et al., "AI-guided few-shot inverse design of HDP-mimicking polymers against drug-resistant bacteria," *Nature Communications* 15, no. 1 (2024): 6288.

20. S. Hemayat, S. Moayed Baharlou, A. Sergienko, and A. Ndao, "Integrating deep convolutional surrogate solvers and particle swarm optimization for efficient inverse design of plasmonic patch nanoantennas," *Nanophotonics* 13, no. 21 (2024): 3963–3983.

21. C. Ma, Z. Wang, H. Zhang, et al., "Inverse design of electromagnetic metamaterials: from iterative to deep learning-based methods," *Journal of Micromechanics and Microengineering* 34, no. 5 (2024): 053001.

22. X. Shen, K. Yan, D. Zhu, et al., "Inverse design framework of hybrid honeycomb structure with high impact resistance based on active learning," *Defence Technology* 55 (2025): 407–421.

23. J. Zhang, Z. Wei, K. Kang, and W.-Y. Yin, "Intelligent inverse designs of impedance matching circuits With generative adversarial network," *IEEE Transactions on Computer-Aided Design of Integrated Circuits and Systems* (2024).

24. J. Song, J. Lee, N. Kim, and K. Min, "Artificial intelligence in the design of innovative metamaterials: A comprehensive review," *International Journal of Precision Engineering and Manufacturing* 25, no. 1 (2024): 225–244.

25. L. Jin, X. Zhai, K. Wang, et al., "Big data, machine learning, and digital twin assisted additive manufacturing: A review," *Materials & Design* 244 (2024): 113086.

26. O. Khatib, S. Ren, J. Malof, and W. J. Padilla, "Deep learning the electromagnetic properties of metamaterials-a comprehensive review," *Advanced Functional Materials* 31, no. 31 (2021): 2101748.

27. W. Ma, Z. Liu, Z. A. Kudyshev, A. Boltasseva, W. Cai, and Y. Liu, "Deep learning for the design of photonic structures," *Nature Photonics* 15, no. 2 (2021): 77–90.

28. Z. Ballard, C. Brown, A. M. Madni, and A. Ozcan, "Machine learning and computation-enabled intelligent sensor design," *Nature Machine Intelligence* 3, no. 7 (2021): 556–565.

29. M. Dijkstra and E. Luijten, "From predictive modelling to machine learning and reverse engineering of colloidal self-assembly," *Nature Materials* 20, no. 6 (2021): 762–773.

30. B. Mortazavi, "Recent advances in machine learning-assisted multiscale design of energy materials," *Advanced Energy Materials* 15, no. 9 (2025): 2403876.

31. L. Jin, X. Zhai, W. Xue, et al., "Finite element analysis, machine learning, and digital twins for soft robots: state-of-arts and perspectives," *Smart Materials and Structures* 34, no. 3 (2025): 033002.

32. Z. Yang, C.-H. Yu, K. Guo, and M. J. Buehler, "End-to-end deep learning method to predict complete strain and stress tensors for complex hierarchical composite microstructures," *Journal of the Mechanics and Physics of Solids* 154 (2021): 104506.

33. S. Goel, S. Leedumrongwatthanakun, N. H. Valencia, et al., "Inverse design of high-dimensional quantum optical circuits in a complex medium," *Nature Physics* 20, no. 2 (2024): 232–239.

34. M. Berardi, F. V. Difonzo, and M. Icardi, "Inverse physics-informed neural networks for transport models in porous materials," *Computer Methods in Applied Mechanics and Engineering* 435 (2025): 117628.

35. P. R. Wiecha, A. Arbouet, C. Girard, and O. L. Muskens, "Deep learning in nano-photonics: inverse design and beyond," *Photonics Research* 9, no. 5 (2021): B182–B200.

36. M. Cheng, C.-L. Fu, R. Okabe, et al., "Artificial intelligence-driven approaches for materials design and discovery," *Nature Materials* 25 (2026): 174–190.

37. A. F. Villaverde and J. R. Banga, "Reverse engineering and identification in systems biology: strategies, perspectives and challenges," *Journal of the Royal Society Interface* 11, no. 91 (2014): 20130505.

38. P. Marcal and I. P. King, "Elastic-plastic analysis of two-dimensional stress systems by the finite element method," *International Journal of Mechanical Sciences* 9, no. 3 (1967): 143–155.

39. Z. Zeng, P. K. Venuthurumilli, and X. Xu, "Inverse design of plasmonic structures with FDTD," *ACS Photonics* 8, no. 5 (2021): 1489–1496.

40. K. Yee, "Numerical solution of initial boundary value problems involving Maxwell's equations in isotropic media," *IEEE Transactions on Antennas and Propagation* 14, no. 3 (1966): 302–307.

41. M. Clemens and T. Weiland, "Discrete electromagnetism with the finite integration technique," *Progress In Electromagnetics Research* 32, no. 32 (2001): 65–87.

42. M. Ahmadi and W. S. Ghaly, "Aerodynamic inverse design of turbomachinery cascades using a finite volume method on unstructured meshes," *Inverse Problems in Engineering* 6, no. 4 (1998): 281–298.

43. R. Eymard, T. Gallouët, and R. Herbin, "Finite volume methods," *Handbook of Numerical Analysis* 7 (2000): 713–1018.

44. C. Eys, V. Ky, H. Yoshida, N. Shiba, and T. Ide, "Discrete element analysis in musculoskeletal biomechanics," *Molecular & Cellular Biomechanics* 7, no. 3 (2010): 175.

45. Y. Jiang, E. Byrne, J. Glassey, and X. Chen, "Integrating graph neural network-based surrogate modeling with inverse design for granular flows," *Industrial & Engineering Chemistry Research* 63 (2024): 9225–9235.

46. V. D. Fachinotti, A. Cardona, and P. Jetteur, "Finite element modelling of inverse design problems in large deformations anisotropic hyperelasticity," *International Journal for Numerical Methods in Engineering* 74, no. 6 (2008): 894–910.

47. O. C. Zienkiewicz and R. L. Taylor, *The finite element method for solid and structural mechanics* (Elsevier, 2005).

48. M. V. Reddy, B. Hemasunder, S. Ramana, P. R. Babu, P. Thejasree, and J. Joseph, "State of art on FEM approach in inverse heat transfer problems for different materials," *Materials Today: Proceedings* (2023).

49. F. Teixeira, C. Sarris, Y. Zhang, et al., "Finite-difference time-domain methods," *Nature Reviews Methods Primers* 3, no. 1 (2023): 75.

50. T. Rylander, P. Ingelström, and A. Bondeson, *Computational electromagnetics* (Springer Science & Business Media, 2012).

51. N. Yu, P. Genevet, M. A. Kats, et al., "Light propagation with phase discontinuities: generalized laws of reflection and refraction," *Science* 334, no. 6054 (2011): 333–337.

52. R. J. LeVeque, *Finite volume methods for hyperbolic problems*, Vol. 31 (Cambridge University Press, 2002).

53. Á. Veress and J. Rohács, "Application of Finite Volume Method in Fluid Dynamics and Inverse Design Based Optimization," in *Finite Volume Method - Powerful Means of Engineering Design*, ed. R. Petrova (IntechOpen, 2012), 1–34.

54. J.-P. Plassiard and F.-V. Donzé, "Optimizing the design of rockfall embankments with a discrete element method," *Engineering Structures* 32, no. 11 (2010): 3817–3826.

55. Y. Ryu, M. Haririan, C. Wu, and J. Arora, "Structural design sensitivity analysis of nonlinear response," *Computers & Structures* 21, no. 1-2 (1985): 245–255.

56. S. R. Kennon and G. S. Dulikravich, "Inverse design of multiholed internally cooled turbine blades," *International Journal for Numerical Methods in Engineering* 22, no. 2 (1986): 363–375.

57. G. B. Olson, "Computational design of hierarchically structured materials," *Science* 277, no. 5330 (1997): 1237–1242.

58. M. P. Bendsøe and O. Sigmund, "Material interpolation schemes in topology optimization," *Archive of Applied Mechanics* 69 (1999): 635–654.

59. A. Hakansson, J. Sánchez-Dehesa, and L. Sanchis, "Inverse design of photonic crystal devices," *IEEE Journal on selected areas in communications* 23, no. 7 (2005): 1365–1371.

60. H. Xiang, B. Huang, E. Kan, S.-H. Wei, and X. Gong, "Towards direct-gap silicon phases by the inverse band structure design approach," *Physical review letters* 110, no. 11 (2013): 118702.

61. T. Nomura, A. Kawamoto, T. Kondoh, et al., "Inverse design of structure and fiber orientation by means of topology optimization with tensor field variables," *Composites Part B: Engineering* 176 (2019): 107187.

62. R. E. Christiansen and O. Sigmund, "Inverse design in photonics by topology optimization: tutorial," *Journal of the Optical Society of America B* 38, no. 2 (2021): 496–509.

63. D. Nelson, S. Kim, and K. B. Crozier, "Inverse design of plasmonic nanotweezers by topology optimization," *ACS Photonics* 11, no. 1 (2023): 85–92.

64. D. Thillaithevan, R. Murphy, R. Hewson, and M. Santer, "Inverse design of periodic microstructures with targeted nonlinear mechanical behaviour," *Structural and Multidisciplinary Optimization* 67, no. 4 (2024): 55.

65. J. Cui, Y. Wang, L. Zhang, and H. Li, "An intelligent design system for tailored metamaterial properties," *International Journal of Mechanical Sciences* 282 (2024): 109595.

66. Q. Zeng, S. Duan, Z. Zhao, P. Wang, and H. Lei, "Inverse design of energy-absorbing metamaterials by topology optimization," *Advanced Science* 10, no. 4 (2023): 2204977.

67. M. Abu-Mualla and J. Huang, "Inverse design of 3D cellular materials with physics-guided machine learning," *Materials & Design* 232 (2023): 112103.

68. W. Xiong and G. B. Olson, "Cybermaterials: materials by design and accelerated insertion of materials," *npj Computational Materials* 2, no. 1 (2016): 1–14.

69. S. Grieu, O. Faugeroux, A. Traoré, B. Claudet, and J.-L. Bodnar, "Artificial intelligence tools and inverse methods for estimating the thermal diffusivity of building materials," *Energy and Buildings* 43, no. 2-3 (2011): 543–554.

70. W.-C. Lu, X.-B. Ji, M.-J. Li, L. Liu, B.-H. Yue, and L.-M. Zhang, "Using support vector machine for materials design," *Advances in Manufacturing* 1, no. 2 (2013): 151–159.

71. B. Sanchez-Lengeling, C. Outeiral, G. L. Guimaraes, and A. Aspuru-Guzik, "Optimizing distributions over molecular space: an objective-reinforced generative adversarial network for inverse-design chemistry (ORGANIC)," *ChemRxiv: 10.26434* (2017).

72. K. Kim, S. Kang, J. Yoo, et al., "Deep-learning-based inverse design model for intelligent discovery of organic molecules," *npj Computational Materials* 4, no. 1 (2018): 67.

73. X. Shi, T. Qiu, J. Wang, X. Zhao, and S. Qu, "Metasurface inverse design using machine learning approaches," *Journal of Physics D: Applied Physics* 53, no. 27 (2020): 275105.

74. J. Hou, H. Lin, W. Xu, et al., "Customized inverse design of metamaterial absorber based on target-driven deep learning method," *IEEE Access* 8 (2020): 211849–211859.

75. R. Gómez-Bombarelli, J. N. Wei, D. Duvenaud, et al., "Automatic chemical design using a data-driven continuous representation of molecules," *ACS Central Science* 4, no. 2 (2018): 268–276.

76. J.-H. Bastek and D. M. Kochmann, "Inverse design of nonlinear mechanical metamaterials via video denoising diffusion models," *Nature Machine Intelligence* 5, no. 12 (2023): 1466–1475.

77. K. Choudhary, "Atomgpt: Atomistic generative pretrained transformer for forward and inverse materials design," *The Journal of Physical Chemistry Letters* 15, no. 27 (2024): 6909–6917.

78. J. Jung and G. X. Gu, "Data-driven airfoil shape optimization framework for enhanced flutter performance," *Physics of Fluids* 36, no. 10 (2024): 101706.

79. X. Fang, H.-S. Shen, and H. Wang, "Nonlinear vibration analysis of sandwich plates with inverse-designed 3D auxetic core by deep generative model," *Thin-Walled Structures* 206 (2025): 112599.

80. Y. Wang, Q. Jin, C. Zhang, et al., "Inverse design of triply periodic minimal surfaces structure based on point cloud generation network," *Composite Structures* 354 (2025): 118814.

81. X. Hou, W. Zhao, K. Zhang, and Z. Deng, "Inverse design of a NURBS-based chiral metamaterial via machine learning for programmable mechanical deformation," *Acta Mechanica Solida Sinica* 38, no. 5 (2025): 739–748.

82. J. Wang, J. Li, Y. Wei, S. Meng, T. Yang, and C. Wang, "Inverse Design of Broadband Optimal Power Amplifiers Enabled by Deep Learning," *IEEE Transactions on Microwave Theory and Techniques* 73, no. 10 (2025): 7500–7514.

83. H. Li, H. Zheng, T. Yue, et al., "Machine learning-accelerated discovery of heat-resistant polysulfates for electrostatic energy storage," *Nature Energy* 10, no. 1 (2025): 90–100.

84. M. Li, Y. Zhao, R. Long, Z. Liu, and W. Liu, "Synergic inverse design of adsorbent bed topology and heterogeneous adsorbent porosity distribution for adsorption desalination via data-free deep learning," *International Journal of Heat and Mass Transfer* 241 (2025): 126771.

85. M. H. Tahersima, K. Kojima, T. Koike-Akino, et al., "Deep neural network inverse design of integrated photonic power splitters," *Scientific Reports* 9, no. 1 (2019): 1368.

86. S. Sarkar, A. Ji, Z. Jermain, et al., "Physics-informed machine learning for inverse design of optical metamaterials," *Advanced Photonics Research* 4, no. 12 (2023): 2300158.

87. E. Adibnia, M. Ghadrdan, and M. A. Mansouri-Birjandi, "Chirped apodized fiber Bragg gratings inverse design via deep learning," *Optics & Laser Technology* 181 (2025): 111766.

88. Z. Yu and R. Hao, "Inverse design of High-Q topological corner states nanocavities based on deep reinforcement learning," *Optics Communications* 577 (2025): 131402.

89. X. Q. Wang, Z. Jin, D. Ravichandran, and G. X. Gu, "Artificial intelligence and multiscale modeling for sustainable biopolymers and bioinspired materials," *Advanced Materials* 37, no. 22 (2025): 2416901.

90. B. Sanchez-Lengeling and A. Aspuru-Guzik, "Inverse molecular design using machine learning: Generative models for matter engineering," *Science* 361, no. 6400 (2018): 360–365.

91. M. Elzouka, C. Yang, A. Albert, R. S. Prasher, and S. D. Lubner, "Interpretable forward and inverse design of particle spectral emissivity using common machine-learning models," *Cell Reports Physical Science* 1, no. 12 (2020): 100259.

92. M. Li, Y. Zhao, R. Long, Z. Liu, and W. Liu, "Heterogeneous inverse design for adsorption desalination via data-free deep learning," *Applied Thermal Engineering* 263 (2025): 125334.

93. Y. Ling, Z. Mao, W. Liu, et al., "Severity indices of diquat poisoning for triage and prognosis in acute diquat poisoning: a multicenter prospective cohort study," *Annals of Emergency Medicine* 85, no. 6 (2025): 512–520.

94. J. Nie, T. Huang, Y. Sun, et al., "Influence of the enterovirus 71 vaccine and the COVID-19 pandemic on hand, foot, and mouth disease in china based on counterfactual models: observational study," *JMIR Public Health and Surveillance* 10, no. 1 (2024): e63146.

95. S. Chen, Y. Ling, F. Zhou, X. Qiao, and J. D. Reinhardt, "Trajectories of cognitive function among people aged 45 years and older living with diabetes in China: Results from a nationally representative longitudinal study (2011˜ 2018)," *Plos One* 19, no. 5 (2024): e0299316.

96. Q. Yang, L. Wang, X. Zhang, et al., "Impact of an enhanced recovery after surgery program integrating cardiopulmonary rehabilitation on post-operative prognosis of patients treated with CABG: protocol of the ERAS-CaRe randomized controlled trial," *BMC Pulmonary Medicine* 24, no. 1 (2024): 512.

97. C. S. Ha, D. Yao, Z. Xu, et al., "Rapid inverse design of metamaterials based on prescribed mechanical behavior through machine learning," *Nature Communications* 14, no. 1 (2023): 5765.

98. J. Feng, L. Wang, X. Zhai, et al., "Constructing boundary-identical microstructures via guided diffusion for fast multiscale topology optimization," *Computer Methods in Applied Mechanics and Engineering* 436 (2025): 117735.

99. T. Dai, L. Jin, C. Shang, et al., "Advances in intelligent design of metamaterials," *Journal of Computer-Aided Design & Computer Graphics* 37, no. 1 (2025): 1–27.

100. S. Jain, G. Seth, A. Paruthi, U. Soni, and G. Kumar, "Synthetic data augmentation for surface defect detection and classification using deep learning," *Journal of Intelligent Manufacturing* 33, no. 4 (2022): 1007–1020.

101. W. Zhou, S. Wang, Q. Wu, et al., "An inverse design paradigm of multi-functional elastic metasurface via data-driven machine learning," *Materials & Design* 226 (2023): 111560.

102. Y. Zhao, L. Wang, X. Zhai, et al., "Near-isotropic, extreme-stiffness, continuous 3D mechanical metamaterial sequences using implicit neural representation," *Advanced Science* 12, no. 3 (2025): 2410428.

103. C.-T. Chen and G. X. Gu, "Generative deep neural networks for inverse materials design using backpropagation and active learning," *Advanced Science* 7, no. 5 (2020): 1902607.

104. S. So, T. Badloe, J. Noh, J. Bravo-Abad, and J. Rho, "Deep learning enabled inverse design in nanophotonics," *Nanophotonics* 9, no. 5 (2020): 1041–1057.

105. L. Wang, J. Jiang, Y. Tian, et al., "Prediction of Process Parameters Based on Stress-Strain Behaviour in 3D Printing Using Deep Neural Network," in *2025 International Conference on Intelligent Digitization of Systems and Services (IDSS)* (IEEE, 2025), 161–166.

106. N. N. Vlassis and W. Sun, "Denoising diffusion algorithm for inverse design of microstructures with fine-tuned nonlinear material properties," *Computer Methods in Applied Mechanics and Engineering* 413 (2023): 116126.

107. M. E. Celebi and K. Aydin, *Unsupervised learning algorithms*, Vol. 1 (Springer, 2016).

108. K. Zhou, E. Diehl, and J. Tang, "Deep convolutional generative adversarial network with semi-supervised learning enabled physics elucidation for extended gear fault diagnosis under data limitations," *Mechanical Systems and Signal Processing* 185 (2023): 109772.

109. V. François-Lavet, P. Henderson, R. Islam, et al., "An introduction to deep reinforcement learning," *Foundations and Trends in Machine Learning* 11, no. 3-4 (2018): 219–354.

110. H. Huo, Z. Rong, O. Kononova, et al., "Semi-supervised machine-learning classification of materials synthesis procedures," *npj Computational Materials* 5, no. 1 (2019): 62.

111. P. Deng, S. Huo, C. Zhao, et al., "Inverse structural design of flexible electronics based on improved random forest," *Mechanics of Advanced Materials and Structures* (2025): 1–22.

112. S. Li and A. S. Barnard, "Inverse design of nanoparticles using multi-target machine learning," *Advanced Theory and Simulations* 5, no. 2 (2022): 2100414.

113. P. Naseri and S. V. Hum, "A generative machine learning-based approach for inverse design of multilayer metasurfaces," *IEEE Transactions on Antennas and Propagation* 69, no. 9 (2021): 5725–5739.

114. C. Cleeton and L. Sarkisov, "Inverse design of metal-organic frameworks using deep dreaming approaches," *Nature Communications* 16, no. 1 (2025): 4806.

115. N. Gao, M. Wang, B. Cheng, and H. Hou, "Inverse design and experimental verification of an acoustic sink based on machine learning," *Applied Acoustics* 180 (2021): 108153.

116. Q. Wang and L. Zhang, "Inverse design of glass structure with deep graph neural networks," *Nature Communications* 12, no. 1 (2021): 5359.

117. J. Chen, H. Duan, and G. Huang, "Transformer-based inverse-design model for optimal multilayer microperforated panels," *Physical Review Applied* 23, no. 2 (2025): 024044.

118. R. Azad, P. Lenßen, Y. Jia, et al., "Modeling the temperature-dependent size change of polydisperse nano-objects using a deep generative model," *Nano Letters* 24, no. 15 (2024): 4447–4453.

119. N. Zhang, F. Gao, R. Wang, et al., "Deep-Learning empowered customized chiral metasurface for calibration-free biosensing," *Advanced Materials* 37, no. 1 (2025): 2411490.

120. X. Li, A. H. H. Ngu, and V. Metsis, "Tts-cgan: A transformer time-series conditional gan for biosignal data augmentation," *Arxiv Preprint Arxiv: 2206.13676* (2022).

121. J. Xiong, O. Fink, J. Zhou, and Y. Ma, "Controlled physics-informed data generation for deep learning-based remaining useful life prediction under unseen operation conditions," *Mechanical Systems and Signal Processing* 197 (2023): 110359.

122. S. Singh, R. Kumar, P. Singh, and R. S. Hegde, "Active learning-driven framework for efficient inverse design in large nanophotonic design spaces," *Authorea Preprints* (2025).

123. C. Bowles, L. Chen, R. Guerrero, et al., "Gan augmentation: Augmenting training data using generative adversarial networks,"*ArXiv Preprint ArXiv: 1810.10863* (2018).

124. T. Brzin and M. Brojan, "Using a generative adversarial network for the inverse design of soft morphing composite beams," *Engineering Applications of Artificial Intelligence* 133 (2024): 108527.

125. H. Wang, Z. Du, F. Feng, Z. Kang, S. Tang, and X. Guo, "DiffMat: Data-driven inverse design of energy-absorbing metamaterials using diffusion model," *Computer Methods in Applied Mechanics and Engineering* 432 (2024): 117440.

126. B. Liu, L. Xu, Y. Wang, and J. Huang, "Diffusion model-based inverse design for thermal transparency," *Journal of Applied Physics* 135, no. 12 (2024): 125101.

127. J. Zhang, S. Chen, R. J. Martin, B. Liu, R. Zhang, and D. Xiao, "Conditional diffusion models for the inverse design of lattice structures," *Structural and Multidisciplinary Optimization* 68, no. 3 (2025): 1–23.

128. Z. Zhang, C. Yang, Y. Qin, H. Feng, J. Feng, and H. Li, "Diffusion probabilistic model based accurate and high-degree-of-freedom metasurface inverse design," *Nanophotonics* 12, no. 20 (2023): 3871–3881.

129. J. Park, A. P. S. Gill, S. M. Moosavi, and J. Kim, "Inverse design of porous materials: a diffusion model approach," *Journal of Materials Chemistry A* 12, no. 11 (2024): 6507–6514.

130. W. Ma, F. Cheng, Y. Xu, Q. Wen, and Y. Liu, "Probabilistic representation and inverse design of metamaterials based on a deep generative model with semi-supervised learning strategy," *Advanced Materials* 31, no. 35 (2019): 1901111.

131. Z.-H. Lee, P. C. Lin, and T. Yang, "Inverse design of ligands using a deep generative model semi-supervised by a data-driven ligand field strength metric," *Journal of the Chinese Chemical Society* 70, no. 5 (2023): 1095–1101.

132. R. Li, C. Zhang, W. Xie, et al., "Deep reinforcement learning empowers automated inverse design and optimization of photonic crystals for nanoscale laser cavities," *Nanophotonics* 12, no. 2 (2023): 319–334.

133. S. Yang, S. Lee, and K. Yee, "Inverse design optimization framework via a two-step deep learning approach: application to a wind turbine airfoil," *Engineering with Computers* 39, no. 3 (2023): 2239–2255.

134. S. Ruder, "An overview of gradient descent optimization algorithms,"*Arxiv Preprint Arxiv: 1609.04747* (2016).

135. Y. Dan, Y. Zhao, X. Li, S. Li, M. Hu, and J. Hu, "Generative adversarial networks (GAN) based efficient sampling of chemical composition space for inverse design of inorganic materials," *npj Computational Materials* 6, no. 1 (2020): 84.

136. T. Bartz-Beielstein, J. Branke, J. Mehnen, and O. Mersmann, "Evolutionary algorithms," *Wiley Interdisciplinary Reviews: Data Mining and Knowledge Discovery* 4, no. 3 (2014): 178–195.

137. A. G. Gad, "Particle swarm optimization algorithm and its applications: A systematic review," *Archives of Computational Methods in Engineering* 29, no. 5 (2022): 2531–2561.

138. Y. Liu, H. He, Y. Cao, Y. Liang, and J. Huang, "Inverse design of TPMS piezoelectric metamaterial based on deep learning," *Mechanics of Materials* 198 (2024): 105109.

139. Y. Tang, A. Kurtz, and Y. F. Zhao, "Bidirectional evolutionary structural optimization (BESO) based design method for lattice structure to be fabricated by additive manufacturing," *Computer-Aided Design* 69 (2015): 91–101.

140. C. Bao, Y. Guo, and Y. Wang, "Interactive inverse design of periodic non-uniform/inhomogeneous rod structures based on q-learning method," *Composite Structures* 341 (2024): 118233.

141. X. Sun, L. Yue, L. Yu, et al., "Machine learning-enabled forward prediction and inverse design of 4D-printed active plates," *Nature Communications* 15, no. 1 (2024): 5509.

142. H. Zhang, J. Liu, W. Ma, et al., "Learning to inversely design acoustic metamaterials for enhanced performance," *Acta Mechanica Sinica* 39, no. 7 (2023): 722426.

143. N. Morrison and E. Y. Ma, "Efficiency of machine learning optimizers and meta-optimization for nanophotonic inverse design tasks," *APL Machine Learning* 3, no. 1 (2025): 016101.

144. C. Qiu, X. Wu, Z. Luo, H. Yang, G. He, and B. Huang, "Nanophotonic inverse design with deep neural networks based on knowledge transfer using imbalanced datasets," *Optics Express* 29, no. 18 (2021): 28406–28415.

145. E. Yilmaz and B. German, "A deep learning approach to an airfoil inverse design problem," in 2018 multidisciplinary analysis and optimization conference (2018), 3420.

146. Z. Liu, D. Zhu, L. Raju, and W. Cai, "Tackling photonic inverse design with machine learning," *Advanced Science* 8, no. 5 (2021): 2002923.

147. C. Yeung, B. Pham, R. Tsai, K. T. Fountaine, and A. P. Raman, "DeepAdjoint: an all-in-one photonic inverse design framework integrating data-driven machine learning with optimization algorithms," *ACS Photonics* 10, no. 4 (2022): 884–891.

148. L. He, Z. Wen, Y. Jin, D. Torrent, X. Zhuang, and T. Rabczuk, "Inverse design of topological metaplates for flexural waves with machine learning," *Materials & Design* 199 (2021): 109390.

149. R. Zhu, T. Qiu, J. Wang, et al., "Phase-to-pattern inverse design paradigm for fast realization of functional metasurfaces via transfer learning," *Nature Communications* 12, no. 1 (2021): 2974.

150. Y. Long, J. Ren, Y. Li, and H. Chen, "Inverse design of photonic topological state via machine learning," *Applied Physics Letters* 114, no. 18 (2019): 181105.

151. T. Long, N. M. Fortunato, I. Opahle, et al., "Constrained crystals deep convolutional generative adversarial network for the inverse design of crystal structures," *npj Computational Materials* 7, no. 1 (2021): 66.

152. M. Kiani, M. Zolfaghari, and J. Kiani, "Transfer learning for inverse design of tunable graphene-based meta-surfaces," *Journal of Materials Science* 59, no. 8 (2024): 3516–3530.

153. Z. Fan, C. Qian, Y. Jia, et al., "Transfer-learning-assisted inverse metasurface design for 30% data savings," *Physical Review Applied* 18, no. 2 (2022): 024022.

154. Z. Fang and J. Zhan, "Deep physical informed neural networks for metamaterial design," *IEEE Access* 8 (2019): 24506–24513.

155. Y. Chen, L. Lu, G. E. Karniadakis, and L. Dal Negro, "Physics-informed neural networks for inverse problems in nano-optics and metamaterials," *Optics Express* 28, no. 8 (2020): 11618–11633.

156. L. Lu, R. Pestourie, W. Yao, Z. Wang, F. Verdugo, and S. G. Johnson, "Physics-informed neural networks with hard constraints for inverse design," *SIAM Journal on Scientific Computing* 43, no. 6 (2021): B1105–B1132.

157. Q. Li, J. Wang, T. Lei, T. Xiang, C. Qin, and M. Yang, "Design of metamaterials for absorbers based on variational autoencoder," *IEEE Access* 12 (2024): 92328–92336.

158. X. Liu, H. Zhao, Y. Tang, et al., "Few-shot learning-based generative design of metamaterials with zero Poisson's ratio," *Materials & Design* 244 (2024): 113224.

159. X.-L. Peng and B.-X. Xu, "Data-driven inverse design of composite triangular lattice structures," *International Journal of Mechanical Sciences* 265 (2024): 108900.

160. B. Liu, H. Cai, and Y. Wang, "Metamaterial-based realization for thermal transparency: A conditional variational autoencoder approach," *Physica B: Condensed Matter* 684 (2024): 415975.

161. Y. Chen, X. Wang, X. Deng, et al., "MatterGPT: A generative transformer for multi-property inverse design of solid-state materials,"*Arxiv Preprint Arxiv: 2408.07608* (2024).

162. J. Han, X. Zhai, L. Wang, et al., "Inverse-designed 3D sequential metamaterials achieving extreme stiffness," *Materials & Design* 247 (2024): 113350.

163. R. Dong, Y. Dan, X. Li, and J. Hu, "Inverse design of composite metal oxide optical materials based on deep transfer learning and global optimization," *Computational Materials Science* 188 (2021): 110166.

164. R. Yu, Y. Liu, and L. Zhu, "Inverse design of high degree of freedom meta-atoms based on machine learning and genetic algorithm methods," *Optics Express* 30, no. 20 (2022): 35776–35791.

165. Y. Kim, Y. Kim, C. Yang, K. Park, G. X. Gu, and S. Ryu, "Deep learning framework for material design space exploration using active transfer learning and data augmentation," *npj Computational Materials* 7, no. 1 (2021): 140.

166. L. Grbcic, J. Müller, and W. A. de Jong, "Efficient inverse design optimization through multi-fidelity simulations, machine learning, and boundary refinement strategies," *Engineering with Computers* 40, no. 6 (2024): 4081–4108.

167. L. Grbčić, M. Park, M. Elzouka, et al., "Inverse design of photonic surfaces via multi fidelity ensemble framework and femtosecond laser processing," *npj Computational Materials* 11, no. 1 (2025): 35.

168. J. Gu, Z. Ye, T. Rae-Grant, et al., "Optimization and control of actuator networks in variable geometry truss systems using genetic algorithms," *Nature Communications* 16, no. 1 (2025): 8432.

169. P. Naseri, S. Pearson, Z. Wang, and S. V. Hum, "A combined machine-learning/optimization-based approach for inverse design of nonuniform bianisotropic metasurfaces," *IEEE Transactions on Antennas and Propagation* 70, no. 7 (2021): 5105–5119.

170. J. N. Kumar, Q. Li, K. Y. Tang, T. Buonassisi, A. L. Gonzalez-Oyarce, and J. Ye, "Machine learning enables polymer cloud-point engineering via inverse design," *npj Computational Materials* 5, no. 1 (2019): 73.

171. A. Ajagekar and F. You, "Molecular design with automated quantum computing-based deep learning and optimization," *npj Computational Materials* 9, no. 1 (2023): 143.

172. T. Van Huynh, S. Tangaramvong, B. Do, and W. Gao, "A novel decoupled approach combining invertible cross-entropy method with Gaussian process modeling for reliability-based design and topology optimization," *Computer Methods in Applied Mechanics and Engineering* 427 (2024): 117006.

173. R. L. Pereira, H. N. Lopes, and R. Pavanello, "Topology optimization of acoustic systems with a multiconstrained BESO approach," *Finite Elements in Analysis and Design* 201 (2022): 103701.

174. D. Vercruysse, N. V. Sapra, L. Su, R. Trivedi, and J. Vučković, "Analytical level set fabrication constraints for inverse design," *Scientific Reports* 9, no. 1 (2019): 8999.

175. X. Chen, X. Zhao, Y. Li, and Y. Yin, "Inverse design of air supply distribution using coupled adjoint and parametric level set method," *Building and Environment* 279 (2025): 113106.

176. P. Kudela, A. Ijjeh, M. Radzienski, M. Miniaci, N. Pugno, and W. Ostachowicz, "Deep learning aided topology optimization of phononic crystals," *Mechanical Systems and Signal Processing* 200 (2023): 110636.

177. X. Zhai, Y. Gai, L. Jin, W.-H. Liao, F. Chen, and P. Hu, "Isogeometric topology optimization of auxetic materials based on moving morphable components method," *Advanced Topics in Mechanics of Materials, Structures and Construction: AToMech1* 31 (2023): 172.

178. A. M. Hammond, A. Oskooi, M. Chen, Z. Lin, S. G. Johnson, and S. E. Ralph, "High-performance hybrid time/frequency-domain topology optimization for large-scale photonics inverse design," *Optics Express* 30, no. 3 (2022): 4467–4491.

179. H. Chi, Y. Zhang, T. L. E. Tang, et al., "Universal machine learning for topology optimization," *Computer Methods in Applied Mechanics and Engineering* 375 (2021): 112739.

180. N. Napier, S.-A. Sriraman, H. T. Tran, and K. A. James, "An artificial neural network approach for generating high-resolution designs from low-resolution input in topology optimization," *Journal of Mechanical Design* 142, no. 1 (2020): 011402.

181. Z. Chai, Z. Zong, H. Yong, et al., "Tailoring stress-strain curves of flexible snapping mechanical metamaterial for on-demand mechanical responses via data-driven inverse design," *Advanced Materials* 36, no. 33 (2024): 2404369.

182. M. M. Behzadi and H. T. Ilieş, "Gantl: Toward practical and real-time topology optimization with conditional generative adversarial networks and transfer learning," *Journal of Mechanical Design* 144, no. 2 (2022): 021711.

183. B. Peng, Y. Wei, Y. Qin, et al., "Machine learning-enabled constrained multi-objective design of architected materials," *Nature Communications* 14, no. 1 (2023): 6630.

184. Z. Huang, X. Liu, and J. Zang, "The inverse design of structural color using machine learning," *Nanoscale* 11, no. 45 (2019): 21748–21758.

185. Q. Guan, A. Raza, S. S. Mao, L. F. Vega, and T. Zhang, "Machine learning-enabled inverse design of radiative cooling film with on-demand transmissive color," *ACS Photonics* 10, no. 3 (2023): 715–726.

186. M. A. Hossain, L. Hao, W. Xiong, and C. M. Stewart, "Discovering chemistry to creep rupture equations in Alloy 617 with machine learning," *Scientific Reports* 15, no. 1 (2025): 6051.

187. R. Riganti, Y. Zhu, W. Cai, S. Torquato, and L. D. Negro, "Multiscale physics-informed neural networks for the inverse design of hyperuniform optical materials," *Advanced Optical Materials* 13, no. 16 (2025): 2403304.

188. T. Hospedales, A. Antoniou, P. Micaelli, and A. Storkey, "Meta-learning in neural networks: A survey," *IEEE Transactions On Pattern Analysis And Machine Intelligence* 44, no. 9 (2021): 5149–5169.

189. Q. Ma, K. Dong, F. Li, M. Yu, and Y. Xiong, "Inverse design of material, structure, and process for dielectric properties of additively manufactured PLA/BaTiO3 polymer composites," *Composites Communications* 55 (2025): 102314.

190. J. Sun, J. Zhang, X. Zhang, and W. Zhou, "A deep learning-based method for heat source layout inverse design," *IEEE Access* 8 (2020): 140038–140053.

191. R. Babbar and B. Schölkopf, "Data scarcity, robustness and extreme multi-label classification," *Machine Learning* 108, no. 8 (2019): 1329–1351.

192. C. Zhang, C. Huang, Y. Tian, et al., "Diving into unified data-model sparsity for class-imbalanced graph representation learning,"*Arxiv Preprint Arxiv: 2210.00162* (2022).

193. Z. Wang, P. Wang, K. Liu, et al., "A comprehensive survey on data augmentation,"*Arxiv Preprint Arxiv: 2405.09591* (2024).

194. A. E. Forte, P. Z. Hanakata, L. Jin, et al., "Inverse design of inflatable soft membranes through machine learning," *Advanced Functional Materials* 32, no. 16 (2022): 2111610.

195. M. Elgendi, M. U. Nasir, Q. Tang, et al., "The effectiveness of image augmentation in deep learning networks for detecting COVID-19: A geometric transformation perspective," *Frontiers in Medicine* 8 (2021): 629134.

196. G. Ramponi, P. Protopapas, M. Brambilla, and R. Janssen, "T-cgan: Conditional generative adversarial network for data augmentation in noisy time series with irregular sampling,"*Arxiv Preprint Arxiv: 1811.08295* (2018).

197. J. P. Yun, W. C. Shin, G. Koo, M. S. Kim, C. Lee, and S. J. Lee, "Automated defect inspection system for metal surfaces based on deep learning and data augmentation," *Journal of Manufacturing Systems* 55 (2020): 317–324.

198. X. Zheng and G. Jia, "Active learning based reverse design of hydrogen production from biomass fuel," *Fuel* 357 (2024): 129948.

199. I. T. Jolliffe and J. Cadima, "Principal component analysis: a review and recent developments," *Philosophical Transactions of the Royal Society A: Mathematical, Physical and Engineering Sciences* 374, no. 2065 (2016): 20150202.

200. Z. Zhou, Y. Shang, X. Liu, and Y. Yang, "A generative deep learning framework for inverse design of compositionally complex bulk metallic glasses," *npj Computational Materials* 9, no. 1 (2023): 15.

201. Y. Tang, K. Kojima, T. Koike-Akino, et al., "Generative deep learning model for inverse design of integrated nanophotonic devices," *Laser & Photonics Reviews* 14, no. 12 (2020): 2000287.

202. J. Lim, S. Ryu, J. W. Kim, and W. Y. Kim, "Molecular generative model based on conditional variational autoencoder for de novo molecular design," *Journal of Cheminformatics* 10, no. 1 (2018): 31.

203. M. Lee and K. Min, "MGCVAE: multi-objective inverse design via molecular graph conditional variational autoencoder," *Journal of Chemical Information and Modeling* 62, no. 12 (2022): 2943–2950.

204. J. Peurifoy, Y. Shen, L. Jing, et al., "Nanophotonic particle simulation and inverse design using artificial neural networks," *Science Advances* 4, no. 6 (2018): eaar4206.

205. M. Maurizi, C. Gao, and F. Berto, "Inverse design of truss lattice materials with superior buckling resistance," *npj Computational Materials* 8, no. 1 (2022): 247.

206. Y. Xu, J.-Q. Yang, K. Fan, et al., "Physics-informed Inverse Design of Multi-bit Programmable Metasurfaces,"*Arxiv Preprint Arxiv: 2405.16795* (2024).

207. A. Vaswani, N. Shazeer, N. Parmar, et al., "Attention is all you need," *Advances in Neural Information Processing Systems* 30 (2017): 1–11.

208. N. Fu, L. Wei, Y. Song, et al., "Material transformers: deep learning language models for generative materials design," *Machine Learning: Science and Technology* 4, no. 1 (2023): 015001.

209. J. Sohl-Dickstein, E. Weiss, N. Maheswaranathan, and S. Ganguli, "Deep unsupervised learning using nonequilibrium thermodynamics," in *International Conference on Machine Learning* Proceedings of Machine Learning Research, (2015) 2256–2265.

210. X. Zheng, X. Zhang, T.-T. Chen, and I. Watanabe, "Deep learning in mechanical metamaterials: from prediction and generation to inverse design," *Advanced Materials* 35, no. 45 (2023): 2302530.

211. S. Ghosh, G. Anantha Padmanabha, C. Peng, et al., "Inverse aerodynamic design of gas turbine blades using probabilistic machine learning," *Journal of Mechanical Design* 144, no. 2 (2022): 021706.

212. B. Deng, A. Zareei, X. Ding, J. C. Weaver, C. H. Rycroft, and K. Bertoldi, "Inverse design of mechanical metamaterials with target nonlinear response via a neural accelerated evolution strategy," *Advanced Materials* 34, no. 41 (2022): 2206238.

213. Y. Wang, H. Gao, and X. Li, "Machine learning-guided design of shell-based multistable lattices for superior energy absorption and reusability," *Small* 21, no. 45 (2025): 2502789.

214. X. Guo, X. Zheng, J. Zhou, T. Yamada, Y. Yi, and I. Watanabe, "Spring-based mechanical metamaterials with deep-learning-accelerated design," *Materials & Design* 252 (2025): 113800.

215. X. Li, Y. Qin, L. Sun, and X. Guo, "Multimaterial metamaterial inverse design via machine learning for tailorable and reusable energy absorption," *ACS Applied Materials & Interfaces* 17, no. 26 (2025): 38203–38214.

216. X. Li, X. Han, Y. Qin, L. Sun, and X. Guo, "Inverse design of NiTi alloy-based chiral metamaterials with multi-level rotational capabilities for reusable high-performance impact absorption," *Composite Structures* 370 (2025): 119387.

217. K. Zhang, J. Jiang, L. Jin, et al., "Low-melting-point alloy/polyurethane auxetic composite foam for outstanding impact protection with favorable shape memory effect," *Smart Materials and Structures* 34, no. 4 (2025): 045025.

218. K. Zhang, Q. Gao, J. Jiang, et al., "High energy dissipation and self-healing auxetic foam by integrating shear thickening gel," *Composites Science and Technology* 249 (2024): 110475.

219. H. Ye, C. Li, S. Yu, et al., "Adaptive energy dissipator with compression-to-tension design," *Advanced Functional Materials* 36, no. 19 (2026): e21393.

220. S. Wang, P. Ling, G. Yan, H. Ma, and B. Yan, "Multi-stage quasi-zero stiffness vibration isolation with linear-to-torsion magnetic negative stiffness mechanism for variable load," *Mechanical Systems and Signal Processing* 249 (2026): 114055.

221. H. Ye, X. Huang, L. Jin, et al., "Multi-material 3D printed compression-induced stretching lattice metamaterials with superior reusable energy absorption," *Virtual and Physical Prototyping* 21, no. 1 (2026): e2637380.

222. G. Sun, D. Chen, G. Zhu, and Q. Li, "Lightweight hybrid materials and structures for energy absorption: A state-of-the-art review and outlook," *Thin-Walled Structures* 172 (2022): 108760.

223. Y. Chang, H. Wang, and Q. Dong, "Machine learning-based inverse design of auxetic metamaterial with zero Poisson's ratio," *Materials Today Communications* 30 (2022): 103186.

224. Y. Gao, X. Chen, and Y. Wei, "Graded honeycombs with high impact resistance through machine learning-based optimization," *Thin-Walled Structures* 188 (2023): 110794.

225. Z.-Y. Chang, H.-T. Liu, G.-B. Cai, and D. Zhen, "Inverse design of a petal-shaped honeycomb with zero Poisson's ratio and bi-directional tunable mechanical properties," *Composite Structures* 358 (2025): 118967.

226. S. Zhou, K. Zhang, L. Jin, Q. Gao, and W.-H. Liao, "Efficient data driven optimization framework for designing B-spline honeycombs with excellent energy absorption," *Thin-Walled Structures* 209 (2025): 112941.

227. A. Satpati, M. Maurizi, D. Yao, et al., "Multi-objective automatic discovery of optimized metamaterials for varying velocity impact protection," *Materials & Design* 258 (2025): 114657.

228. Z. Hu, J. Ding, S. Ding, et al., "Machine learning–enabled inverse design of shell-based lattice metamaterials with optimal sound and energy absorption," *Virtual and Physical Prototyping* 19, no. 1 (2024): e2412198.

229. M. Zhao, X. Li, X. Yan, et al., "Machine learning accelerated design of lattice metamaterials for customizable energy absorption," *Thin-Walled Structures* 208 (2025): 112845.

230. X. Tang, H. Ma, J. Zhang, et al., "Research progress on carbon-based materials for aerospace applications," *Composites Part B: Engineering* 309 (2025): 113105.

231. W. Zhang and J. Xu, "Advanced lightweight materials for Automobiles: A review," *Materials & Design* 221 (2022): 110994.

232. S. Wu, R. Wang, L. Jin, et al., "Digital light processing 3D printing of large-scale and crack-free ceramics with perforated internal honeycomb structures," *Virtual and Physical Prototyping* 20, no. 1 (2025): e2589472.

233. W. Gao, D. Lu, H. Wang, et al., "The Development and Utilization of Ecofriendly and High-Performance Materials in the Marine Environment," *Advanced Engineering Materials* 27, no. 15 (2025): 2500149.

234. L. Jin, X. Zhai, K. Zhang, J. Jiang, and W.-H. Liao, "Spider web-inspired additive manufacturing: unleashing the potential of lightweight support structures," in *MATEC Web of Conferences*, Vol. 401 (EDP Sciences, 2024), 02003.

235. W. Xu, N. Zhang, H. Xu, L. Jin, and J. Jiang, "Stress-guided lightweight design and optimisation for 3D printing sacrificial moulds," *Materials & Design* 255 (2025): 114161.

236. A. Challapalli, D. Patel, and G. Li, "Inverse machine learning framework for optimizing lightweight metamaterials," *Materials & Design* 208 (2021): 109937.

237. N. Bhat, A. S. Barnard, and N. Birbilis, "Inverse design of aluminium alloys using multi-targeted regression," *Journal of Materials Science* 59, no. 4 (2024): 1448–1463.

238. X. Wang, L. F. Ladinos Pizano, S. Sridar, C. Sudbrack, and W. Xiong, "Aging heat treatment design for Haynes 282 made by wire-feed additive manufacturing using high-throughput experiments and interpretable machine learning," *Science and Technology of Advanced Materials* 25, no. 1 (2024): 2346067.

239. S. Kim, L. Zhang, S.-H. Kim, and Y. S. Choi, "Diffusion model for inverse design of 7xxx-series aluminum alloys with desired property," *Metals and Materials International* 30, no. 7 (2024): 1817–1830.

240. H. Aharoni, Y. Xia, X. Zhang, R. D. Kamien, and S. Yang, "Universal inverse design of surfaces with thin nematic elastomer sheets," *Proceedings of the National Academy of Sciences* 115, no. 28 (2018): 7206–7211.

241. X. Dang, F. Feng, P. Plucinsky, R. D. James, H. Duan, and J. Wang, "Inverse design of deployable origami structures that approximate a general surface," *International Journal of Solids and Structures* 234 (2022): 111224.

242. H. Huang, S. Zhang, and Y. Li, "Inverse design of performance-oriented cellular metamaterials," *Engineering Structures* 332 (2025): 120048.

243. W. Xue, L. Jin, B. Jian, and Q. Ge, "Origami-based flexible robotic grippers via hard-soft coupled multimaterial 3D printing," *Soft Robotics* 12, no. 5 (2025): 537–552.

244. W. Xue, B. Jian, L. Jin, R. Wang, and Q. Ge, "Origami robots: design, actuation, and 3D printing methods," *Advanced Materials Technologies* 10, no. 17 (2025): e00278.

245. W. Xu, M. Zhang, H. Xu, et al., "INPR-Connector: Interlocking negative Poisson's ratio connectors design for deployable energy absorption structures," *Composites Part B: Engineering* 297 (2025): 112243.

246. L. Ma, M. Mungekar, V. Roychowdhury, and M. K. Jawed, "Rapid design of fully soft deployable structures via kirigami cuts and active learning," *Advanced Materials Technologies* 9, no. 5 (2024): 2301305.

247. T. Brzin, M. K. Jawed, and M. Brojan, "Generative adversarial network-based inverse design of self-deploying soft kirigami composites for targeted shape transformation," *Engineering Applications of Artificial Intelligence* 149 (2025): 110417.

248. C. Truong-Quoc, J. Y. Lee, K. S. Kim, and D.-N. Kim, "Prediction of DNA origami shape using graph neural network," *Nature Materials* 23, no. 7 (2024): 984–992.

249. Z. Zhang, D. Huang, B. Pan, et al., "Inverse design method of deployable cylindrical composite shells for solar sail structure," *Composite Structures* 352 (2025): 118698.

250. X. Zhai, L. Jin, and J. Jiang, "A survey of additive manufacturing reviews," *Materials Science in Additive Manufacturing* 1, no. 4 (2022): 21.

251. J. Cheng, R. Wang, Z. Sun, et al., "Centrifugal multimaterial 3D printing of multifunctional heterogeneous objects," *Nature Communications* 13, no. 1 (2022): 7931.

252. J. Jiang, X. Zhai, K. Zhang, et al., "Low-melting-point alloys integrated extrusion additive manufacturing," *Additive Manufacturing* 72 (2023): 103633.

253. B. MacNider, H. Xiu, C. Tamur, et al., "Customizable wave tailoring nonlinear materials enabled by bilevel inverse design," *Nature Communications* 16, no. 1 (2025): 3425.

254. J. Jiang, X. Zhai, L. Jin, et al., "Design for reversed additive manufacturing low-melting-point alloys," *Journal of Engineering Design* 36, no. 10 (2025): 1617–1630.

255. L. Jin, X. Zhai, K. Zhang, J. Jiang, and W.-H. Liao, "3D printing soft robots integrated with low-melting-point alloys," *Materials Science in Additive Manufacturing* 3, no. 3 (2024): 4144.

256. L. Jin, X. Zhai, K. Zhang, and J. Jiang, "Unlocking the potential of low-melting-point alloys integrated extrusion additive manufacturing: insights into mechanical behavior, energy absorption, and electrical conductivity," *Progress in Additive Manufacturing* 10, no. 4 (2025): 2733–2745.

257. X. Kuang, D. J. Roach, J. Wu, et al., "Advances in 4D printing: materials and applications," *Advanced Functional Materials* 29, no. 2 (2019): 1805290.

258. K. Mirasadi, M. A. Yousefi, L. Jin, et al., "4D printing of magnetically responsive shape memory polymers: Toward sustainable solutions in soft robotics, wearables, and biomedical devices," *Advanced Science* 13, no. 15 (2025): e13091.

259. Z. Xu, S. Zhang, X. Sun, S. Mao, and R. Xiao, "Machine Learning-Assisted Inverse Design of 3D Shape Morphing in Liquid Crystal Elastomer Composite Strips," *Advanced Functional Materials* (2025): e26924.

260. X. Sun, K. Zhou, F. Demoly, R. R. Zhao, and H. J. Qi, "Perspective: machine learning in design for 3D/4D printing," *Journal of Applied Mechanics* 91, no. 3 (2024): 030801.

261. K. A. Brown and G. X. Gu, "Computational challenges in additive manufacturing for metamaterials design," *Nature Computational Science* 4, no. 8 (2024): 553–555.

262. C. Liu, L. Jin, W.-H. Liao, Z. Wang, and Q. He, "Achieving rapid actuation in liquid crystal elastomers," *National Science Open* 4, no. 2 (2025): 20240013.

263. L. Jin, X. Zhai, J. Jiang, K. Zhang, and W.-H. Liao, "Optimizing stimuli-based 4D printed structures: a paradigm shift in programmable material response," in *Sensors and Smart Structures Technologies for Civil, Mechanical, and Aerospace Systems 2024*, Vol. 12949 (SPIE, 2024), 321–332.

264. L. Jin, K. Zhang, S. Zhou, G. Xie, and W.-H. Liao, "Modulus tunability in hierarchical architectures: a machine learning-enabled approach," in *Multifunctional Materials and Structures*, Vol. 13433 (SPIE, 2025), 133–143.

265. A. Zolfagharian, L. Jin, Q. Ge, et al., "Roadmap on artificial intelligence-augmented additive manufacturing," *Advanced Intelligent Systems* (2026): e202500484.

266. X. Sun, L. Yu, L. Yue, et al., "Machine learning and sequential subdomain optimization for ultrafast inverse design of 4D-printed active composite structures," *Journal of the Mechanics and Physics of Solids* 186 (2024): 105561.

267. M. Wang, Z. Liu, H. Furukawa, et al., "Fast reverse design of 4D-Printed voxelized composite structures using deep learning and evolutionary algorithm," *Advanced Science* 12, no. 12 (2025): 2407825.

268. Q. Tao, P. Xu, M. Li, and W. Lu, "Machine learning for perovskite materials design and discovery," *npj Computational Materials* 7, no. 1 (2021): 23.

269. Z. Liu, N. Rolston, A. C. Flick, et al., "Machine learning with knowledge constraints for process optimization of open-air perovskite solar cell manufacturing," *Joule* 6, no. 4 (2022): 834–849.

270. C. Wei and X. Jing, "A comprehensive review on vibration energy harvesting: Modelling and realization," *Renewable and Sustainable Energy Reviews* 74 (2017): 1–18.

271. H. Ryu, H.-J. Yoon, and S.-W. Kim, "Hybrid energy harvesters: toward sustainable energy harvesting," *Advanced Materials* 31, no. 34 (2019): 1802898.

272. J. Zhu, M. Zhu, Q. Shi, et al., "Progress in TENG technology-A journey from energy harvesting to nanoenergy and nanosystem," *EcoMat* 2, no. 4 (2020): e12058.

273. S. Fang, X. Wang, X. Zhang, et al., "High output, lightweight and small-scale rotational piezoelectric energy harvester utilizing internal impact effect," *Energy Conversion and Management* 322 (2024): 119180.

274. B. Zhang, G. Yang, B. Hu, Y. Xiong, and S. Zhou, "Optimized design of self-powered SSHI interface circuit for enhanced vibration energy harvesting," *Smart Materials and Structures* 34, no. 2 (2025): 025025.

275. J. Choi, I. Jung, and C.-Y. Kang, "A brief review of sound energy harvesting," *Nano Energy* 56 (2019): 169–183.

276. C. Liu, W. Wang, Z. Wang, B. Ding, Z. Wu, and J. Feng, "Data-driven modeling and fast adjustment for digital coded metasurfaces database: Application in adaptive electromagnetic energy harvesting," *Applied Energy* 365 (2024): 123303.

277. P. Jiao, Z. L. Wang, and A. H. Alavi, "Maximizing triboelectric nanogenerators by physics-informed AI inverse design," *Advanced Materials* 36, no. 5 (2024): 2308505.

278. X. Cai, F. Liu, A. Yu, et al., "Data-driven design of high-performance $MASn_xPb_{1-x}I_3$ perovskite materials by machine learning and experimental realization," *Light: Science & Applications* 11, no. 1 (2022): 234.

279. J. Wu, L. Torresi, M. Hu, et al., "Inverse design workflow discovers hole-transport materials tailored for perovskite solar cells," *Science* 386, no. 6727 (2024): 1256–1264.

280. D. V. Anand, Q. Xu, J. Wee, K. Xia, and T. C. Sum, "Topological feature engineering for machine learning based halide perovskite materials design," *npj Computational Materials* 8, no. 1 (2022): 203.

281. L. Zhang, J. Miao, J. Li, and Q. Li, "Halide perovskite materials for energy storage applications," *Advanced Functional Materials* 30, no. 40 (2020): 2003653.

282. J.-S. Kim, J. Noh, and J. Im, "Machine learning-enabled chemical space exploration of all-inorganic perovskites for photovoltaics," *npj Computational Materials* 10, no. 1 (2024): 97.

283. X. Yuan, X. Liu, and J. Zuo, "The development of new energy vehicles for a sustainable future: A review," *Renewable and Sustainable Energy Reviews* 42 (2015): 298–305.

284. E. Goikolea, V. Palomares, S. Wang, et al., "Na-ion batteries-approaching old and new challenges," *Advanced Energy Materials* 10, no. 44 (2020): 2002055.

285. H. Geng, X. Zou, Y. Min, Y. Bu, and Q. Lu, "Advances and challenges in perovskite oxide design for high-performance zinc–air batteries: integrating experimental strategies and machine learning," *Advanced Functional Materials* 35, no. 32 (2025): 2500657.

286. A. Bhowmik, I. E. Castelli, J. M. Garcia-Lastra, P. B. Jørgensen, O. Winther, and T. Vegge, "A perspective on inverse design of battery interphases using multi-scale modelling, experiments and generative deep learning," *Energy Storage Materials* 21 (2019): 446–456.

287. C. Sui, Y.-Y. Li, X. Li, et al., "Bio-inspired computational design of vascularized electrodes for high-performance fast-charging batteries optimized by deep learning," *Advanced Energy Materials* 12, no. 6 (2022): 2103044.

288. M. Duquesnoy, C. Liu, D. Z. Dominguez, V. Kumar, E. Ayerbe, and A. A. Franco, "Machine learning-assisted multi-objective optimization of battery manufacturing from synthetic data generated by physics-based simulations," *Energy Storage Materials* 56 (2023): 50–61.

289. S. Li and A. S. Barnard, "Inverse design of MXenes for high-capacity energy storage materials using multi-target machine learning," *Chemistry of Materials* 34, no. 11 (2022): 4964–4974.

290. Y. Wang, C. Wu, W. Ji, et al., "Machine learning-assisted precision inverse design research of ternary cathode materials: A new paradigm for material design," *Journal of Colloid and Interface Science* 680 (2025): 505–517.

291. X. Li, Y. Qin, G. He, F. Lian, S. Zuo, and C. Cai, "Machine learning-assisted inverse design of wide-bandgap acoustic topological devices," *Journal of Physics D: Applied Physics* 57, no. 13 (2023): 135303.

292. C. Luo, S. Ning, Z. Liu, and Z. Zhuang, "Interactive inverse design of layered phononic crystals based on reinforcement learning," *Extreme Mechanics Letters* 36 (2020): 100651.

293. K. Huang, Y. Lin, Y. Lai, and X. Liu, "Inverse design of nonlinear phononic crystal configurations based on multi-label classification learning neural networks," *Chinese Physics B* 33, no. 10 (2024): 104301.

294. X.-H. Wan, Y. Zhang, Q.-H. Guo, and L.-Y. Zheng, "Deep learning-based inverse design of irregular phononic crystals," *International Journal of Mechanical Sciences* 297 (2025): 110335.

295. V. Digiorgio, U. Senica, P. Micheletti, M. Beck, J. Faist, and G. Scalari, "On-chip, inverse-designed active wavelength division multiplexer at THz frequencies," *Nature Communications* 16, no. 1 (2025): 7711.

296. K. Zhang, Y. Guo, X. Liu, F. Hong, X. Hou, and Z. Deng, "Deep learning-based inverse design of lattice metamaterials for tuning bandgap," *Extreme Mechanics Letters* 69 (2024): 102165.

297. E. A. Karahan, Z. Liu, A. Gupta, et al., "Deep-learning enabled generalized inverse design of multi-port radio-frequency and sub-terahertz passives and integrated circuits," *Nature Communications* 15, no. 1 (2024): 10734.

298. W. W. Ahmed, M. Farhat, X. Zhang, and Y. Wu, "Deterministic and probabilistic deep learning models for inverse design of broadband acoustic cloak," *Physical Review Research* 3, no. 1 (2021): 013142.

299. W. Chen, R. Sun, D. Lee, C. M. Portela, and W. Chen, "Generative inverse design of metamaterials with functional responses by interpretable learning," *Advanced Intelligent Systems* 7, no. 6 (2025): 2400611.

300. A. Avina, S. Gerges, F. A. Amirkulova, and W. Du, "Acoustic Cloak Design via Gradient-Based Optimization," in *ASME International Mechanical Engineering Congress and Exposition*, Vol. 87615 (American Society of Mechanical Engineers, 2023), V004T04A049.

301. Z. Yang and X. Huang, "An acoustic cloaking design based on topology optimization," *The Journal of the Acoustical Society of America* 152, no. 6 (2022): 3510–3521.

302. G. Fujii, M. Takahashi, and Y. Akimoto, "Acoustic cloak designed by topology optimization for acoustic–elastic coupled systems," *Applied Physics Letters* 118, no. 10 (2021): 101102.

303. H. P. Kunc, K. E. McLaughlin, and R. Schmidt, "Aquatic noise pollution: implications for individuals, populations, and ecosystems," *Proceedings of the Royal Society B: Biological Sciences* 283, no. 1836 (2016): 20160839.

304. X. Fan, L. Li, L. Zhao, et al., "Environmental noise pollution control of substation by passive vibration and acoustic reduction strategies," *Applied Acoustics* 165 (2020): 107305.

305. P. Zhu, W. Tao, X. Lu, F. Mo, F. Guo, and H. Zhang, "Optimisation design and verification of the acoustic environment for multimedia classrooms in universities based on simulation," in *Building Simulation* (Springer, 2022), 1–18.

306. D. Wang, L. Ying, W. Wang, C. Pei, and J. Wang, "Indoor substation low-noise design and sound absorbing structure improvement considering power transformer acoustic radiation characteristics," *Building and Environment* 149 (2019): 390–403.

307. X. Li, J. W. Chua, X. Yu, et al., "3D-printed lattice structures for sound absorption: current progress, mechanisms and models, structural-property relationships, and future outlook," *Advanced Science* 11, no. 4 (2024): 2305232.

308. L. Cao, Q. Fu, Y. Si, B. Ding, and J. Yu, "Porous materials for sound absorption," *Composites Communications* 10 (2018): 25–35.

309. F. Feng, L. Diao, C. He, and M. Tao, "Topology optimization of multi-material acoustic metamaterials for low-frequency and broadband sound absorption," *Materials & Design* 254 (2025): 114136.

310. J. Yan, Y. Li, G. Yin, G. Yan, and H. P. Lee, "Inverse-designed multifunctional metamaterials for broadband acoustic absorption and ventilation," *Composite Structures* 362 (2025): 119106.

311. B. Zheng, J. Yang, B. Liang, and J.-C. Cheng, "Inverse design of acoustic metamaterials based on machine learning using a Gauss–Bayesian model," *Journal of Applied Physics* 128, no. 13 (2020): 134902.

312. H. Weeratunge, Z. Shireen, S. Iyer, et al., "A machine learning accelerated inverse design of underwater acoustic polyurethane coatings," *Structural and Multidisciplinary Optimization* 65, no. 8 (2022): 213.

313. B. Cheng, M. Wang, N. Gao, and H. Hou, "Machine learning inversion design and application verification of a broadband acoustic filtering structure," *Applied Acoustics* 187 (2022): 108522.

314. Y. Zhou, L. Ma, X. Kang, and Z. Zhu, "Reverse design of broadband sound absorption structure based on deep learning method," *Scientific Reports* 15, no. 1 (2025): 1946.

315. K. Mahesh, S. K. Ranjith, and R. Mini, "A deep autoencoder based approach for the inverse design of an acoustic-absorber," *Engineering with Computers* 40, no. 1 (2024): 279–300.

316. Z. Xiao, P. Gao, D. Wang, X. He, Y. Qu, and L. Wu, "Accelerated design of low-frequency broadband sound absorber with deep learning approach," *Mechanical Systems and Signal Processing* 211 (2024): 111228.

317. M. Massoudinejad, N. Amanidaz, R. M. Santos, and R. Bakhshoodeh, "Use of municipal, agricultural, industrial, construction and demolition waste in thermal and sound building insulation materials: A review article," *Journal of Environmental Health Science and Engineering* 17 (2019): 1227–1242.

318. M. Zarastvand, M. Ghassabi, and R. Talebitooti, "Acoustic insulation characteristics of shell structures: a review," *Archives of Computational Methods in Engineering* 28 (2021): 505–523.

319. X. Zhang, Q. Yu, C. Zhao, et al., "Modular reverse design of acoustic metamaterial and sound barrier engineering applications: High ventilation and broadband sound insulation," *Thin-Walled Structures* 196 (2024): 111498.

320. C. Song, X. Wang, S. Xu, C. Zhao, and Z. Huang, "Inverse design of laminated plate-type acoustic metamaterials for sound insulation based on deep learning," *Applied Acoustics* 218 (2024): 109906.

321. X. Sun, Y. Yang, H. Jia, et al., "Acoustic structure inverse design and optimization using deep learning," *Journal of Sound and Vibration* 596 (2025): 118789.

322. L. Fan, X. Zhang, and Y. Wu, "Machine learning driven inverse design of broadband acoustic superscattering," *Advanced Intelligent Discovery* (2026): e202500210.

323. I. Chowdhury, R. Prasher, K. Lofgreen, et al., "On-chip cooling by superlattice-based thin-film thermoelectrics," *Nature Nanotechnology* 4, no. 4 (2009): 235–238.

324. A. H. Khalaj and S. K. Halgamuge, "A Review on efficient thermal management of air-and liquid-cooled data centers: From chip to the cooling system," *Applied Energy* 205 (2017): 1165–1188.

325. T.-J. Lu, "Thermal management of high power electronics with phase change cooling," *International Journal of Heat and Mass Transfer* 43, no. 13 (2000): 2245–2256.

326. W. Wu, S. Wang, W. Wu, K. Chen, S. Hong, and Y. Lai, "A critical review of battery thermal performance and liquid based battery thermal management," *Energy Conversion and Management* 182 (2019): 262–281.

327. Z. Rao, S. Wang, M. Wu, Z. Lin, and F. Li, "Experimental investigation on thermal management of electric vehicle battery with heat pipe," *Energy Conversion and Management* 65 (2013): 92–97.

328. M. Ramandi, I. Dincer, and G. Naterer, "Heat transfer and thermal management of electric vehicle batteries with phase change materials," *Heat and Mass Transfer* 47, no. 7 (2011): 777–788.

329. L. Chen, W. Zhang, and F. Sun, "Power, efficiency, entropy-generation rate and ecological optimization for a class of generalized irreversible universal heat-engine cycles," *Applied Energy* 84, no. 5 (2007): 512–525.

330. F. Lu, M. Kaviany, B. Veyera, and J. Williams, "Axial-vapor-flow induced, low-liquid-saturation heat-pipe effect in wet insulation: Simulation and experiment," *International Journal of Heat and Mass Transfer* 244 (2025): 126857.

331. F. Lu, L. Franceschetti, K. Krippner, M. Kaviany, and T. Daimaru, "Analytic thermal conductance for square channel, flat plate oscillating heat pipe: CFD simulations of Taylor liquid film and experiment," *International Journal of Heat and Mass Transfer* 241 (2025): 126711.

332. J. J. García-Esteban, J. Bravo-Abad, and J. C. Cuevas, "Deep learning for the modeling and inverse design of radiative heat transfer," *Physical Review Applied* 16, no. 6 (2021): 064006.

333. J. Sullivan, A. Mirhashemi, and J. Lee, "Deep learning-based inverse design of microstructured materials for optical optimization and thermal radiation control," *Scientific Reports* 13, no. 1 (2023): 7382.

334. Q. Pan, S. Zhou, S. Chen, C. Yu, Y. Guo, and Y. Shuai, "Deep learning-based inverse design optimization of efficient multilayer thermal emitters in the near-infrared broad spectrum," *Optics Express* 31, no. 15 (2023): 23944–23951.

335. S. Yang, L.-F. Zhu, L.-L. Ke, et al., "Transfer learning-based layout inverse design of composite plates for anticipated thermo-mechanical field," *Applied Thermal Engineering* 263 (2025): 125362.

336. P. Jin, L. Xu, G. Xu, J. Li, C.-W. Qiu, and J. Huang, "Deep learning-assisted active metamaterials with heat-enhanced thermal transport," *Advanced Materials* 36, no. 5 (2024): 2305791.

337. E. Li, Y. Wang, L. Jin, et al., "Current-diffusion model for metasurface structure discoveries with spatial-frequency dynamics," *Nature Machine Intelligence* 8 (2025): 59–69.

338. B. Xu, J. Shao, X. Zhao, et al., "Deep-Learning-Enabled Inverse Design of Large-Scale Metasurfaces With Full-Wave Accuracy," *Laser & Photonics Reviews* 20, no. 5 (2025): e03115.

339. N. Wang, W. Yan, Y. Qu, S. Ma, S. Z. Li, and M. Qiu, "Intelligent designs in nanophotonics: from optimization towards inverse creation," *PhotoniX* 2 (2021): 1–35.

340. Y. Xie, S. Feng, L. Deng, et al., "Inverse design of chiral functional films by a robotic AI-guided system," *Nature Communications* 14, no. 1 (2023): 6177.

341. Z. Li, R. Pestourie, J.-S. Park, Y.-W. Huang, S. G. Johnson, and F. Capasso, "Inverse design enables large-scale high-performance meta-optics reshaping virtual reality," *Nature Communications* 13, no. 1 (2022): 2409.

342. Q. Wang, A. V. Chumak, and P. Pirro, "Inverse-design magnonic devices," *Nature Communications* 12, no. 1 (2021): 2636.

343. C. Dory, D. Vercruysse, K. Y. Yang, et al., "Inverse-designed diamond photonics," *Nature Communications* 10, no. 1 (2019): 3309.

344. M. Camacho, B. Edwards, and N. Engheta, "A single inverse-designed photonic structure that performs parallel computing," *Nature Communications* 12, no. 1 (2021): 1466.

345. J. L. Pita Ruiz, N. Dalvand, and M. Ménard, "Integrated silicon nitride devices via inverse design," *Nature Communications* 16, no. 1 (2025): 9307.

346. A. Sun, S. Xing, X. Deng, et al., "Edge-guided inverse design of digital metamaterial-based mode multiplexers for high-capacity multi-dimensional optical interconnect," *Nature Communications* 16, no. 1 (2025): 1–12.

347. K. Y. Yang, C. Shirpurkar, A. D. White, et al., "Multi-dimensional data transmission using inverse-designed silicon photonics and microcombs," *Nature Communications* 13, no. 1 (2022): 7862.

348. F. A. A. Nugroho, P. Bai, I. Darmadi, et al., "Inverse designed plasmonic metasurface with parts per billion optical hydrogen detection," *Nature Communications* 13, no. 1 (2022): 5737.

349. S. So, J. Mun, and J. Rho, "Simultaneous inverse design of materials and structures via deep learning: demonstration of dipole resonance engineering using core–shell nanoparticles," *ACS Applied Materials & Interfaces* 11, no. 27 (2019): 24264–24268.

350. C. Park, S. Kim, A. W. Jung, et al., "Sample-efficient inverse design of freeform nanophotonic devices with physics-informed reinforcement learning," *Nanophotonics* 13, no. 8 (2024): 1483–1492.

351. Z. Liu, D. Zhu, S. P. Rodrigues, K.-T. Lee, and W. Cai, "Generative model for the inverse design of metasurfaces," *Nano Letters* 18, no. 10 (2018): 6570–6576.

352. S. Harel and K. Radinsky, "Prototype-based compound discovery using deep generative models," *Molecular pharmaceutics* 15, no. 10 (2018): 4406–4416.

353. M. Xu, T. Ran, and H. Chen, "De novo molecule design through the molecular generative model conditioned by 3D information of protein binding sites," *Journal of Chemical Information and Modeling* 61, no. 7 (2021): 3240–3254.

354. Y. Wang, S. Michael, S.-M. Yang, et al., "Retro drug design: from target properties to molecular structures," *Journal of Chemical Information and Modeling* 62, no. 11 (2022): 2659–2669.

355. A. Zhavoronkov, Y. A. Ivanenkov, A. Aliper, et al., "Deep learning enables rapid identification of potent DDR1 kinase inhibitors," *Nature Biotechnology* 37, no. 9 (2019): 1038–1040.

356. S. R. Krishnan, N. Bung, S. R. Vangala, R. Srinivasan, G. Bulusu, and A. Roy, "De novo structure-based drug design using deep learning," *Journal of Chemical Information and Modeling* 62, no. 21 (2021): 5100–5109.

357. N. De Cao and T. Kipf, "MolGAN: An implicit generative model for small molecular graphs,"*Arxiv Preprint Arxiv: 1805.11973* (2018).

358. A. Schneuing, C. Harris, Y. Du, et al., "Structure-based drug design with equivariant diffusion models," *Nature Computational Science* 4, no. 12 (2024): 899–909.

359. I. Igashov, H. Stärk, C. Vignac, et al., "Equivariant 3D-conditional diffusion model for molecular linker design," *Nature Machine Intelligence* 6, no. 4 (2024): 417–427.

360. H. Wang, Y. Lyu, J. Jiang, and H. Zhu, "Data-driven inverse design of novel spinodoid bone scaffolds with highly matched mechanical properties in three orthogonal directions," *Materials & Design* 251 (2025): 113697.

361. P. Jiao, C. Zhang, W. Meng, et al., "Artificial intelligence-guided inverse design of deployable thermo-metamaterial implants," *ACS Applied Materials & Interfaces* 17, no. 2 (2025): 2991–3001.

362. J. Zhang, Y. Zhuang, C. Feng, et al., "Inverse design of skull osteoinductive implants with multi-level pore structures through machine learning," *Journal of Materials Chemistry B* 12, no. 39 (2024): 9991–10003.

363. Y. Jia, K. Liu, and X. S. Zhang, "Modulate stress distribution with bio-inspired irregular architected materials towards optimal tissue support," *Nature Communications* 15, no. 1 (2024): 4072.

364. Z. Liu, M. Cai, S. Hong, et al., "Data-driven inverse design of flexible pressure sensors," *Proceedings of the National Academy of Sciences* 121, no. 28 (2024): e2320222121.

365. J. Wekalao, N. Mandela, A. Obed, and A. Bouhenna, "Design and evaluation of tunable terahertz metasurface biosensor for malaria detection with machine learning optimization using artificial intelligence," *Plasmonics* 20, no. 5 (2025): 2569–2593.

366. J. G. Freeze, H. R. Kelly, and V. S. Batista, "Search for catalysts by inverse design: artificial intelligence, mountain climbers, and alchemists," *Chemical Reviews* 119, no. 11 (2019): 6595–6612.

367. B. Kim, S. Lee, and J. Kim, "Inverse design of porous materials using artificial neural networks," *Science Advances* 6, no. 1 (2020): eaax9324.

368. D. H. Mok and S. Back, "Generative pretrained transformer for heterogeneous catalysts," *Journal of the American Chemical Society* 146, no. 49 (2024): 33712–33722.

369. Z. Song, L. Fan, S. Lu, C. Ling, Q. Zhou, and J. Wang, "Inverse design of promising electrocatalysts for CO_2 reduction via generative models and bird swarm algorithm," *Nature Communications* 16, no. 1 (2025): 1053.

370. J. Li, T. Liu, K. N. Palansooriya, et al., "Zeolite-catalytic pyrolysis of waste plastics: Machine learning prediction, interpretation, and optimization," *Applied Energy* 382 (2025): 125258.

371. S. Jiang, W. Xu, Q. Xia, et al., "Application of machine learning in the study of cobalt-based oxide catalysts for antibiotic degradation: An innovative reverse synthesis strategy," *Journal of Hazardous Materials* 471 (2024): 134309.

372. K. S. Chandana, S. Karka, M. K. Gujral, R. Kamesh, and A. Roy, "Machine learning aided catalyst activity modelling and design for direct conversion of CO_2 to lower olefins," *Journal of Environmental Chemical Engineering* 11, no. 2 (2023): 109555.

373. R. Xin, C. Wang, Y. Zhang, et al., "Efficient removal of greenhouse gases: machine learning-assisted exploration of metal–organic framework space," *ACS Nano* 18, no. 30 (2024): 19403–19422.

374. H. Park, S. Majumdar, X. Zhang, J. Kim, and B. Smit, "Inverse design of metal–organic frameworks for direct air capture of CO_2 via deep reinforcement learning," *Digital Discovery* 3, no. 4 (2024): 728–741.

375. B. Yan, X. Wang, H. Ma, W. Lu, and Q. Li, "Hybrid time-delayed feed-forward and feedback control of lever-type quasi-zero-stiffness vibration isolators," *IEEE Transactions on Industrial Electronics* 71, no. 3 (2023): 2810–2819.

Biographies

Weihao Lin is a Ph.D. candidate in the School of Automation and Intelligent Manufacturing at The Southern University of Science and Technology (SUSTech), supervised by Prof. Guopin Liu. He was awarded the Liyuan Star Scholarship during his undergraduate studies at Shenzhen University and achieved high rankings in multiple disciplinary competitions, including the Electronic Design Contest and the Internet of Things Competition. As a doctoral candidate in a joint program between SUSTech and Peng Cheng Laboratory, he will focus on applying machine learning to control systems, such as robotic (manipulator) control and 3D/4D printing technologies.

Liuchao Jin is a Ph.D. candidate in the Department of Mechanical and Automation Engineering at The Chinese University of Hong Kong, supervised by Prof. Wei-Hsin Liao. He is a recipient of the Hong Kong PhD Fellowship Scheme (HKPFS). His research focuses on 3D/4D printing, adaptive structures, soft robotics, metamaterials, and AI for science. Liuchao obtained a bachelor's degree from Sichuan University - Pittsburgh Institute. He has also gained research experience as a visiting student at the Southern University of Science and Technology and Shenzhen University, and as a research assistant at McGill University and Westlake University.

Zhifei Jiang is currently a PhD candidate in the Department of Materials Science and Engineering at the National University of Singapore, supervised by Professor Konstantin Novoselov. His research focuses on two-dimensional materials, batteries and supercapacitors, hydrogen storage materials, and AI-driven approaches for materials science. He received his First-Class Honors Bachelor Degree in Materials Science and Engineering from the University of Manchester, followed by an MSc (Distinction) from Imperial College London. He has also gained extensive research experience as a research assistant at Zhejiang University and Westlake University.

Mingjing Cai received the Ph.D. degree in mechanical and automation engineering from The Chinese University of Hong Kong, Shatin, Hong Kong, China, in 2020. He is currently an Associate Professor with Guangzhou Institute of Technology, Xidian University, Guangzhou, China. His current research interests include energy harvesting from human motion, self-powered IoT applications and advanced robotics.

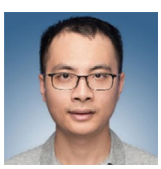

Zhihui Lai received the B.Eng. degree and the master's and Ph.D. degrees in mechanical engineering from Tianjin University, Tianjin, China in 2010 and 2015, respectively. He currently works as a Professor with the College of Mechatronics and Control Engineering, Shenzhen University, China. His research interests include vibration energy harvesting, mechanical fault diagnosis, and vibration control. Dr. Lai has published more than 80 peer-review papers. He was ranked among the world's top 2% most-cited scientists in 2024/2025. He served as an editor for one SCI journal, and guest editors for three SCI journals, including Smart Materials and Structures.

Daniil Yurchenko is an expert in Nonlinear and Stochastic Dynamics, mathematical and experimental modelling of complex dynamical systems. He has received his Ph.D. degree in mechanical engineering from Worcester Polytechnic Institute, USA. He is currently the Head of Dynamics group at the Institute of Sound and Vibration Research, University of Southampton. He has published over 200 scientific publications, including peer-reviewed journals and conference proceedings. He received a Young Scientists Award from the Russian Science Council in 2008. He is an Associate Editor of MSSP, CNSNS, JVTSD. He is also a Fellow of the International Institute of Acoustics and Vibration.

Bo Yan is a full Professor and Vice Dean with the School of Mechanical Engineering, Zhejiang Sci-Tech University, Zhejiang, China. He became an Assistant Professor in 2016, an Associate Professor in 2018, a Professor in 2022 with the School of Mechanical Engineering, Zhejiang Sci-Tech University. He has been funded by 6 NSFCs including Excellent Young Scientist Fund. He has authored more than 90 peer reviewed journal articles and published 1 academic book. His research interests include low-frequency vibration isolation, bio-inspired vibration structure, and dynamics and control of high-end equipment.

Shengxi Zhou joined the School of Aeronautics, Northwestern Polytechnical University, Xi'an, China, in 2018 as a professor (full). His research interests include vibration energy harvesting, fluid energy harvesting, signal processing, structural health monitoring, nonlinear dynamics, vibration control, robotics, and so on. Currently, he is an Associate Editor of ASME Journal of Computational and Nonlinear Dynamics, an Associate Editor of ASME Journal of Dynamic Systems, Measurement and Control, an Associate Editor of Mechanical Systems and Signal Processing, an Editorial Board Member of Smart Materials and Structures, an Editorial Board Member of Applied Nonlinear Dynamics and Vibrations.

Kostya S. Novoselov received M.Sc. degree from Moscow Institute of Physics and Technology, Moscow, Russia, in 1997, and Ph.D. degree from University of Nijmegen, Nijmegen, The Netherlands, in 2004. He is a Fellow of the Royal Society and Royal Society Research Professor. He was with The University of Manchester, Manchester, U.K., in 2001, and the National University of Singapore, Singapore, in 2019. Prof. Novoselov is an expert in condensed matter physics, mesoscopic physics, and nanotechnology, best known for isolating graphene in 2004. Prof. Novoselov was awarded the Nobel Prize for Physics in 2010 for his pioneering experiments with this material.

Wei-Hsin Liao received his Ph.D. from The Pennsylvania State University, University Park, USA. Since 1997, Dr. Liao has been with The Chinese University of Hong Kong, where he is Choh-Ming Li Professor of Mechanical and Automation Engineering. His research has led to publications of over 400 technical papers and 28 patents. Prof. Liao is the recipient of 2020 ASME Adaptive Structures and Material Systems Award. He serves as an Associate Editor for Journal of Intelligent Material Systems and Structures, and on the Executive Editorial Board of Smart Materials and Structures. Dr. Liao is a Fellow of ASME, HKIE, and IOP.

Shitong Fang received the Ph.D. degree from the Chinese University of Hong Kong in 2021. She currently works as an Associate Professor and the Associate Chairman with Shenzhen University, China. Her research interests include self-powered sensing techniques and metamaterials. Dr. Fang was ranked among the world's top 2% most-cited scientists in 2024/2025. She received the ASME Best Paper Award (2021, 2023), the Best PhD Thesis Award at CUHK, and the ICAST Best Paper Gold Award. She served as a guest editor for three SCI journals including Smart Materials and Structures as well as a youth editor for the SCI journal International Journal of Dynamics and Control.